DOKUZ EYLÜL UNIVERSITY

GRADUATE SCHOOL OF NATURAL AND APPLIED SCIENCES

WEAR AND CORROSION BEHAVIOUR OF ELECTROCHEMICALLY DEPOSITED BIOACTIVE HYDROXYAPATITE COATINGS ON IMPLANT MATERIALS

by

Erhan ÖZKAN

July, 2006

İZMİR

WEAR AND CORROSION BEHAVIOUR OF ELECTROCHEMICALLY DEPOSITED BIOACTIVE HYDROXYAPATITE COATINGS ON IMPLANT MATERIALS

A Thesis Submitted to the
Graduate School of Natural and Applied Sciences of Dokuz Eylül University
In Partial Fulfillment of the Requirements for the Degree of Master of Science
in Metallurgical and Materials Engineering, Materials Science Program

by

Erhan ÖZKAN

July, 2006

İZMİR

M.Sc. THESIS EXAMINATION RESULT FORM

We have read the thesis entitled **"WEAR AND CORROSION BEHAVIOUR OF ELECTROCHEMICALLY DEPOSITED BIOACTIVE HYDROXYAPATITE COATINGS ON IMPLANT MATERIALS"** completed by Erhan ÖZKAN under supervision of Prof. Dr. Ahmet ÇAKIR and we certify that in our opinion it is fully adequate, in scope and in quality, as a thesis for the degree of Master of Science.

Prof. Dr. Ahmet ÇAKIR

Supervisor

Assoc. Prof. Dr. A. Bülent ÖNAY

(Jury Member)

Prof. Dr. Mustafa DEMİRCİOĞLU

(Jury Member)

Prof. Dr. Cahit HELVACI
Director
Graduate School of Natural and Applied Sciences

ACKNOWLEDGMENTS

First and foremost, I would like to express my sincere gratitude to my advisor Prof. Dr. Ahmet ÇAKIR for his constant support in the construction of the original idea of this dissertation and for his efforts to improve my theoretical background. I have both privileged and fortunate to have had such an advisor.

I would like to thank Sandvick Company for supplying 316L Stainless Steels, Eczacıbaşı A.Ş. for supplying lactated Ringer's solutions, and especially Devlet Planlama Teşkilatı (DPT) for supplying all experimental possibilities.

I would like to present my gratitude to Prof. Dr. Mustafa DEMİRCİOĞLU, who is my external advisor. I never forget his attention on the control for my thesis. His respect to my thesis affected me too much.

I would also like to thank my family for their patience, trust and endless support through all my life.

I would like to extend my appreciation to my friends and colleagues Çağrı TEKMEN, Murat KUŞOĞLU, Süleyman AKPINAR, Osman ÇULHA, Faruk EBEOĞLUGIL, Bahadır UYULGAN and the others for their big help and friendship.

Erhan ÖZKAN

WEAR AND CORROSION BEHAVIOUR OF ELECTROCHEMICALLY DEPOSITED BIOACTIVE HYDROXYAPATITE COATINGS ON IMPLANT MATERIALS

ABSTRACT

Calcium phosphate-based ceramics are attractive materials as bone substitutes in biomedical applications due to their inherent biocompatibility. They promise better properties over existing biomaterials because of their ability to promote intimate bone growth and rapid fixation.

In particular, hydroxyapatite (HA) formulated as $[Ca_{10}(PO_4)_6(OH)_2]$ has been recognised as a bioactive material usable as a bone substitute and bone repair material. Among several methods for preparing HA coatings, electrochemical deposition using aqueous electrolyte containing Ca and P bearing has attracted considerable attention for a decade because it is claimed to have a variety of advantages for coating fabrication, such as low process temperature, ability to deposit uniform coatings on bodies of complex shape, easy control of deposit thickness, and achieving high purity to a certain degree.

The objective of this study was to form HA coatings on 316 Stainless Steel by using electrochemical deposition technique, and investigate the wear and corrosion behaviour of these coatings. The HA deposits were characterized using, scanning electron microscopy (SEM) with energy dispersive X-ray microanalysis (EDS), X-ray diffraction (XRD), optical microscope with image analyser and Fourier Transform Infrared spectroscopy (FTIR).

Key words: Hydroxyapatite, electrochemical deposition, corrosion, wear

İMPLANT MALZEME YÜZEYLERİNDE ELEKTROKİMYASAL OLARAK ÇÖKTÜRÜLEN BİYOAKTİF HİDROKSİAPATİT KAPLAMALARIN AŞINMA VE KOROZYON DAVRANIŞLARI

ÖZ

Kalsiyum fosfat esaslı seramikler biyouyumlu oluşlarından dolayı biyomedikal uygulamalarda kemik yerine geçebilen ilgi çekici malzemelerdir. Var olan biyomalzemelerden daha çok gelecek vaat etmeleri, kemik büyümesini teşvik ederek protezlerin daha hızlı tespitini sağlamalarındandır.

Özellikle hidroksiapatit (HA) [$Ca_{10}(PO_4)_6(OH)_2$] kemik yerine geçen ve kemik tamir malzemesi olarak bilinen biyoaktif bir malzemedir. HAP kaplamaların hazırlanmasında kullanılan çeşitli metotlar arasında Ca ve P taşıyan sıvı elektrolitler kullanılarak yapılan elektrokimyasal çöktürme son yıllarda tüm dikkatleri üzerinde toplamıştır. Bunun nedeni kaplama üretiminde çeşitli avantajlara sahip olmasıdır. Düşük işlem sıcaklığı, karmaşık şekilli parçalar üzerinde homojen kaplama çöktürme kabiliyeti, çöktürme kalınlığının kolay kontrolü, bir dereceye kadar yüksek saflık temini gibi unsurlar bu avantajlar arasında sayılabilir.

Bu çalışmanın amacı implant uygulamalarında kullanılan protez yüzeylerini elektrokimyasal çöktürme yöntemi ile biyoaktif HA tabakası ile kaplamak ve bu kaplamaların aşınma ve korozyon davranışlarını incelemektir. HA çökeltilerin karakterizasyonu; taramalı elektron mikroskobu (SEM) enerji dağılım spektrometresi (EDS), X-ışınları difraktometresi (XRD), görüntü analiz sistemi aparatlı optik mikroskop ve FTIR ile gerçekleştirilmiştir.

Anahtar sözcükler: Hidroksiapatit, elektrokimyasal çöktürme, korozyon, aşınma

CONTENTS

Page

CHAPTER ONE
INTRODUCTION

A biomaterial is any synthetic material that is used to replace or restore function to a body tissue and continuously or intermediately in contact with body fluids. This definition is somewhat restrictive, because it excludes materials used for devices such as surgical or dental instruments. Although these instruments are exposed to body fluids, they do not replace or augment the function of human tissue. Also excluded from the aforementioned definition are materials that are used for external prostheses, such as artificial limbs or devices such as hearing aids. These materials are not exposed to body fluids (Agrawal, 1998).

One of primary reasons that biomaterials are used is to physically replace hard or soft tissues that have become damaged or destroyed through some pathological process. Although the issues and structures of the body perform for an extended period of time in most people, they do suffer from a variety of destructive processes, including fracture, infection, and cancer that cause pain, disfigurement, or loss of function. Under these circumstances, it may be possible to remove the diseased tissue and replace it with some synthetic material (Williams, 1990).

Most synthetic biomaterials used for implants are common materials familiar to materials engineer or scientists. In general, these materials can be divided into the following categories: metals, ceramics, polymers, and composites.

Austenitic stainless steels (especially 316L) are popular for implant applications because they are relatively inexpensive, they can be formed with common techniques, and their mechanical properties can be controlled over a wide range for optimal strength and ductility. Stainless steels of 316L are not sufficiently corrosion resistant for long-term use as an implant material. They find use as bone screws, bone plates, intramedullary nails and rods and temporary fixation devices (Davis 2003).

Calcium phosphate base bioceramics have been in use in medicine and dentistry over thirty years. Applications include dental implants, periodontal treatment, alveolar ridge augmentation, orthopaedics, maxillofacial surgery, and otolaryngology. Being one of these, Hydroxyapatite [HA; chemical formula $Ca_{10}(PO_4)_6(OH)_2$] has been extensively studied lately due to its chemical and structural similarities to naturally occurring biological apatite in hard tissues. It cannot be used directly in bulk form for implant production due to its inefficient mechanical properties (Sridhar et al., 2001). However its use as coating materials continues to be a point of interest because of its excellent biocompatibility, bioactivity, stimulating effect on bone formation onto itself (Osseo-integration) (Yu-Peng Lu et al., 2006). Plasma-sprayed HAP coatings on implant materials, titanium alloys in particular, have been used commercially for some time (Gu et al., 2003). However low adherence to the substrate and co-existence of stable crystals of HA with other amorphous CaP structures with high solubility and porosities remains to be a main problem faced in practice today. Besides argument is still going on at present whether the degree of crystalline structure of HA in coating layers has anything to do to promote bio-compatibility and osseo-integration (Sridhar et al., 2001).

In dealing with the shortcomings of CaP coatings, to better control the film adherence particularly, various deposition technologies, electrochemical deposition (ECD) being the first (Lin et al., 2003), have been developed. When compared to the other deposition techniques, ECD methods have several advantages and are in the most important place with high flexibility to control the coating chemistry and characteristics because of several numbers of process variables they have. However, it should be noted that electrochemical deposition is not a simple dip and dunk process. It is probably one of the most complex unit operations known because of the unusually large number of critical elementary phenomena or process steps which control the overall process. Electrochemical deposition involves surface phenomena, solid state processes, and processes occurring in the liquid state on many scientific disciplines.

The objective of this study was to form HA coatings on 316 Stainless Steel by using electrochemical deposition technique, and investigate the wear and corrosion behaviour of these coatings. The coatings were characterised by using X-ray diffraction (XRD), scanning electron microscope (SEM) with attached energy dispersive spectroscopy (EDS), optical microscope, image analyzer, Fourier transform infrared (FTIR), differential thermal analyzer/thermogravimetry (DTA/TG). Electrochemical corrosion studies were also employed to determine the corrosion characteristics of HA coatings on stainless steel substrates in Ringer's Solution at 37 °C by using potentiostat/galvanostat. The changes in morphology and chemistry of the coatings as a result of corrosion tests were investigated by conducting characterization before and after corrosion tests. Tribological and mechanical properties of the coatings were measured by using dynamic ultra micro-hardness tester, scratch tester, and friction-wear tester.

CHAPTER TWO
BIOMATERIALS

2.1 A Short History of Biomaterials

The modern field we call biomaterials is too new for a formal history to have been compiled. However, a few comments are appropriate to place both ancient history and rapidly moving contemporary history in perspective. The Romans, Chinese, Aztec used gold in dentistry more than 2000 years ago. Through much of recorded history, glass eyes and wooden teeth have been in common use. At the turn of this century, synthetic plastics became available. Their ease of fabrication to many implantation experiments, most of them, in light our contemporary understanding of biomaterials toxicology, doomed to failure. Poly methyl methacrylate (PMMA) was introduced in dentistry in 1937. During World War II, shards PMMA from shattered gunnery turrets, unintentionally implanted in the eyes of aviators, suggested that some materials might evoke only a mild foreign body reaction. Just after World War II, Voorhees experimented with parachute cloth (Vinyon N) as a vascular prosthesis. In 1958, in a cardiovascular surgery textbook by Rob, the suggestion was offered that surgeons might visit their local draper's shop and purchase Dacron fabric could be cut with pinking shears to fabricate an arterial prosthesis. In the early 1960s Charnley used PMMA, ultrahigh molecular weight polyethylene, and stainless steel for total hip replacement. While these applications for synthetic materials medicine spanned much of written history, the term “biomaterial” was not invoked.

It is difficult to pinpoint the precise origins of them “biomaterial”. However, it is probable that the field we recognize today was solidified through the early Clemson University biomaterials symposia in the late 1960s and early 1970s. The scientific success of these symposia led to formation of the society for biomaterials in 1975. The individual physician-visionaries who implanted miscellaneous materials to find a solution to pressing, often life-threatening, medical problems were, with these Clemson symposia, no longer the dominant force. We had researchers and engineers designing materials meet specific criteria, and scientists exploring the nature biocompatibility. Around this term "biomaterial" a unique scientific discipline

evolved. The evolution of this field and Society For Biomaterials were intimately connected. From biomaterials ideas, many of which originated at society meetings, other fields evolved. Drug delivery, biosensors, and bioseparations owe much to biomaterials. There are now academic departments of biomaterials, many biomaterials programs, and research institutes devoted to education and exploration in biomaterials science and engineering. Paralleling research and educational effort, hundreds of companies that incorporate biomaterials into devices have developed (Ratner, 1996).

2.2 Biomaterials Science

Biomaterials are materials used for making devices that can interact with biological systems to coexist for longer service with minimal failure. Williams (1981) defined biomaterials as "nonviable materials used in medical devices, intended to interact with the biological systems". Biomaterials are widely used in repair, replacement, or augmentation of diseased or damaged parts of the musculoskeletal system such as bones, joints and teeth. A majority of the applications are summarized in Figure 2.1 (Hench, 1985). The fundamental requirement of a biomaterial is that the material and the tissue environment of the body should coexist without having any undesirable or inappropriate effect on each other. Biocompatibility, an essential requirement for any biomaterial, implies the ability of the material to perform effectively with an appropriate host response for the desired application. Common medical devices made of biomaterials include hip replacements, prosthetic heart valves and the less common neurological prostheses and implanted drug delivery systems. These devices when placed inside the body are termed implants when they are intended to remain there for a substantial period of time, and as prosthesis when they are permanently fixed in the body for long-term application till the end of lifetime (Von Recum, 1999).

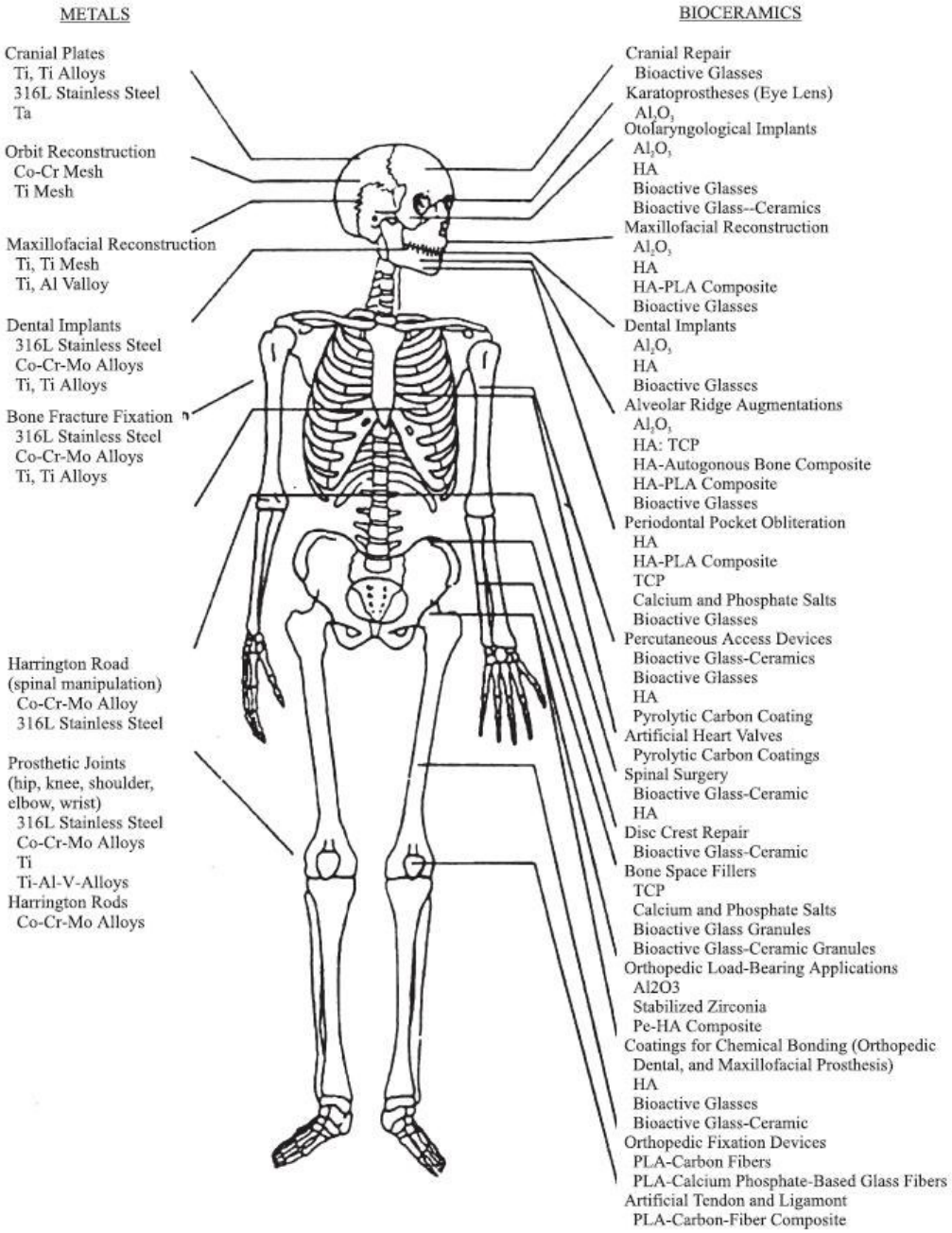

Figure 2.1 Clinical uses of inorganic biomaterials (Hench, 1985)

Orthopaedic implant devices are generally mounted on to the skeletal system of the human body for aiding healing, correcting deformities and restoring the lost functions of the original part. These are supporting bone plates, screws, total hip

joints, knee joints, elbow joints, shoulder joints and reattachments for tendons or ligaments. The implants are exposed to the biochemical and dynamic environment of the human body and their design is dictated by anatomy and restricted by physiological conditions. In the past few decades, increase in the utilization of self-operating machines, participation of many persons in sports, defence activities, increased interest in motorcycles and bicycles, and day-to-day increasing traffic, has resulted in enormous increase in the number of accidents. This has necessarily led people to opt for orthopaedic implants for early and speedy recovery and resumption of their routine activities (Ratner, 1996).

2.3 Materials For Orthopaedic Application

Orthopaedic implants have improved the quality of life for millions of people over the last quarter of a century. The clinical objective is to relieve pain and increase ease of movement in the joint. The engineering objective is to provide minimal physiological stress to the remaining bone system so that the integrity and functionality of the bone and prosthetic materials are maintained over a long service life. Thus, materials suitable for implantation are those that are well tolerated by the body and can withstand cyclic loading in the aggressive environment of the body. Materials that are selectively used in orthopaedics are metals and alloys, ceramics polymers and composites.

2.3.1 Metals and Alloys

Metallic implant materials have a significant economic and clinical impact on the biomaterials field. The total U.S. markets for implants and instrumentation in orthopaedics was about $ 2.908 million in 1991, according to recent estimates. This includes $ 1.379 million for joint prostheses made of metallic materials, plus a variety of trauma products ($ 340 million), instrumentation devices ($ 266 million), bone cement accessories ($ 66 million), and bone replacement materials ($ 29 million). Projections for 2002 indicate that the total global biomaterials market will be $ 6 billion. The clinical numbers are equally impressive. Of the $ 3.6 million orthopaedic operations per year in the U.S., four of ten most frequent involve

metallic implants: open reduction of a fracture and internal fixation, placement or removal of an internal fixation device without reduction of a fracture, arthoplasty of the knee or ankle, and total hip replacement or arthoplasty of the hip.

Besides orthopaedics, there are other markets for metallic implants and devices, including oral and maxillofacial surgery (e.g., dental implants, craniofacial plates and screws) and cardiovascular surgery (e.g. parts of artificial hearts, pacemakers, balloon catheters, valve replacements, aneurysm clips). Interestingly, in 1988, about 11 million Americans (about 4.6% of the civilian population) had at least one implant (Moss et al., 1990)

In view of this wide utilization of metallic implants, the objective of this part is to describe the metallurgical properties of current metallic implant alloys.

2.3.1.1 Currently Used Metallic Implant Materials

The fundamental criterion for choosing a metallic implant material is that it should possess biocompatibility. Metals and alloys have been widely used in various forms as implants, which provide the required mechanical strength and reasonable corrosion resistance. Metallic implants are usually made of one of the three types of materials: austenitic stainless steels, cobalt–chromium alloys and titanium and its alloys (Sivakumar *et al.,* 1992, 1994). The mechanical properties of these metals and alloys as recommended by ASTM are given in Table 2.1. The body environment because of their passive and inert oxide layer formed on the surface accepts these materials. The body in trace amounts usually tolerates the main elemental constituents, as well as the minor alloying constituents of these materials, since most of these alloying elements have specific biological role. Cobalt–chromium alloys have the excellent corrosion resistance property. However, they are not recommended for joint prosthesis because of their poor frictional properties with itself or with other materials. They are susceptible to work hardening and special fabrication procedures need to be employed. Amongst all these materials, titanium and its alloys are the most corrosion resistant materials. Several. ($\alpha+\beta$) titanium alloys provide sufficient strength and corrosion resistance: Ti-6Al-4V, Ti-5Al-2.5Fe,

Ti-6Al-7Nb, etc. However, the main disadvantages are their high cost, inferior wear properties, diffusion of oxygen into titanium during fabrication and heat treatment, and the dissolved oxygen embrittles titanium. Hence, special fabrication and welding procedures are required for joining. Titanium is regarded as highly passive and the passive film formed on titanium and its alloys are quite unreactive. In these alloys passive state is not entirely stable and under certain circumstances, localized breakdown on a highly microscopic scale has been found to occur. These deficiencies in applications have demanded the surface modification of the material, which would enhance corrosion and wear resistance without altering the mechanical properties. The presence of titanium in the surrounding tissues of these implants in the form of titanium compounds and subsequent failure of implants due to fatigue, stress corrosion cracking and poor wear resistance have been reported (Dobbs, 1982).

Table 2.1 Mechanical properties of the implant alloys and human bone

Material	Tensile strength $(MN/m)^2$	Yield strength $(MN/m)^2$	Elongation at fracture	Vickers hardness (H_v)	Young's modulus $(GN/m)^2$	Fatigue limit $(GN/m)^2$
316L SS (annealed)	650	280	45	190	211	0·28
Wrought Co–Cr alloy	1540	1050	9	450	541	0·49
Cast Co–Cr alloy	690	490	8	300	241	0·30
Titanium	710	470	30	–	121	0·30
Ti-6Al-4V	1000	970	12	–	121	–
Human bone	137·3	–	1·49	26·3	30	–

Also, Ti6Al4V alloy contains aluminium, which is well known to cause certain bone diseases and neurological disorders. Vanadium is considered to be an essential element in the body, but may become toxic at excessive levels. The toxicity of vanadium is well known, and can be aggravated when an implant is fractured and subsequently undergoes fretting. Release of titanium ions into the tissues adjacent to the implants results in discolouration of the tissues. This may also be detrimental to the bone attachment and further bone growth on the implant surface. Austenitic stainless steels, especially AISI (American Iron and Steel Institute) Type 316L stainless steel is the most widely used material for implant fabrication in India for orthopaedic applications because of its lower cost, ease of fabrication and welding as

compared to Co–Cr alloys and Ti and its alloys. Austenitic type 316L stainless steel possesses reasonable corrosion resistance, biocompatibility, tensile strength, fatigue resistance and suitable density for load-bearing purposes thus making this material a desirable surgical-implant material

2.3.1.1.1 Stainless Steel, While several types or stainless steels are available for implant (Figure 2.1), in practice the most common is 316L (ASTM F138, F139), grade *2.* This steel has less than 0.030% (wt. %) carbon in order to reduce the possibility of *in vivo* corrosion. The "L" in the designation 316L denotes its low carbon content. The 316L alloy is predominantly iron (60-65%) alloyed with major amounts of chromium (17—19%) and nickel (12-14%), plus minor amounts of nitrogen, manganese, molybdenum, phosphorous, silicon, and sulphur.

The rationale for the alloying additions involves the metals surface and bulk microstructure. The key function or chromium is to permit the development of corrosion-resistant steel by forming a strongly adherent surface oxide (Cr_2O_3). However, the downside is that chromium tends to stabilize the ferritic (BCC, body-centered cubic) phase, which is weaker than the austenitic (FCC, face-centered cubic) phase. Molybdenum and silicon are also ferrite stabilizers. To counter this tendency to form ferrite, nickel is added to stabilize the austenitic phase.

The most important reason for the low carbon content relates to corrosion. If the carbon content of the steel significantly exceeds 0.03%, there is increased danger of formation carbides such as $Cr_{23}C_6$. These tend to precipitate at grain boundaries when the carbon concentration and thermal history have been favourable to the kinetics of carbide growth. In turn, this carbide precipitation depletes the adjacent grain boundary regions of chromium, which has the effect of diminishing formation of the protective chromium-based oxide Cr_2O_3. Steels in which such carbides have formed are called "sensitized" and are prone to fail through corrosion-assisted fractures that originate at the sensitized (weakened) grain boundaries (Brunski, 1996).

2.3.1.1.2 Cobalt Based Alloys, Cobalt-based alloys include Haynes-Stellite 21 and 25 (ASTM F75 and F90, respectively), forged Co-Cr-Mo alloy (ASTM F799),

and multiphase (MP) alloy MP35N (ASTM F562). The F75 and F799 alloys are virtually identical in composition, each being about 58-69% Co and 26-30% Cr. The key difference is their processing history. The other two alloys, F90 and F562, have slightly less Co and Cr, but more Ni in the case of F562, and more tungsten in case of F 90.

2.3.1.1.3 Titanium Based Alloys, CP titanium (ASTM F67) and extra-low interstitial (ELI) Ti-6Al-4V alloy (ASTM F136) are the two most common titanium-based implant biomaterials. The F67 CP Ti is 98.9-99.6% titanium. Oxygen content of CP Ti affects its yield and fatigue strength significantly. For example, 0.18% oxygen (grade 1), the yield strength is about 170 MPa, while at 0.40% (grade 4), the yield strength increases to about 485 MPa. Similarly, at 0.085 wt.% oxygen (slightly purer than grade 1) the fatigue limit (107 cycles) is about 88.2 MPa, while at 0.27 wt.% oxygen (slightly purer than grade 2) the fatigue limit (107 cycles) is about 216 MPa.

With Ti-6Al-4V ELI alloy, the individual Ti-Al and Ti-V phase diagrams suggest the effects of the alloying additions in the ternary alloy. Al is an alpha (HCP) phase stabilizer while V is a beta (BCC) phase stabilizer. The 6Al-4V alloy used for implants is an alpha-beta alloy; the properties or which vary with prior treatments.

2.3.2 Ceramics

Bioceramics are produced in a variety of forms, phases and serve many different functions in repair of the body. In many applications ceramics are used in the form of bulk materials of a specific shape, called implants, prosthesis, or prosthetic devices. Bioceramics are also used to fill space while natural repair processes restore function. In other situations the ceramic is used as coating on a substrate, or as a second phase in a composite, combining the characteristics of both into a new material with enhanced mechanical and biomechanical properties (Hench et al., 1982).

Ceramics and glasses have been used for long time outside the body for a variety of applications in the health care industry. Eyeglasses, diagnostic instruments, chemical ware, thermometers, tissue culture flasks, chromatography column, lasers and fibre optics for endoscopies are commonplace products in the multi-billion dollar industry. Ceramics are widely used in density as restorative materials, gold porcelain crowns, glass-filled ionomer cements, endodontic treatments, dentures, etc. Use of ceramics inside the body as implants is relatively new; alumina hip implants have been used for just over 20 years (Hulbert et al., 1987, for a review of the history of bioceramics).

2.3.2.1 Mechanism of the Ligament

Bio-ceramic substances/materials need to form a steady ligament with the neighbour tissue in order to be resistant in the body ambiance. Mechanism of ligaments depends on the way the tissue reacts in the interface of the implant. No material implanted in the living tissue is inert; all the materials receive a reaction from the tissue.

The most common response of tissues to an implant is formation of a non-adherent fibrous capsule. The fibrous tissue is formed in order to “wall off” or isolate the implant from the host. It is a protective mechanism and with time can lead to complete encapsulation of an implant within the fibrous layer. Metals and most polymers produce this type of interfacial response.

Biological inactive, nearly inert ceramics, such as alumina or zirconia, also develop fibrous capsules at their interface. This thickness of the fibrous layer depends on the factors listed in Table 2.2. The chemical in inertness of alumina and zirconia results in a very thin fibrous layer under optimal conditions. More chemically reactive metallic implants elicit thicker interfacial layers. However, it is important to remember that thickness of an interfacial fibrous layer also depends upon motion and fit at the interface, as well as other factors indicated in Table 2.2.

Table 2.2 Factors affecting implant-tissue interfacial response

Tissue Side	Implant Side
Type of tissue	Composition of Implant
Health of tissue	Phases in Implant
Age of tissue	Phase Boundaries
Blood Circulation in Tissue	Surface morphology
Blood Circulation at interface	Surface porosity
Motion at interface	Chemical reactions
Closeness of Fit	Closeness of Fit
Mechanical Load	Mechanical Load

The third type of interfacial response, indicated in Table 2.3, is when a bond forms across the interface between implant and tissue. This is termed a "bioactive" interface. The interfacial bond prevents motion between the two materials and mimics the type of interface that is formed when natural tissues repair themselves. This type of interface requires the material to have a controlled rate of chemical reactivity. An important characteristic of a bioactive interface is that it changes with time, as do natural tissues, which are in a state of dynamic equilibrium.

Table 2.3 Consequences of implant tissue interactions

Implant-Tissue Reaction	Consequence
Toxic	Tissue dies
Biologically nearly inert	Tissue forms a non-adherent fibrous capsule around the implant
Bioactive	Tissue forms an interfacial bond with the implant
Dissolution of implant	Tissue replaces implant

The mechanism of attachment of tissues to an implant is directly related to the tissue response at the implant interface. There are four types of bioceramics, each with a different type of tissue attachment, summarized in Table 2.4 with examples. The factors that influence the implant-tissue interfacial response listed in Table 2.4 also affect the type and stability of tissue attachment listed in Table 2.4.

Table 2.4 Types of tissue attachment of bioceramic prostheses

Type of Implant	Type of Attachment	Example
Ceramics whose surface irregularities are bond with bone growth, and that are intensive semi-inert but not porous	Mechanical interlock (Morphological Fixation)	Al_2O_3 ZrO_2
For porous implants, bone growth forms and the bone is connected to the material.	Ingrowths of tissues into pores (Biological Fixation)	Hydroxyapatite (HA) HA coated porous metals
Ceramics, glasses, glass ceramics with surface- reaction connect to the bone directly through the chemical bond/ligament.	Interfacial bonding with tissues (Bioactive Fixation)	Bioactive glasses Bioactive glass-ceramics HA
Ceramics and glasses that are designed to be placed by the bone slowly and are able to dissolve in the powder or solid form	Replacement with tissues	Tricalcium phosphate Bioactive glasses

2.3.2.2 Inert/Semi Inert Materials/Substances

2.3.2.2.1 Alumina, Alumina has been used in orthopaedic surgery for nearly 20 years as it is able to biologically co-exist perfectly; it has a low breakability coefficient and corrosion rate.

Tribologic features of alumina can be achieved when the grains have the small and narrow dimension distribution. If the grains are wide, there can be regional disintegration.

Other clinical applications of alumina are dentures, bone screws, teeth roof and the replacement of the disintegrated teeth.

2.3.2.2.2 Zirconia, Zirconia ceramics are called as polymorphic as they are subject to many transformations while they are being cooled down to the room temperature in the state of melting. Zirconia includes three well defined polymorphies: monoclinic, tetragonal and cubic, high pressure orthorhombic forms.

SSZ (semi- stabilized zirconia) is the compound of cubic, tetragonal and/or monoclinic phases. TZP (tetragonal zirkonia polycrystalline) is 100% tetragonal. Both SSZ and TZP are ideal for surgical implant applications.

Resistance and breakability hardness of the TZP ceramics is 2 times higher than that of the alumina ceramics that are used in the bio-medical sector. This makes zirconia headspieces which will be connected to metal parts less sensitive against stress.

2.3.2.3 Porous Ceramics

The advantage of a ceramic implant with pores is the mechanical stability of the interface formed at the size of the bone in the pores of the ceramic. Prosthesis limits the use of the porous ceramics with low resistance in the surface applications due to their mechanical requirements. The studies indicate that inert porous ceramics are functional implants in the cases where load carrying is not a basic need.

2.3.2.3.1 Calcium-phosphate Bio-ceramics, Bioceramics with calcium phosphate have been used in the medicine and dental industry for nearly 20 years. Its applications are in the dentures, treatment of dental diseases, orthopaedic, and surgery of jawbone and the treatment of middle ear. Different phases of Ca-P ceramics are used depending on whether the material used is of the melting type or bioactive.

Mechanical features of Ca-P phases affect their use as implant at a significant extent. Their pulling and pressing resistance and exhaustion resistance depends on the total volume of porosity. The porosity can be very small (micro-pores) or macrospores. Mechanisms and properties are described in a later chapter.

2.3.2.3.2 Porcelain, For the opaque, weak and porous-structured ceramic to be used in the dentistry it is compounded with minerals such as caolonesilica and feldspat. This material, which includes these important compounds, is called porcelain.

Porcelain powders can be collected under 3 groups in terms of the melting degree of the porcelain powders:

a) High temperature porcelain
b) Medium temperature porcelain
c) Low temperature porcelain

High temperature porcelain is preferred to others in important constructions as it is opaque, sound and able to protect the model with all details during the cooking period. It provides successful results in the inlay, jackets, kern and bridge prosthesis. In the porcelain powders, all the compounds should be of the required quality and opacity. In order to ensure this, a process, which is called as fritage, is applied. In this process, the temperature of the compounds is increased and thus first combustion is achieved. The material is washed to free the porcelain from the unwanted substances. It is swaged until it becomes a very thin powder. It is served to the dentists and laboratories in the form of special boxes of powders of different colours, colour-changing powders, opaque porcelain powder and basic opaque porcelain powder including enamel and dentin colours.

First colour of the porcelain is white and it is opaque. The colours obtained do not change event when it is diluted or it is under high temperatures. Pigments are metal oxides that are cooked with the compound of porcelain. The appropriate porcelain white can be obtained by adding zircon, soil with clay and silica.

2.3.2.4 Properties of Bioceramics

Bioceramics can be divided into three classes;

a) **Bioinert Ceramics**
b) **Bioactive Ceramics**
c) **Biodegradable Ceramics**

a) Bioinert Ceramics:

Bioinert materials do not cause any response from their host. This is usually because they do not chemically react with the local chemicals due to the fact that the bioinert materials have already reacted with another substances. As a result cells can live adjacent to the material but do not form a bond with it. The most important bioceramics are alumina and zircon.

Properties of bioinert ceramics can be listed as follows:

- High Density
- High Purity
- Optimum Compressive Strength
- High Corrosion Resistance
- High Wear Resistance
- High Fatique Resistance
- Low Porosity
- Simple Manufacturing
- High Biocompability
- High Bending Strength.

b) Bioactive Ceramics

A bioactive material undergoes chemical reactions in the body, but only at its surface. Thus, a bioactive material that elicits a specific biological response at the

interface of the material, which results in the formation of a bond between tissues and the material. The most important bioactive ceramics are hydroxyapatite and glass ceramics.

Properties of bioactive ceramics, which addition to bioinert ceramics properties, are:

- Low Elasticity Modulus
- Low Ductility
- High Biodegeneration Resistance
- Low Friction Factor
- High Resistance for pH changes

c) Biodegradable Ceramics

Refers to the materials degrade in the body while they are replaced by regenerating of natural tissue.

2.3.2.5 Advantages of Bioceramics to Other Materials

Bioceramics offer many advantages compared to other materials;

- Harder Than Materials
- More heat and corrosion resistant than metals or polymers
- Less dense than most metals and their alloys
- Their raw materials are both plentiful and inexpensive

The components of several metallic biomaterials have been indicated as causing an undesirable response in the human body that is similar to heavy metal poisoning

Cobalt chromium → growth cancer cells

Nickel → causes skin irritation and inflammation

Cobalt → Anaemia

Chromium → Damage nervous system and causes Ulcer

Aluminium → Alzheimer and Epilepsy

As a result of these, bioceramics have an important place in medicine because of their developing properties.

2.3.3 Polymers

Polymers are long-chain molecules that consist of a number small repeating unit. The repeat units or "mers" differ from the small molecules, which were used in the original synthesis procedures, the monomers, in the loss of unsaturation or the elimination of a small molecule such as water or HCl during polymerization. The exact difference between the monomer and the mer unit depends on the mode of polymerization.

The wide variety of polymers includes such natural materials as cellulose, starches, natural rubber, and deoxyribonucleic acid (DNA), the genetic material of all living creatures. While these polymers are undoubtedly interesting and have seen widespread use in numerous applications, they are sometimes eclipsed by the seemingly endless variety of synthetic polymers that are available today.

The task of the biomedical engineer is to select a biomaterial with properties that most closely match those required for a particular application. Because polymers are long-chain molecules, their properties tend to be more complex than their short-chain counterparts. Thus, in order to choose a polymer type for a particular application, the unusual properties of polymers must be understood (Visser et al., 1996).

2.3.3.1 Classes of Polymers Used in Medicine

Many types of polymers are used for biomedical purposes. Figure 2.2 illustrates the variety of clinical applications for polymeric biomaterials. This section discusses some of the polymers used in medicine.

Poly(methylmethacrylate) (PMMA) is a hydrophobic, linear chain polymer that is glassy at room temperature and may more easily recognized by such trade names as Lucite or Plexiglas. It has very good light transmittance, toughness, and stability, making it a good material for intraocular lenses and hard contact lenses.

Soft contact lenses are made from the same family of polymers, with the addition of a CH_2OH group to the methyl methacrylate side group, resulting in 2-hydroxyethyl methacrylate (HEMA). The additional methylol group causes the polymer to be hydrophilic. For soft contact lenses the poly(HEMA) slightly cross-linked with ethylene glycol dimethylacrylate EGDM) to prevent the polymer from dissolving when it is hydrated (Rodriguez, 1982). Fully hydrated, it is a swollen hydro gel.

Polyethylene (PE) is used in its high-density form in biomedical applications because low-density material cannot withstand sterilization temperatures. It is used in tubing for drains and catheters, and in very high-molecular-weight form as the acetabular component in artificial hips. The material has good toughness, resistance to fats and oils, and a relatively low cost.

Polypropylene (PP) is closely related to PE and has high rigidity, good chemical resistance, and good tensile strength. Its stress cracking resistance is superior to that of PE, and it is used for many of the same applications as PE.

Polytetrafluoroethylene (PTFE), also known as Teflon, has the same structure as PE, except that the hydrogen in PE is replaced by fluorine. PTFE is a very stable polymer, both thermally and chemically, and as a result it is very difficult to process.

It is very hydrophobic and has excellent lubricity. In microporous (Gore-Tex) form, it is used in vascular grafts.

Polyvinylchloride (PVC) is used mainly in tubing in biomedical applications. Typical tubing uses include blood transfusion, feeding, and dialysis. Pure PVC is a hard, brittle material, but with the addition of plasticizers, it can be made flexible and soft. PVC can pose problems for long-term applications because the body can extract the plasticizers. While these plasticizers have low toxicities, their loss makes the PVC less flexible.

Polydimethylsiloxane (PDMS) is an extremely versatile polymer. It is unique in that it has a silicon-oxygen backbone instead of a carbon backbone. Its properties are less temperature sensitive than other rubbers because of its lower T_g. PDMS is used in catheter and drainage tubing, in insulation for pacemaker leads, and as a component in some vascular graft systems. It is used in membrane oxygenators because of its high oxygen permeability. Because of its excellent flexibility and stability, it is also used in a variety of prostheses such as finger joints, blood vessels, heart valves, breast implants, outer ears, and chin and nose implants (Rosato, 1983).

Polymerization of bisphenol A and phosgene produces polycarbonate, a clear, tough material. Its high impact strength dictates its use as lenses for eyeglasses and safety glasses, and housings for oxygenators and heart-lung bypass machine.

Nylon is the name given by Du Pont to a family of polyamides. Nylons are formed by the reaction of diamines with dibasic acids or by the ring opening polymerization of lactams. Nylons are used in surgical sutures.

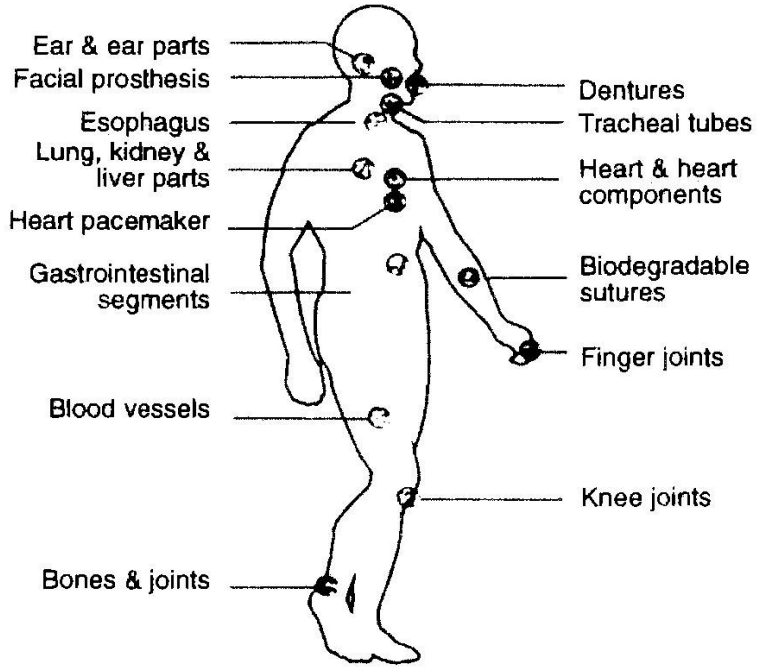

Ear & ear parts: acrylic, polyethylene, silicone, poly(vinyl chloride) (PVC)
Dentures: acrylic, ultrahigh molecular weight polyethylene (UHMWPE), epoxy
Facial prosthesis: acrylic, PVC, polyurethane (PUR)
Tracheal tubes: acrylic, silicone, nylon
Heart & heart components: polyester, silicone, PVC
Heart pacemaker: polyethylene, acetal
Lung, kidney & liver parts: polyester, polyaldehyde, PVC
Esophagus segments: polyethylene, polypropylene (PP), PVC
Blood vessels: PVC, polyester
Biodegradable sutures: PUR
Gastrointestinal segments: silicones, PVC, nylon
Finger joints: silicone, UHMWPE
Bones & joints: acrylic, nylon, silicone, PUR, PP, UHMWPE
Knee joints: polyethylene

Fig. 2.2 Common clinical applications and types of polymers used in medicine. (From D. V. Rosato, in *Biocompatible Polymers, Metals*, and types of polymers used in medicine, Technomic Publ., 1983, p. 1022)

2.3.4 Composites

The word "composite" means, "consisting of two or more distinct parts". At the atomic level, materials such as metal alloys and polymeric materials could be called composite materials in that they consist of different and distinct atomic groupings. At the microstructural level (about 10^{-4} to 10^{-2} cm), a metal such as a plain-carbon steel containing ferrite and pearlite could be called a composite material since the ferrite and pearlite are distinctly visible constituents as observed in the optical microscope.

At the molecular and microstructural level, tissues such as bone and tendon are certainly composites with a number of levels of hierarchy.

In engineering design, a composite material usually refers to a material consisting of constituents in the micro to macro size range, favouring the macro size range. Composites can be considered to be materials consisting of two or more chemically distinct constituents, on a macro scale, having a distinct interface separating them. This definition encompasses the fibre and particulate composite materials of primary interest as biomaterials. Such composites consist of one or more discontinuous phases embedded within continuous phase. The discontinuous phase is usually harder stronger than the continuous phase and is called the reinforcement or reinforcing material, whereas the continuous phase is termed the “matrix”.

The properties of composites are strongly influenced by the properties of their constituent materials, their distribution, and the interaction among them. The properties of a composite may be the volume fraction sum of the properties of the constituents, or the constituents may interact in a synergistic way owing to geometric orientation to provide properties in the composite that are not accounted for by a simple volume fraction sum. Thus, in describing a composite material, besides specifying the constituent materials and their properties, one needs to specify the geometry of the reinforcement, its concentration, distribution, and orientation.

Most composite materials are fabricated to provide mechanical properties such as strength, stiffness, toughness, and fatigue resistance. Therefore, it is natural to study together the composites that have a common strengthening mechanism. This mechanism strongly depends upon the geometry of the reinforcement. It is quite convenient to classify composite materials on the basis of the geometry of a representative unit of reinforcement. Figure 2.3 shows a commonly accepted classification scheme.

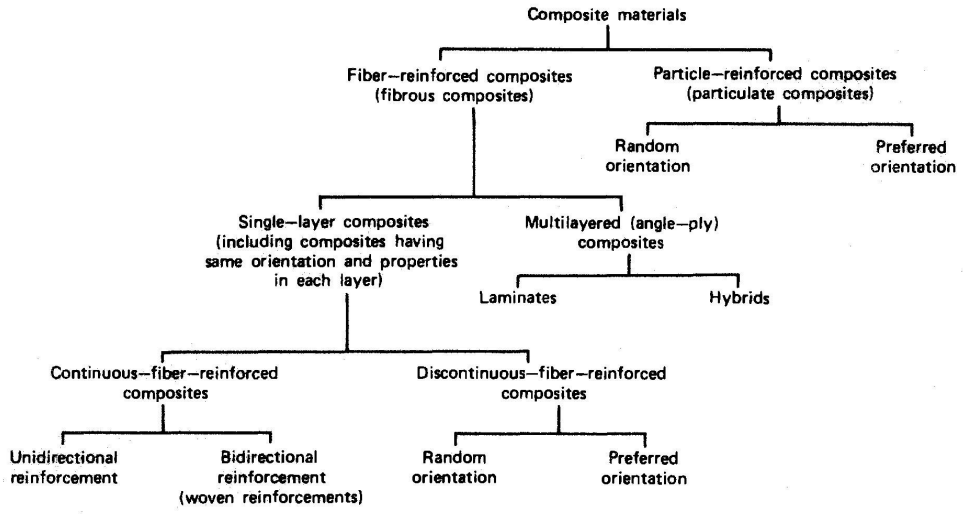

Fig 2.3 Classification of composite materials (Ratner et al., 1996)

With regard to this classification, the distinguishing characteristic of a particle is that it is nonfibrous in nature. It may be spherical, cubic, tetragonal, or other regular or irregular shapes, but it is approximately equiaxial. Its length being much greater than its cross-sectional dimensions characterizes a fibre. Particle-reinforced composites are sometimes referred to as particulate composites. Fibre-reinforced composites are, understandably, called fibrous composites.

In addition to the classic engineering concerns regarding composites, biomedical composites have other unique properties that affect their performance. As with all biomaterials, the question of biocompatibility (tissue response to the composite) is paramount among them. Being composed of two or more materials, composites carry an enhanced probability of causing adverse tissue reactions. Also, the fact that one constituent (the reinforcement) usually has dimensions on the cellular scale always leaves open the possibility of cellular ingestion of particulate debris that can result in either the production of tissue lysing enzymes or transport into the lymph system. One class of composites, absorbable composites, overlay additional requirements for degradation rate kinetics, binding between matrix and reinforcement and biocompatibility of degradation products.

2.3.4.1 Reinforcing Systems

The main reinforcing materials that have been used in biomedical composites are carbon fibres, polymer fibres, ceramics, and glasses. Depending upon the application, the reinforcements have been either inert or absorbable.

2.3.4.1.1 Carbon Fibre, Carbon fibre for biomedical use is produced from polyacrylonitrile (PAN) precursor fibre in a three-step process: (1) stabilization, (2) carbonization, and (3) graphitization. In the stabilization stage, the PAN fibres are first stretched to align the fibrillar networks within each fibre parallel to the fibre axis, and then they are oxidized in air at about 200-220°C while held in tension. The second stage in the production of high-strength carbon fibres is carbonization. In this process, the stabilized PAN-based fibres are pyrolyzed (heated) in a controlled environment until they become transformed into carbon fibres by the elimination of O, H, and N from the precursor fibre. The carbonization heat treatment is usually carried out in an inert atmosphere in the 1000-1500°C range. During the graphitization process, turbostratic graphite like fibrils or ribbons are formed within each fibre, greatly increasing the tensile strength of the material.

In recent years, carbon fibre has been recognized as a biocompatible material with many exciting applications in medicine. Several commercial products have used carbon fibre as a reinforcing material to enhance the mechanical properties of the polymeric resin systems in which it is included used to reinforce porous poly tetra fluor ethylene for soft tissue augmentation and as a surface coating for the attachment of orthopaedic implants. It has also been used to reinforce ultra high molecular weight (UHMW) polyethylene used as a bearing surface in total joint prostheses, as a tendon and ligament repair material, to reinforce fracture fixation devices, and to reinforce total joint replacement components.

2.3.4.1.2 Polymer Fibres, For the majority of applications, polymer fibres are not strong or stiff enough to be used to reinforce other polymers. The possible exceptions are aramid fibres, UHMW polyethylene fibres, and certain fibres that have been used tor their absorbability, not their mechanical superiority. Aramid is the

generic name for aromatic polyamide fibres. Aramid fibres were introduced commercially under the trade name Kevlar. Kevlar composites are used commercially where high strength and stiffness, damage resistance, and resistance to fatigue and stress rupture are important. Potential biomedical applications are in hip prostheses stems, fracture fixation devices, and ligament and tendon prostheses. UHMW polyethylene fibres have recently become available. To date, these fibres have not seen extensive use in biomedical composites. Bulk UHMW polyethylene demonstrates excellent biocompatibility. However, there are preliminary data suggesting a less favourable response to UHMW polyethylene fibres. Questions are always raised when bulk and fibre properties are equated. While in theory the basic materials should be the same, differences associated with surface characteristics and the details of manufacturing and processing can be significant.

Absorbable polymer fibres have been used to reinforce absorbable polymers in fabricating fully absorbable fracture fixation systems. Polylacticacid polymer and polyglycolicacid polymer have been used for this purpose. Both of these polymer fibres have been used for a number of years in absorbable sutures. More recently, they have also been utilized as scaffolds for cellular support in experimental hybrid implants that combine synthetics with living cells.

2.3.4.1.3 Ceramics, Several different ceramic materials have been used to reinforce biomedical composites. Since most biocompatible ceramics, when loaded in tension or shear, are relatively weak and brittle materials compared with metals, the preferred form for this reinforcement has usually been particulate. These reinforcements have included various calcium phosphates, aluminium and zinc based phosphates, glass and glass ceramics, and bone mineral. Minerals in bone are numerous. In the past, bone has been defatted, ground, and calcined or heated to yield a relatively pure mix of the naturally occurring bone minerals. It was recognized early that this mixture of natural bone mineral was poorly defined and extremely variable. Consequently, its use as an implant material was limited.

The calcium phosphate ceramic system has been the most intensely studied ceramic system. Of particular interest are the calcium phosphates having calcium to

phosphorus ratios of 1.5-1.67. Tricalcium phosphate and hydroxyapatite form the boundaries of this compositional range. At present, these two materials are used clinically for dental and orthopaedic applications. Tricalcium phosphate has a nominal composition of $Ca_3(PO_4)_2$. The common mineral name for this material is whitlockite. It exists in two crystallographic forms, α- and β- whitlockite. In general, it has been used in the β form.

The ceramic hydroxyapatite has received a great deal of attention. Hydroxyapatite is, of course, the major mineral component of bone. The nominal composition of this material is $Ca_{10}(PO_4)_6(OH)_2$. Some investigators have suggested that may be a direct bonding of synthetic hydroxyapatite with host bone. Most researchers agree that both tricalcium phosphate and hydroxyapatite are extremely compatible materials. This is particularly true when the materials are contact with bone. This, of course, is not surprising since both materials display an apatitic surface structure.

2.3.4.1.4 Glasses, Glass fibres are used to reinforce plastic matrices in forming structural composites and moulding compounds. Commercial glass fibre-plastic composite materials have the following favourable characteristics: high strength to weight ratio; good dimensional stability; good resistance to heat, cold, moisture, and corrosion; good electrical insulation properties; ease of fabrication; and relatively low cost. Most of these reasons for using glass fibre reinforcement are not relevant to biomedical composites; consequently, conventional glass fibre reinforcement is not generally practiced. However, recently Zimmerman *et al.* (1991) and Lin (1986) introduced an absorbable polymer composite reinforced with an absorbable calcium phosphate glass fibre. This allowed the fabrication of a completely absorbable composite implant material. Commercial glass fibre produced from a lime-aluminium-borosilicate glass typically has tensile strength of about 3 GPa and a modulus of elasticity 72 GPa. Lin (1986) estimates the absorbable glass fibre to have a modulus of 48 GPa, which compares favourably with the commercial fibre. The tensile strength, however, was significantly lower-approximately 500 MPa.

2.3.4.2 Matrix Systems

Biomedical composite have been fabricated with both absorbable and nonabsorbable matrices. The most common matrices are synthetic nonabsorbable polymers. However, natural polymers and calcium salts have all been used. By far the largest literature exists for the use of poly sulfone, ultra high molecular weight (UHMW) polyethylene, polytetrafluoroethylene, poly(etheretherketone), and poly (methyl methacrylate). These matrices, reinforced with carbon fibres and ceramics, have been used as prosthetic hip stems, fracture fixation devices, artificial joint bearing surfaces, artificial tooth roots, and bone cements.

Absorbable composite implants can be produced from absorbable α-polyester materials such as polylactic and polyglycolic polymers. Previous work has demonstrated that for most applications, it is necessary to reinforce these polymers to obtain adequate mechanical strength. Poly(glycolicacid) (PGA) was the first biodegradable polymer synthesized (Frazza and Schmitt, 1971). It was followed by polylacticacid (PLLA) and copolymers of the two (Gilding and Reed, 1979).

These α-polyesters have been investigated for use as sutures and as implant materials for repairing a variety of osseous and soft tissues. Important biodegradable polymers developed in recent years include polyorthoesters (POEs), synthesized by Heler and co-workers, and a new class of biodegradable dimethyl-trimethylene carbonates (DMTMCs). A good review of absorbable polymers by Barrows (1986) included PLA, PGA, polylactide-coglycolide, polydioxanone, polyglycolide-cotrimethylenecarbonate, polyethylenecarbonate, polyiminocarbonates, polycaprolactone, polyhydroxybutyrate, polyaminoacids, polyesteramides, polyorthoesters, polyanhydrides, and cyanoacrylates.

Absorbable polymers of natural origin have also been utilized in biomedical composites. Purified bovine collagen, because of its biocompatibility, resorbability, and availability in a well-characterized implant form, has been used as a composite matrix, mainly as a ceramic composite binder. A commercially available fibrin adhesive and calcium sulphate have similarly been used for this purpose.

CHAPTER THREE
HYDROXYAPATITE

3.1 A Short History of Hydroxyapatite

Successful repair of a bony defect with a calcium phosphate reagent, described, as "triple calcium phosphate compound" was first reported by Albee in 1920. A half a century later, Levitt et al., in 1969 and Monroe et al., in 1971 described a method of preparing a ceramic apatite from mineral fluoarapatite, $Ca_{10}(PO_4)_6F_2$ and suggested the possible use of this apatite ceramic in dental and medical applications. Clark et al., and Hubbard described methods of preparing calcium phosphate ceramics from commercially available calcium phosphate reagents. However, these ceramics were not appropriately characterized so that was described as "tricalciumphosphate" or TCP ceramic in the first clinical application reported by Nery et al., was actually a mixture of beta-tricalcium phosphate (β-TCP, $Ca_3(PO_4)_6$), and hydroxyapatite [HA, $Ca_{10}(PO_4)_6(OH)_2$]. (LeGeros, 1988)

In the mid-seventies, three groups: Jarcho et al. in USA, deGroot et al. and Denison in Europe and Aoki et al. in Japan simultaneously but independently worked towards the development and commercialization of hydroxyapatite (HA) more accurately, calcium hydroxyapatite, as a biomaterial for bone repair, augmentation and described as "hydroxyapatite" and followed the observation reported in the early seventies by Hench of a "chemical bonding" of bone with a bioactive glass ceramic through a calcium phosphate-rich layer.

HA can be prepared as dense or as macroporous forms, with pores as large as 500μ. Dense HA is described as having a maximum microporosity of 5% by volume with the micropores measuring about 1 μm in diameter and consisting of crystals with size exceeding 2000 Å. This chapter will attempt to provide basic information on the general properties of pure HA and biological apatites and then discuss the processing, composition, properties, surface chemistry, tissue response and clinical application of HA (Denissen, et al., 1985).

3.2 General Structure and Properties of HA

The term apatite describes a family of compounds having similar structures but not necessarily having identical compositions. Hence, apatite is a description and not a composition. HA, is a compound of a definite composition $Ca_{10}(PO_4)_6(OH)_2$, and a definite crystallographic structure. The structure of HA, showing the exact atomic positions in the crystal, was determinated by Beevers and Melntyre from a mineral and later refined by Kay et al. with a synthetic HA. HA belongs to the hexagonal system, with a space group, $P6_3/m$. This space group characterized by a six-fold c-axis perpendicular to three equivalent a-axes (a_1, a_2, a_3) at angles 120° to each other. (Young, et al., 1966) The smallest building unit, known as the unit cell, contains a complete representation of the apatite crystal, consisting of Ca, PO_4, and OH groups closely packed together in an arrangement shown in Fig. 3.1.

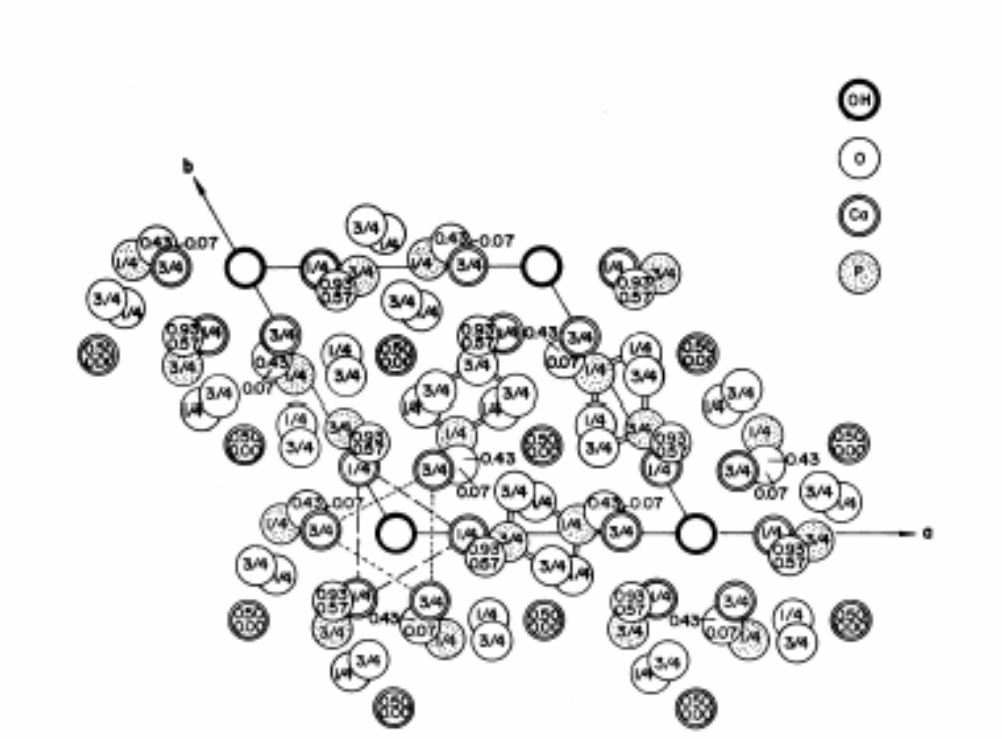

Fig. 3.1 The atomic arrangement of HA, in a hexagonal unit cell. The OH ions located in the corners of the unit-cell are surrounded by two groups of Ca (II) atoms arranged in a triangle positions at z = 0.25 and at 0.75; by two groups of PO_4 tetrahedra also arranged in triangle positions; and by a hexagonal array of Ca(I) atoms at the outermost distance

The ten calcium atoms belong to either Ca(I) or Ca(II) subsets depending on their environment. Four calcium atoms occupy the Ca(I) positions, two at levels z = 0 and two at z = 0.5. Six calcium atoms occupy the Ca(II) positions: one group of three calcium atoms describing a triangle located at z = 0.25, the other group of three at z = 0.75, surrounding the OH groups located at the corners of the unit cell at z = 0.25 and z = 0.75, respectively (Fig 3.2).

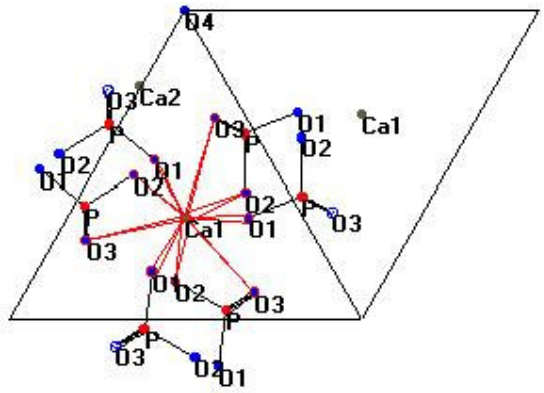

Fig 3.2 The upper side appearance of HA cell structure

The six phosphate (PO_4) tetrahedra are in a helical arrangement from levels z = 0.25 to z = 0.75. The network of PO_4 groups provides the skeletal framework, which gives the apatite structure its stability (Fig. 3.3). The oxygens of the phosphate groups are described as one O_1, one O_2, and two O_3. The atomic arrangements of F-apatite, $Ca_{10}(PO_4)_6F_2$, and of Cl-apatite, $Ca_{10}(PO_4)_6Cl_2$, in which fluoride (F) and chloride (Cl), respectively, substituted for the OH groups in the apatite structure, are similar. The F or Cl atoms substituted for OH differ in the respective position of the OH for which they substitute. The O-H, F and Cl atoms lie along the c- axis at the centre of the Ca (II) triangles. Fig 3.4 shows the O_4 structures in the HA cell.

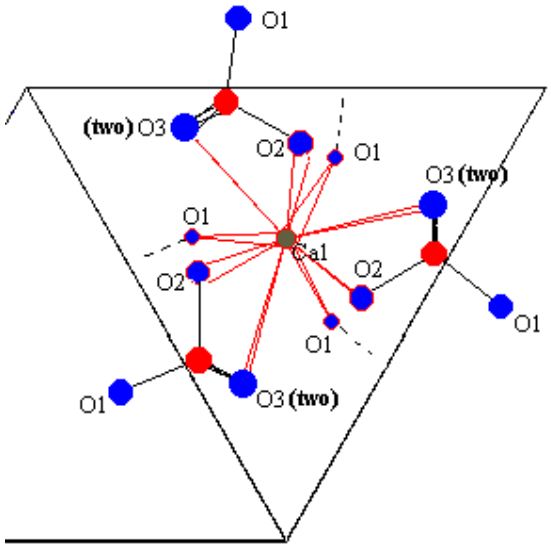

Fig. 3.3 The upper side of HA cell and PO_4 structures

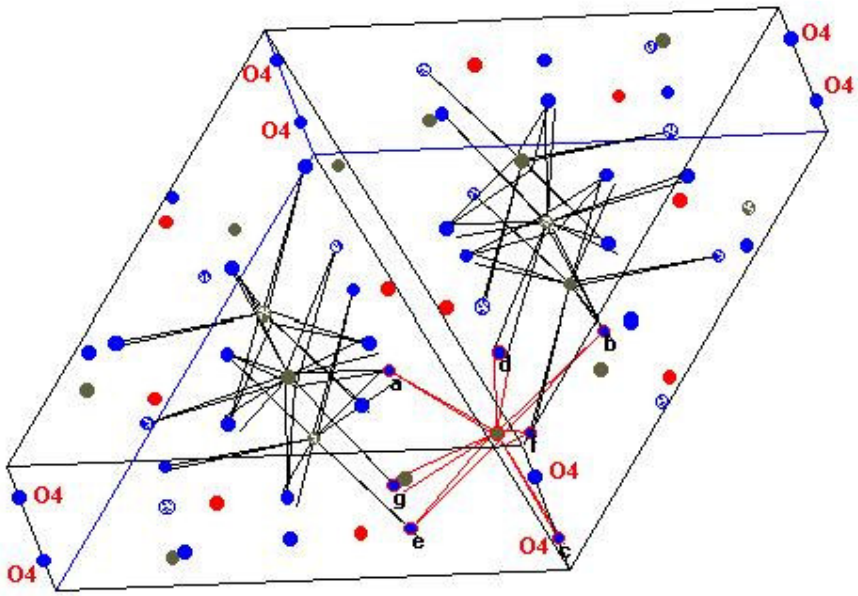

Fig. 3.4 The O_4 structures in a HA cell

The apatite structure is very hospitable one allowing the substitutions of many other ions. Substitutions in the apatite structure for (Ca), (PO_4) or (OH) groups result in changes in properties: e.g. lattice parameters (Table 3.1), morphology, solubility, without significantly changing the hexagonal symmetry. However, Elliot and Young showed that Cl substitution causes the loss of hexagonal symmetry and exhibits monoclinic symmetry because of the alternating positions of the Cl atoms and an enlargement of the cell in the b direction. For example, substitution of F for OH, cause a contraction in the a-axis dimensions without changing the c-axis (Table 3.1), is usually associated with an increase in the crystallinity, reflecting increase in crystal size (and/or decrease in crystal strain); and imparts greater stability to the structure. Fig. 3.5 shows the cell structure of HA.

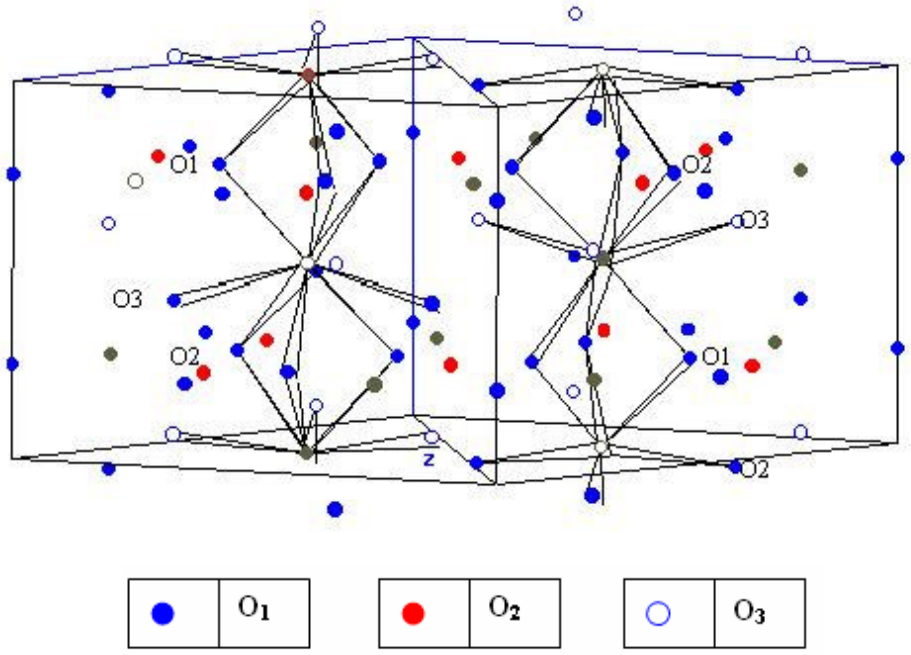

Fig. 3.5 Structure of the HA cell

Table 3.1 Lattice parameters of mineral, synthetic and biological apatites

Apatite	**Major substitutent**	**Lattice Parameters**	**(+0.003 Å)**
Mineral			
OH Apatite (Holly Springs)	-	9.422	6.880
F-apatite (Drungo, Mex)	F	9.375	6.880
Dahllite (Wyoming)	CO_3	9.380	6.885
Staffelite (Staffel, Germany)	CO_3, F	9.345	6.880
Marine phosphorite (w. USA)	CO_3, F	9.322	6.882
Synthetic (Non-aqueous)			
OH apatite	-	9,441	6.882
F-apatite	F	9.375	6.880
Cl-apatite	Cl	9.646	6.771
CO_3 apatite	CO_3	9.544	6.859
Synthetic (Aqueous)			
OH apatite (Ca-deficient)	HPO_4	9.438	6.882
F-apatite	F	9.382	6.880
(Cl, OH)-apatite	Cl	9.515	6.858
CO_3-OH apatite	CO_3	9.298	6.924
CO_3-F-apatite	CO_3, F	9.268	6.924
Sr-apatite	Sr	9.739	6.913
Pb-apatite	Pb	9.894	7.422
Ba-apatite	Ba	10.162	7.422
Biological			
CO_3-OH-apatite (human enamel)	HPO_4, Cl, CO_3, Mg	9.441	6.882
F-apatite (Shark enameloid)	F, CO_3, HPO_4	9.382	6.880

Carbonate can substitute either for the hydroxyl (OH) or phosphate (PO_4) groups; designed as Type A or Type B substitutions, respectively. These two types of substitution have opposite effects on the lattice parameters, a-axis and c-axis dimensions (Table 3.1). In the case of Type A, the substitution of larger planar CO_3 group for smaller linear OH group, cause an expansion in the a-axis and contraction in the c-axis dimensions, while for Type B, the substitution of smaller planar CO_3 group for a larger tetrahedral PO_4 group, cause a contraction in the a-axis and expansion in the c-axis dimensions compared to the CO_3-free apatites. LeGeros and co-workers also demonstrated that the coupled CO_3-for PO_4 and Na-for-Ca substitution cause changes in the size and shape of the apatite crystal: from acicular crystals to rods to equi-axed crystals with increasing carbonate content; and in dissolution properties: the CO_3 substituted apatite being more soluble than CO_3 free synthetic apatites (LeGeros et al., 1983).

Other ions to which the apatite structure may play host include: strontium (Sr), magnesium (Mg), barium (Ba), lead (Pb), etc. for calcium; vanadates, borates, manganates, etc., substituting for phosphate. Differences in lattice parameters between substituted and unsubstituted HA reflect the size and amount of the substituting ions (Table 3.1). Various substitutions in the apatite besides those of F-or-Cl for-OH or CO_3- for-OH or CO_3-for-PO_4 mentioned above, also affect properties, e.g., crystallinity, thermal stability, and dissolution properties or solubility of the apatite crystals. Sr-for-Ca or Mg-for-Ca substitution causes an increase in the extent of dissolution of the apatite. When simultaneously present, the substituents in the apatite structure can have synergistic or antagonistic effects on the properties of the apatite. For example, magnesium and carbonate have synergistic effects on the crystallinity and dissolution properties of synthetic apatites; magnesium and fluoride or carbonate and fluoride have antagonistic effects, the fluoride effect being the more dominant one (LeGeros et al., 1984).

A comprehensive understanding of both the individual effects of substituents in the structure on the properties of apatite is important to the development of substituted HA as new biomaterials and to an improved understanding of the interaction between bone mineral and the HA materials presently used for bone

repair, augmentation, substitution and coatings of metal dental and orthopaedic implants.

3.3 Biological Apatites

Biological apatites, which comprise the mineral phases of calcified tissues (enamel, dentin, bone) and of some pathological calcifications (e.g., human dental calculi, salivary and urinary stones), are usually referred to as calcium HA meaning [$Ca_{10}(PO_4)_6(OH)_2$]. Actually, the biological apatites differ from pure HA in stoichiometry, composition, and crystallinity and in other physical and mechanical properties. Biological apatites are usually calcium-deficient and are always carbonate substituted. It is therefore more appropriate that biological apatites be referred to as carbonate apatite and not as HA. The carbonate in biological apatites substitutes primarily for the phosphate groups in a coupled manner, i.e., Ca-for-Na, CO_3-for-PO_4, referred to as a Type B substitution. The coupled substitution is necessary to balance charges for the substitution of a CO_3 (divalent) for PO_4 (trivalent). Biological apatites of enameloids of some species of fish of shark enameloid are substituted with F and CO_3. Other minor elements, e.g., Na and F and some trace elements (e.g., stroncium, lead, barium, etc.) are associated with biological apatites and may be substituents in the apatite structure, as described below;

$$(Ca, M)_{10}(PO_4,CO_3,Y)_6(OH,F,Cl)_2 \quad (1)$$

where M represents other minor (e.g., Magnesium, Sodium, Potassium, etc.) and trace elements (e.g., Sr, Pb, Ba); Y represents acid phosphate, HPO_4^{2-}, sulphates, borates, vanadates, etc. Some of these minor and trace elements may be surface- rather than lattice-bound. Lattice bound elements will contribute to changes in lattice parameters: surface elements, will not, but contribute the changes in crystal properties (Glimeher, 1984).

The biological apatites of enamel differ from those of dentin or bone in crystallinity and in the concentration of the minor elements, carbonate and

magnesium and have the largest crystal size compared to either dentin or than bone apatites. In terms of dissolution properties, enamel apatite is less soluble than dentin or bone but much more soluble than dense HA which is prepared at high temperature as ceramic HA. The difference in crystal size and in dissolution properties among enamel, dentin and bone may be attributed in part to the differences in the carbonate and magnesium concentrations. Magnesium and carbonate have been shown to cause a decrease in crystallinity and an increase in the extent of dissolution of synthetic apatites (LeGeros et al., 1983).

Biological apatites of human enamel, dentin and bone also give different end products after sintering above 800 °C reflecting the differences in their composition and calcium deficiencies. Sintering enamel and dentin apatites above 800 ^{0}C give HA and small amounts of β-TCP (about 5 wt % in enamel and about 12 wt % in sintered dentin). The substituted β-TCP phase is magnesium-substituted as determined from lattice parameters and chemical analyses and is therefore sometimes referred to as β-TCMP. Sintering human bone apatite above 800 °C gives mainly HA and minor amounts of CaO. Sintering enamel, bone or dentine apatite results in changes in crystal morphology, crystallinity, and composition. Morphologically, the enamel apatite crystals changed in shape from smaller acicular to large hexagonal or rhombohedral crystals. Compositional changes in biological apatites include the loss of CO_3 and the formation of Mg-substituted β-TCP phase. The formation of the β-TCP after heat treatment of enamel and dentin and calcium-deficient synthetic apatites is attributed to the HPO_4 content of the apatite before sintering. Sintered animal bones result in the formation of β-TCP (Mg-substituted) or CaO depending on the age and specie of the animals (LeGeros et al., 1991).

3.4 Composition of HA

Pure HA, $[Ca_{10}(PO_4)_6(OH)_2]$, has the theoretical composition of 39.68 wt % Ca, 18.45 wt % P, Ca/P wt ratio, 2.151, Ca/P molar ratio of 1.667. Dense HA materials, commercial or non-commercial, vary in Ca/P ratios reflecting the β-TCP/HA ratios in the sintered material which in turn reflect the purity (whether consisting of only the apatite phase or mixed with other Ca-P phases); and/or composition or calcium

deficiency of the apatite preparation before sintering. If the Ca/P is 1.67, only HA will be observed in the X-ray diffraction and infrared spectrum; if the Ca/P is lower than 1.67, β-TCP and other phases such as tetra calcium phosphate, TTCP, CaP_2O_9, or $Ca_4(PO_4)_2O$ will be present with the HA phase in the sintered material, depending on the temperature and condition of sintering. If Ca/P is higher than 1.67, CaO will be present with the HA phase. In addition, there will be minor and trace elements from in the original reagents used to prepare the apatite powder. Some of the commercial and non-commercial dense HA materials contain up to 10 wt % β-TCP mixed with HA. According to ASTM designation: F 1185-88, 1990 Annual Book of ASTM Standards, Section 13, (82) the acceptable composition for commercial HA is a minimum of 95 % HA, as established by x-ray diffraction analyses, and the acceptable concentration of trace elements is limited (maximum ppm) as follows: As=3, Cd=5, Hg=5, Pb=30; total heavy metals (as lead) = 50. The HA is to be associated with less than 5 wt % β-TCP.

The purity, composition and the particle size of the apatite preparation before sintering, the sintering temperature and conditions (e.g. with or without water pressure present) also affect the type and amount of other calcium phosphate phases and/or other calcium compounds which will be present with the HA phase. Many of the inter-relationships of these factors are described by the phase diagrams of deGroot et al. Reported sintering temperatures for commercial and non-commercial HA range from 950 to 1500 °C. In this temperature range, the following calcium phosphates can form with or without the additional calcium oxide phase: β-TCP, α-TCP (resulting from the transformation of β-TCP at temperatures above 1300 °C), TTCP, and oxyapatite according to the reaction outlined below:

$$\underset{\text{Ca-deficient AP}}{\text{“Apatite” preparation (AP)}} \xrightarrow[>900\ ^{\circ}C]{} \underset{\text{HA}}{Ca_{10}(PO_4)_6(OH)_2} + \underset{\beta\text{-TCP}}{Ca_3(PO_4)_2} \qquad (2)$$

$$\beta\text{-TCP} \xrightarrow[>1100\ ^{\circ}C]{} \alpha\text{-TCP} \qquad (3)$$

$$\underset{\text{HA}}{Ca_{10}(PO_4)_6(OH)_2} \xrightarrow[>1100\ ^{\circ}C]{} \underset{\alpha\text{-TCP}}{2Ca_3(PO_4)_2} + \underset{\text{TTCP}}{Ca_4(PO_4)_2O} \qquad (4)$$

$$\underset{\beta\text{-TCP}}{Ca_3(PO_4)_2} + CaO \xrightarrow[>1400\ ^{\circ}C]{} \underset{\text{TTCP}}{Ca_4(PO_4)_2O} \qquad (5)$$

Apatite prepared from highly alkaline solution in the presence of air may often contain CO_3 and can form CaO and HA upon sintering above 900 ^{0}C, TTCP can also result from the reaction between β-TCP and CaO.

Another calcium phosphate compound reported to form with HA upon sintering the apatite preparation above 900 °C is dicalcium phosphate anhydrous, DCP, $CaHPO_4$. However, DCP is not stable at these temperatures, transforming instead to β-TCP and calcium pyrophosphate, $Ca_2P_2O_7$. If sintering is with water vapour pressure of about 500 mm Hg, the formation of the other Ca-P phases (β- and α-TCP, TTCP) will be minimized and HA will be the more stable phase. Thus the Ca/P molar ratio of the apatite preparation, sintering temperature and conditions determine the final composition of the dense HA. Comparisons of Ca/P molar ratios of several commercial HA ceramics reported values ranging from 1.57 to 1.70 (Fisher, et al., 1987).

The composition of dense HA is appropriately determined by using X-ray diffraction (XRD), infrared spectroscopy (IR) and chemical analyses.

XRD determines, the purity (whether single or multiphase); crystallinity of the HA phase, approximate ratios of the other phases (e.g. α- and β-TCP or TTCP or CaO with HA phase); and the lattice parameters of the HA and other phases.

Infrared spectroscopy gives information to support XRD data to detect additional phases, indicate relative crystallinities, and provide evidence of substituents (e.g. CO_3, F).

3.5 Properties of HA

3.5.1 Crystallographic Properties

Powdered HA (from dense or macroporous forms) gives an XRD pattern characterized by diffraction peaks with small line broadening, $B_{1/2}$, and high intensities indicating a high degree of crystallinity similar to mineral OH apatite (Hench, 1982). Lattice parameters (a-and c-axis dimensions) are 9.422 and 6.881 + 0.003 Å, similar to mineral HA. Other crystalline phases, e.g. β-TCP, α-TCP, TTCP, and CaO can be detected with X-ray diffraction when present above 1 wt %. Ceramic HA crystals are large and assume rhombic shapes compared to the much smaller acicular apatite crystals before sintering at IR absorption spectrum.

Daculsi et al. reported for the first time the presence of hexagonal parallelepiped (void type) lattice defects in addition to other defects structure in crystals of ceramic HA sintered at 950 °C but not in those prepared at 1250 °C. It may be logical to assume that the differences in the amount and types of lattice defects could cause differences in reactivity in vivo; the material with more lattice defects would be expected to be more reactive than material with fewer lattice defects. This could explain the observations reported by Niwa et al., (1980) that materials sintered at lower temperatures were more reactive than those sintered at higher temperature.

3.5.2 Mechanical Properties

The properties of the apatite powder and the compression and sintering conditions influence the mechanical properties of the dense HA. Several mechanical properties (compressive strength, etc.) were shown to decrease with increasing amount of microporosity. The density, grain size, compressive, flexural, torsional and dynamic torsional strengths, and modules of elasticity in compression and bending increased with sintering temperature from 1150 to 1350 °C. The facture toughness for HA

ceramic sintered from 1100 to 1150 °C increased but no significant change was observed for HA ceramic sintered from 1150 to 1250 °C. At sintering temperatures above 1250 °C the fracture toughness drops down to a value lower than the value obtained for HA sintered at 1100 °C. In addition, the presence of β-TCP also causes a decrease in fracture toughness. The difference in values of mechanical properties has also been attributed to differences in the preparation of apatite powder. The difference in preparation methods causes difference in grain size (small grain size tends to give greater fracture toughness) and in composition. Table 3.2 shows some important mechanical properties of HA.

Table 3.2 Mechanical properties of HA

Modulus of Elasticity (GPa)	**4.0–117**
Compress Strength (MPa)	**294**
Bending Strength (MPa)	**147**
Hardness (Vickers, GPa)	**3.43**
Poisson Ratio	**0.27**
Density (theoretical, g/cm^3)	**3.16**

3.5.3 Dissolution Properties

In vitro dissolution of HA depends on the type and concentration of the buffered or unbuffered solutions: pH of the solution, degree of saturation of the solution, solid/solution ratio, the length of suspension in the solutions, and the composition and crystallinity (reflecting crystal size and strain) of the HA. In case of ceramic HA, degree of micro- and macro- porosities, defect structure and the amount and type of other phases present also have significant influence. The extent of dissolution of the

HA ceramic was less in lactic acid buffer compared to that in acetic acid buffer. For HA ceramic containing other calcium phosphate phases, the extent of dissolution will be affected by the type and amount of the non-HA phases (Kent et al., 1983). The extent of dissolution decreases in the following order:

$$TTCP>>\alpha\text{-}TCP>>\beta\text{-}TCP>>HA \quad (6)$$

3.5.4 Surface Properties

The surface chemistry of HA ceramic will depend on the composition of the ceramic and on the composition and pH of the solution in the microenvironment. An acid environment will cause partial dissolution of the surface enriching the population of Ca^{2+}, $H_2PO_4^-$, HPO_4^{2-}, PO_4^{3-}, H^+, OH, and ion pairs such as $CaH_2PO_4^+$, and $CaOH^+$ in a hydrate layer. Biological apatites have also been described as having a hydrated layer with ions reflecting the composition of the bone mineral and the biological fluid. In vivo, electrolytes from the biological fluids will also be part of the surface chemistry and will contribute to the development of surface charges on the HA implant. The surface charges will influence cellular interactions interface. Ducheyne et al. reported that the absolute values of zeta potential measured were higher for the unsintered and Ca-deficient apatite compared with those of ceramic and stoichiometric HA and suggested that these values affect the cellular activities involved in bone formation (Ducheyne et al., 1992).

In addition, proteins will absorb on modified HA surfaces, a phenomenon well known in the use of apatite for column chromatography. The relationship of specific functional groups of amino acids to the formation of biological apatites and eventual mineralization has been strongly suggested in studies on mineral organic matrix interactions (Gorbunoff, 1984).

3.6 Hydroxyapatite Coatings on Type 316L SS

The dominant requirements connected with the development of HA coatings on metallic implants are preparation of stoichiometric powder material with required chemical and phase composition established by their chemical identity (Ca/P ratio 1.67) and by close crystallographic affinity with bone tissue and their deposition as coatings without the presence of non-stoichiometric phases of the powder (Sridhar, 2001). A number of novel methods (Sridhar et al., 1997) for coating HA have been proposed offering the potential for better control of film structure such as hot isostatic pressing, flame spraying, ion beam deposition, laser ablation and electrochemical deposition along with plasma spraying which has been widely studied over the decade. The major problems associated with plasma spraying process are that it is a line of sight process that produces non-uniform coating with heterogeneous structure and the high temperature involved alters the HA and metal substrate phases. Hence, electrophoretic deposition of HA on metal substrates has been used to overcome the above drawbacks and to achieve the uniform distribution of fine HA deposits. The advantages of this technique include high purity of layers formed, ease of obtaining the desired thickness and high layer adhesion to the substrate. Hence, it is advantages to attempt to develop thin layers of HA on the surface of type 316L SS by electrochemical deposition and to studying their electrochemical properties for applications as orthopaedic devices.

Plasma spray has been the commercial method for coating on titanium implant surfaces. The major problem of this procedure, however, is the decomposition and phase transformation of HA during the spray coating processes (Yankee, et al., 1990). Another issue of concern is the poor adhesion of the plasma-sprayed HA coating to titanium substrate (Yip, et al., 1997). Furthermore, plasma spray is difficult in microstructure control and modification.

High velocity oxy-fuel (HVOF) spray is expected to be a promising technique for HA coating deposition because it can deposit HA with similar set of advantages that plasma spraying can without the debilitating phase transformations, especially with decreased amorphous calcium phosphate (ACP) content, following thermal

decomposition of HA. Despite the advantage of controlling the microstructure compared to plasma spray technique, high temperature makes this technique no useful.

Laser ablation technique has also place of the commercial HA coatings. High crystallinity, high density and low implant dissolubility are the advantages of this method. On the other hand, high cost and high temperature are the important disadvantages, which become this technique nonviable.

Sol-gel technique is available for the low temperature usages. Oxidizing agents, which the solution includes, help decomposition of the organics. Setting the amount of the additives causes to control the stoichiometric ratio of the Ca/P (1.67). Although this method has like these advantages, it also has some disadvantages such that; delamination, fracture failure, and bacterial infection.

The failure of the implants is mainly due to the incorporated carbonate, crack formation, interfacial stresses, large change in surface morphology, fracture failure, delamination and bacterial infection. Hence, better methods of deposition are required. The current processes and remained issues are listed in Table 3.3.

Among several methods for preparing HA coating, electrochemical deposition using aqueous electrolyte containing Ca and P bearing has attracted considerable attention for a decade because it was claimed to have a variety of advantages for the coating fabrication, such as low process temperature, the ability to deposit uniform coatings on bodies of complex shape, the simple of deposit thickness, and high purity to a degree. However, the drawbacks remains for this technique in terms of lower adhesion strength compared to plasma spray method. Also the mechanism of electrodeposition for HA onto the substrate has not been fully clarified (Zhang, et al., 1998).

Current work on the electrochemically deposited HA has been focused on applying cathodic potential and current at ambient temperature and elevated temperatures in several solutions containing Ca^{2+} and PO_4^{3-}. However HA is

accompanied with other unstable calcium phosphate and the enhancement about the adhesion strength on various substrate is still a challenge. The knowledge effect of temperature, the duration of the process and various electrochemical deposition processes on composition and morphology are still not fully established.

Table 3.3 Current HA coating processes and remained issues

Existing coating processes	Remained issues
Plasma spray	Heterogeneous structure
	Poor adhesion
	Difficult in microstructure control
	High temperature process
Laser Ablation	Crack formation
	Incorporated carbonate
	OH deficient
	Interfacial stress
	High temperature process
HVOF	OH deficient
	Poor adhesion
	Delamination
	High temperature process
Sol-gel	Variable composition
	Fracture failure
	Delamination
	Bacterial infection
Electrophoretic Deposition	Selection of solvents and additives
	Solubility of the binder
	Viscosity of the suspension
	Electrical resistivity of the suspension
Electrochemical Deposition	Low adhesion
	Impurity of HA due to design of EC control
	Poor mechanical property
	Lack of knowledge in kinetics
	Post-deposition process required

Cathodic polarisation is to be carried out for coating substrate in solutions Ca^{2+} and PO_4^{3-} to determine the current applied to deposition the coatings. The cathodic reactions can be expressed into three stages:

- Stage 1: Oxygen reduction

$$O_2 + 2H_2O + 4e^- \rightarrow 4OH^- \quad (1)$$

- Stage 2: Reduction of $H_2PO_4^-$ and HPO_4^{2-}

$$2H_2PO_4^- + 2e^- \rightarrow 2HPO_4^{2-} + H_2 \quad (2)$$

$$2HPO_4^{2-} + 2e^- \rightarrow 2PO_4^{3-} + H_2 \quad (3)$$

- Stage 3: Water reduction

$$2H_2O + 2e^- \rightarrow H_2 + 2OH^- \quad (4)$$

Therefore, positive Ca^{2+} ions migrated to cathodic alloy substrate and could react with PO_4^{3-} and OH^- ions formed on alloy surface to synthesise HA. Since DCPD ($CaHPO_4 \bullet 2H_2O$) can be formed due to reaction 2, the current density control for deposition processes is of extreme importance to have purely HA formed with and without pores. Parameters such as temperature and pH will also be controlled during the process.

CHAPTER FOUR
ELECTRO CHEMICAL DEPOSITION PROCESS

4.1 A Short History of Electrodeposition

The early history of electrodeposition of precious metals onto lesser metal can be reliably traced back to around 1800. Italian chemist and university professor Luigi Brugnatelli is considered by many as the first person to utilize gold in the electroplating process. Brugnatelli was a friend of Allisandro Volta, who had just discovered the chemical principles that would later lead to the development of "voltaic" electrical batteries. Volta's first practical demonstration of this was called a "Voltaic Pile". As a result, Brugnatelli's early work using voltaic electricity enabled him to experiment with various metallic plating solutions. By 1805, he had refined his process enough to plate a fine layer of gold over large silver metals. In a letter to the Belgian Journal of Physics and Chemistry later reprinted in Great Britain, Brugnatelli wrote: "I have lately gilt in a complete manner two large silver medals, by bringing them into communication by means of a steel wire, with a negative pole of a voltaic pile, and keeping them one after the other immersed in ammoniated of gold newly made and well saturated".

Unfortunately, a falling out with the French Academy of Sciences, the leading scientific body of Europe, prevented any of Brugnatelli's important work from being published in the scientific journals of his day. His work remained largely unknown outside of Italy, except for a small group of close associates.

From the early 1800's to about 1845, two main commercial processes for coating objects in gold were utilized. For low costs, immersing an object in a diluted form of gold chloride solution (water gilding) allowed a very thin flash of gold to be deposited onto inexpensive objects. For objects where durability and value were required, a dangerous process utilizing mercury amalgam and gold leaf (fire gilding) was the main technique for achieving a thick, durable gold plate over a surface.

By 1839, scientists in Great Britain and Russia had independently devised metal deposition processes similar to Brugnatelli's, for the copper electroplating of printing

press plates. By 1840, this discovery was adapted and refined by Henry and George Elkington of Birmingham, England for gold and silver plating. Collaborating with partner John Wright, and his innovative formulas for potassium cyanide plating baths, the Elkington's were able to secure the first viable patents for gold and silver electroplating.

Struggling at first to commercialize their patented processes, the Ellington's met stiff resistance from the traditional Sheffield plate manufacturers. Unable to license their patents, they later would set up their own respective factories to produce plated silverware, spectacle frames, gift novelties and numerous other low cost plated items. They were so successful in adapting their processes that they soon dominated the decorative metals industry in their region.

From Great Britain, the electroplating process for gold and silver quickly spread throughout the rest of Europe and later to the United States. In France, electroplated decorative objects were readily accepted by upper society to display their affluence and fashion sense.

In Russia, large scale gold plating for cathedral domes, icons and religious statues were being successfully completed. Electroplating baths and equipment based on the patents of the Elkingtons were scaled up to accommodate the plating of numerous large scale objects. Eventually the electroplating process largely displaced the use of old techniques such as mercury amalgam gold gilding and water gilding.

As knowledge of electrochemistry broaden and its relationship to the electrodeposition process became more widely known, other types of non-decorative metal plating would soon be developed. Electrodeposition processes for bright nickel, brass, tin, and zinc were adapted for commercial purposes by the 1850's. Many of these types of plating were utilized for specific manufacturing and engineering applications. As the industrial age and financial capital expanded form Great Britain to the rest of the world, electrodeposition processes would find more usages in the manufacturing of goods and services.

Despite the expansion of electrodeposition processes to other industries, no significant scientific developments were discovered until the emergence of the electronics industry in the mid-1940. With the exception of some technical improvements to direct current (D.C.) power supplies, the period from 1870 to 1940 was a quiet period, characterized by gradual improvements in manufacturing processes, anodic principles and plating bath formulas.

The late 1940's witnessed the rediscovery of heavy gold plating for electronic components. By the mid-1950's, the utilization of new and safer plating baths based on acid formulas, began to displace some of the traditional cyanide based formulas in large scale commercial use.

The 1970's led to numerous regulatory laws for waste water emissions and disposal that set the direction for the electroplating industry for the next 30 years. Improvements in chemical formulas and technical hardware allowed for the rapid and continuous plating of wire, metal strips, semiconductors and complex metal shapes.

Today, chemical developments and a greater understanding of their underlying electrochemical principles, have led to sophisticated plating bath formulas. Greater control over the working characteristics, layer thickness, and performance of electroplated finishes are being achieved. New chemical developments have enabled greater plating speed, throwing power and high quality reliable plated finishes. The electrodeposition of exotic materials such as platinum, ruthenium and osmium are now finding broader usages on electronic connectors, circuit boards and contacts. Many experts believe that the expansion of the telecommunication industry will be increasingly dependent on new and innovative electrodeposition technology. The electronics industry and the need to support the expansion of their underlying infrastructure continue to drive improvements worldwide in the electroplating industry.

Future progress in waveform technologies for D.C. power supplies may lead to even greater achievements for the electrodeposition and metal finishing industry. In addition, safer "closed loop" manufacturing processes and wastewater recycling will

continue to reduce work related exposure to harmful chemicals and waste by products.

Electrodeposition processes for all types of decorative and technical plating applications will continue to find new applications as manufacturing capabilities expand into emerging global markets. (www.artisanplating.com)

4.2 What is Electrochemical Deposition?

When a metallic salt is dissolved in water it dissociates to form positively charged ions. The solution that contains these charged ions is referred to as an electrolyte or a plating solution. By passing a sufficient amount of electric current through this electrolyte, one can reduce the metal ions to form solid metal. This process is most commonly referred to electroplating or electrochemical deposition. (Schlesinger et al., 2000)

Electroplating is often also called "electro chemical deposition", and the two terms are used interchangeably. As a matter of fact, "electroplating" can be considered to occur by the process of electro chemical deposition. Electro chemical deposition is the process of producing a coating, usually metallic, on a surface by the action of electric current. The deposition of a metallic coating onto an object is: achieved by putting a negative charge on the object to be coated and immersing it into a solution, which contains a salt of the metal to be deposited (in other words, the object to be plated is made the cathode of an electrolytic cell). The metallic ions of the salt carry a positive charge and are thus attracted to the object. When they reach the negatively charged object (that is to be electroplated), it provides electrons to reduce the positively charged ions to metallic form. Figure 4.1 is a schematic presentation of an electrolytic cell for electroplating a metal "M" from an aqueous (water) solution of metal salt "MA".

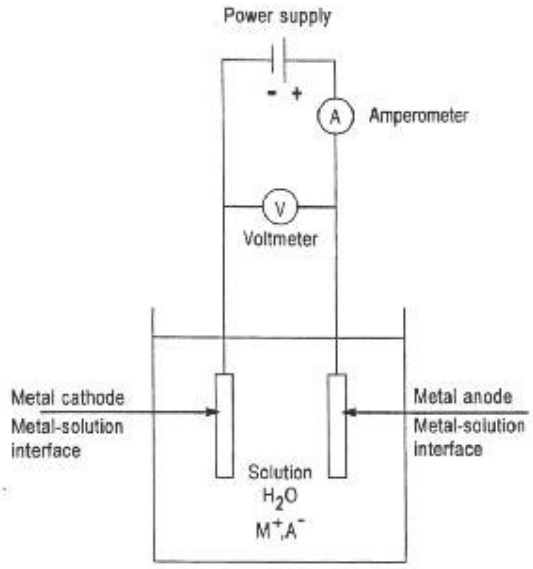

Figure 4.1 Schematics of an electrolytic cell for plating metal "M" from a solution of the metal salt "MA"

4.2.1 Theory of Electrochemical Deposition Process

Faraday's Laws state that:

1. The weight of a substance formed at an electrode is proportional to the amount of current passed through the cell.
2. The weights of different substances produced at an electrode by the same amount of current are proportional to their equivalent weights.

Equivalent weight in an oxidation-reduction reaction is the ratio of molar weight of the compound to the algebraic change in oxidation number of the atom that is oxidized or reduced. This amount of electricity, which exposes an equivalent weight, is called as 1 Faraday.

1 Faraday ~ 96500 Coulomb/mol, 1 Ampere x 1 hour = 3600 Coulomb

1 Faraday = 96500 / 3600 = 26.8 (Ampere x hour)/mol

Explaining Faraday's Law mathematically:

$m = (A \times I \times t) / (96500 \times n)$

m is the amount of material that formed at electrodes (gram), A is atomic weight (gram/mol), n is valence, I is current (ampere), t is time (second).

Based on the mass of the metal deposited, the thickness can be calculated for the objects of known surface area, because

Mass deposited = Density of the metal × Surface area × Thickness. (Paunovic et al., 1998)

4.2.2 Electrodeposition System

Electrodeposition is an extremely important technology. Covering inexpensive and widely available base materials with plated layers of different metals with superior properties extends their use to applications which otherwise would have been prohibitively expensive (Landau, 1982). However, it should be noted that electroplating is not a simple dip and dunk process. It is probably one of the most complex unit operations known because of the unusually large number of critical elementary phenomena or process steps, which control the overall process (Ettel, 1984). An excellent example is the system model from Rudzki (Figure 4.2) for metal distribution showing the interrelation of plating variables and their complexity (Rudzki, 1983). Figure 4.3 is a simplified version summarizing the factors that influence the properties of deposits. Electrodeposition involves surface phenomena, solid state processes, and processes occurring in the liquid state, thereby drawing on many scientific disciplines as shown in Table 4.1 (Landau, 1982).

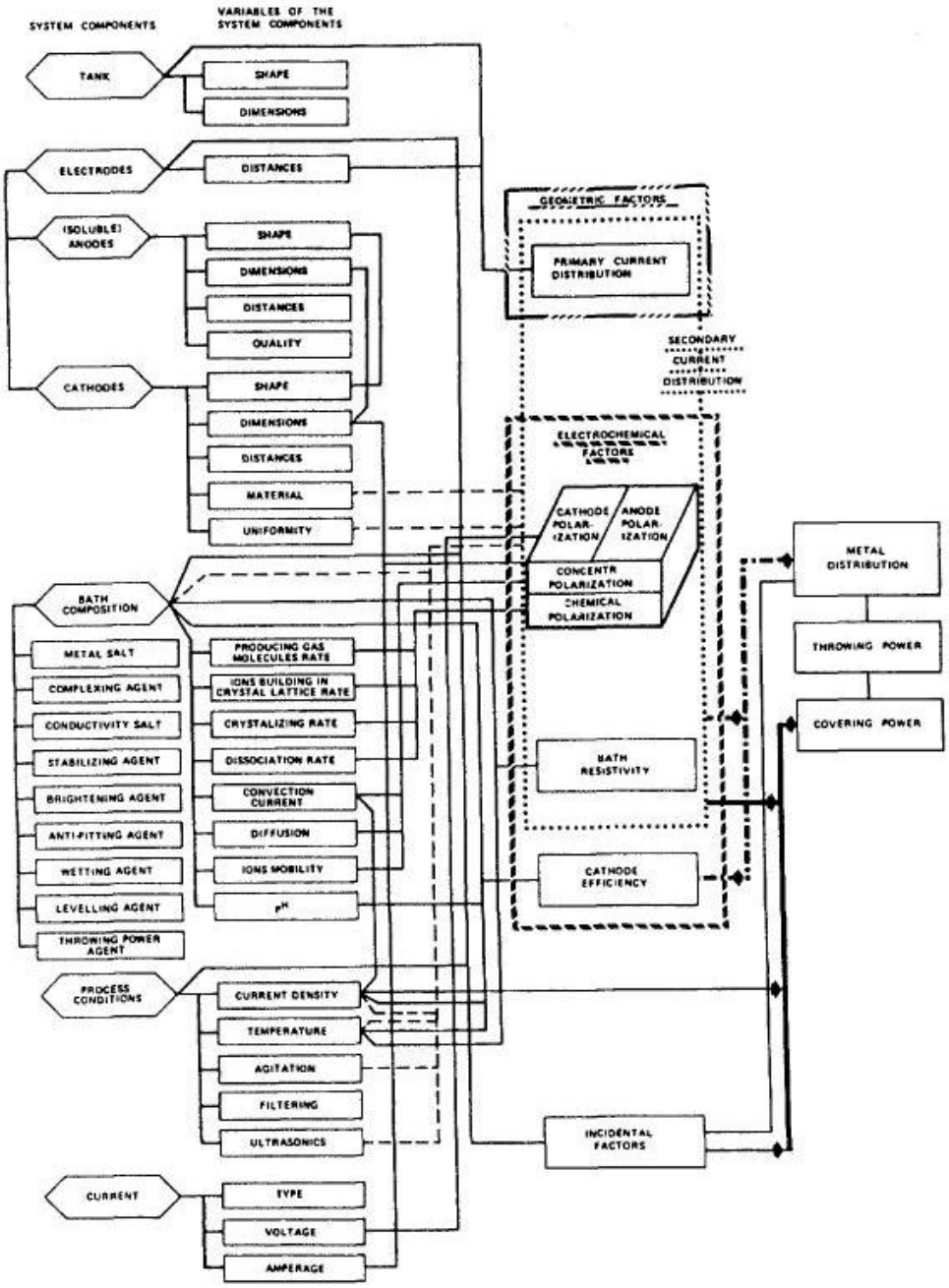

Figure 4.2 System model illustrating metal distribution relationships

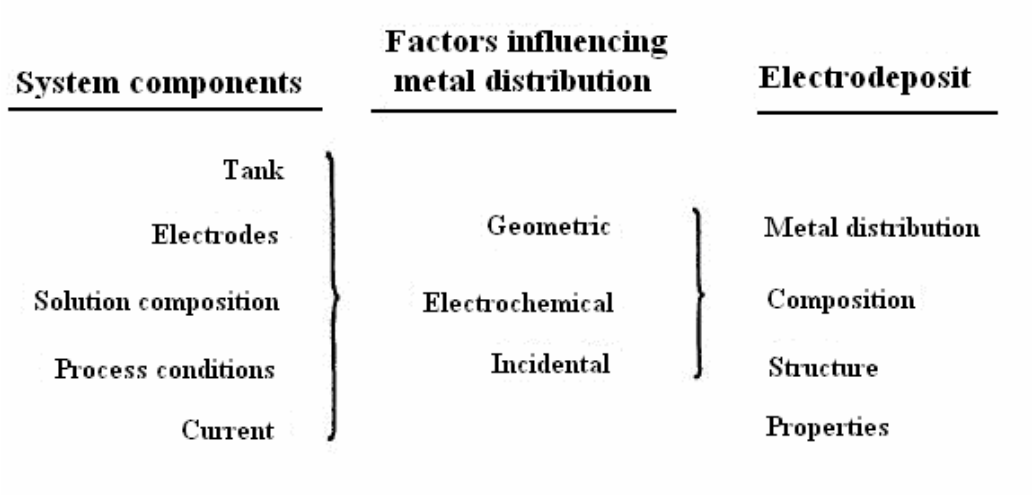

Figure 4.3 Metal distribution relationships in electrodeposition

Table 4.1 Interdisciplinary nature of electrodeposition

Discipline	Involvement
Electrochemistry	Electrode processes
Electrochemical engineering	Transport phenomena
Surface science	Analytical tools
Solid state physics	Use of quantum mechanical solid state concepts to study electrode processes
Metallurgy and materials science	Properties of deposits
Electronics	Modern instrumentation

4.2.3 Factors Affecting Coatings

It has been suggested those four different zones:

1) The substrate
2) The substrate-coating interface
3) The coating
4) The coating-environment interface

has to be considered when protecting materials with coatings (Holleck, 1986). Figure 4.4 shows these zones.

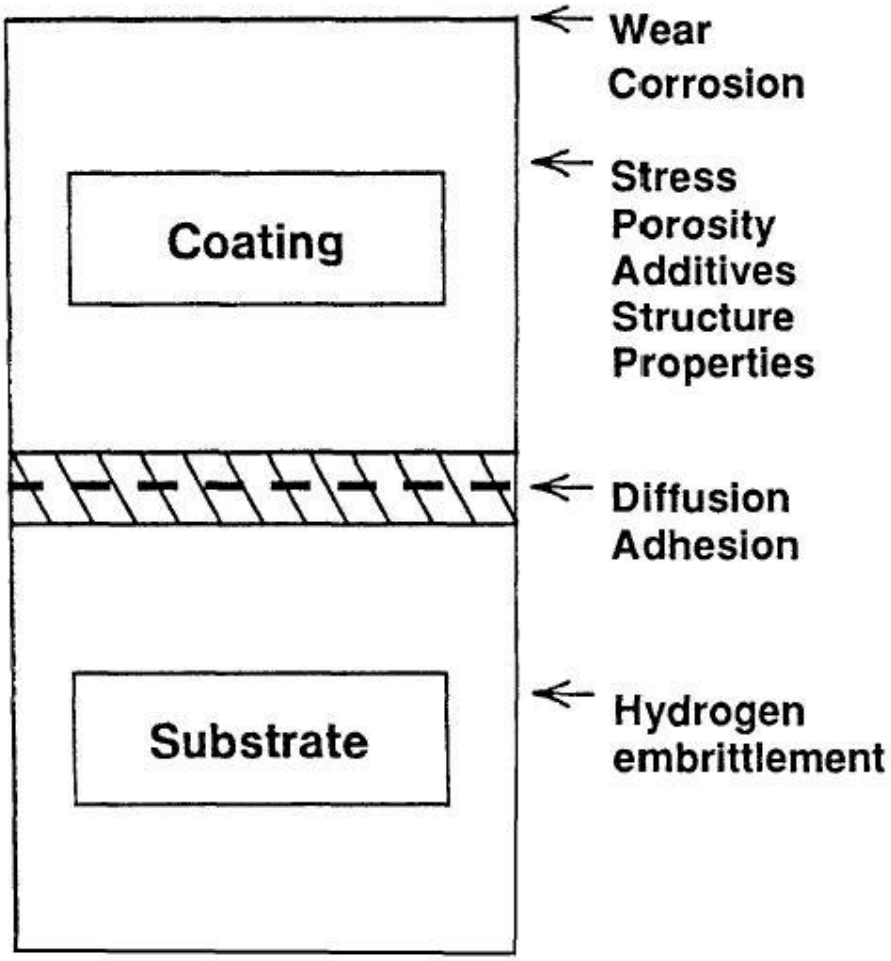

Figure 4.4 Important criteria when selecting coatings

First layer is the substrate where potential hydrogen embrittlement effects are of concern. The second zone is the basis metal interface where adhesion of the coating and interdiffusion between the coating and substrate are of importance. The third zone is the coating itself where composition and microstructure determine properties and factors such as stress; phase transformations and grain growth exert noticeable influences. The final zone is the environmental interface where the interaction of the coating in its intended application has to be considered in terms of corrosion and/or wear.

Clearly, many of the items are important in more than one zone. For example; porosity and/or stress in the substrate (rather than just in the coating) can noticeably

influence coating properties; porosity can noticeably affect corrosion resistance and tensile properties; hydrogen embrittlement is a factor not only for substrates but also for some coatings; and diffusion of codeposited alloying impurities to the surface can noticeably affect wear and corrosion properties.

Hydrogen embrittlement concentrates heavily on steels since these substrates are particularly susceptible to damage by hydrogen. Hydrogen embrittlement is a generic term used to describe a wide variety of fracture phenomena having a common relationship to the presence of hydrogen in the alloy as a solute element or in the atmosphere as a gas (Birnbaum, 1986). Nickel, titanium, aluminium (Nguyen et al., 1987) and even electroless copper deposits (Nakahara, 1983) exhibit the phenomenon. It appears that any material can become embrittled by a pressure effect if hydrogen bubbles are introduced by a means such as electrodeposition and this state remains unchanged until hydrogen atoms escape from the bubbles. In some cases, the failure can be so abrupt and forceful as to seem almost explosive (Durney, 1985).

Adhesion refers to the bond (chemical or physical) between two adjacent materials, and is related to the force required to effect their complete separation. Cohesive forces are involved when the separation occurs within one of them rather than between the two (Davies et al., 1967). The ASTM defines adhesion as the "condition in which two surfaces are held together by either valence forces or by mechanical anchoring or by both together" (ASTM D907-70). Adhesion is a macroscopic property, which depends on three factors:

1) Bonding across the interfacial region,
2) Type of interfacial region (including amount and distribution of intrinsic stresses)
3) The fracture mechanism, which results in failure (Mattox, 1978).

Equating adhesion, which is a gross effect, to bonding or cleanliness may be very misleading. Failure of adhesion may be more related to fracture mechanisms than to bonding. In thin films, the intrinsic stress may result in adhesive failure even though chemical bonding may be high. Also, the interfacial morphology may lead to easy

fracture though bonding is strong. With copper, if an acid dip prior to plating is too strong so that the etching results in the development of large areas with (111) planes constituting the surface, the subsequently deposited films may not only grow non-epitaxially, but also lose adhesion to the substrate forming an interfacial crack because of the voids (Felder et al., 1981). Good adhesion is promoted by: 1) strong bonding across the interfacial region, 2) low stress gradients, either from intrinsic or applied stress, 3) absence of easy fracture modes, and 4) no long term degradation modes. Adhesion is broken down into four categories; interfacial adhesion, interdiffusion adhesion, intermediate layer adhesion and mechanical interlocking. Processes that have been used to provide adhesion of coatings on difficult-to-plate substrates are discussed and supported with quantitative data. The relatively new approach of combining physical vapour deposition with electroplating which offers considerable promise for obtaining adherent bonds between coatings and difficult-to-plate substrates is also covered. Other techniques such as interface tailoring, alloying surface layers with metals exhibiting a high negative free energy of formation, use of partial pressure of various gases during deposition, reactive ion mixing and phase-in deposition are also discussed.

Diffusion, which is the attempt of a system to achieve equilibrium through elimination of concentration gradients, can result in degradation of properties and appearance. Diffusion mechanisms are discussed with particular emphasis placed on Kirkendall voids, which can lead to loss of adhesion. The nature of the atoms, temperature, concentration gradients, nature of the lattice crystal structure, grain size, amount of impurities and the presence of cold work influence diffusion (Nakahara, 1979). An effective way to minimize or eliminate potential diffusion problems is the use of barrier coatings. In some instances, diffusion can benefit coating applications. Examples include deposition of alloy coatings and diffusion welding which utilizes diffusion to produce high integrity joints in a range of both similar and dissimilar metals.

The properties of electrodeposits are important for a broad spectrum of applications. A fundamental concern of materials science is the relationship between structure and properties and this is true for both bulk and coated materials (Rickerby

et al., 1989). Topics include tensile property measurements, strength and ductility of thin deposits, the Hall-Petch relationship between strength and grain size, and the influence of impurities on properties. Super plasticity, which refers to the ability of a material to be stretched to many times its original length, is covered since electrodeposition offers some potential in this area.

The properties of all materials are determined by their structure. Even minor structural differences often have profound effects on the properties of electrodeposited metals (Safranek, 1986). Four typical structures encountered with electrodeposited metals include; 1) columnar, 2) fibrous, 3) fine-grained, and 4) banded (Lamb, 1968). Texture of deposits is an important structural parameter for bulk materials and coatings and a good illustration of how properties can be tailored for applications such as formability, corrosion resistance, etching characteristics, contact resistance, magnetism, wear resistance, and porosity. Fractals, which offer the materials scientist a new way to analyze microstructures, provide a new tool for studying surfaces and corrosion processes.

The use of additives in aqueous electroplating solutions is extremely important owing mainly to the interesting and important effects produced on the growth and structure of deposits. The potential benefits of additives include: brightening the deposit, reducing grain size, reducing the tendency to tree, increasing the current density range, promoting levelling, changing mechanical and physical properties, reducing stress and reducing pitting. The striking effects on electrocrystallization processes of small concentrations of addition agents, ranging from a few mg/L to a few percent but generally with an effective concentration range of 10^{-4} to 10^{-2} M, point to their adsorption on a high energy surface and deposition on growth sites, thereby producing a poisoning or inhibiting effect on the most active growth sites**.** (Schwartz, 1982)

Porosity is one of the main sources of discontinuities in electrodeposited coatings. It can noticeably enhance corrosion resistance, mechanical properties, electrical properties and diffusion characteristics. Items, which influence porosity, include the substrate, the plating solution and its operating characteristics, and post plating

treatments. An effective way to minimize porosity is to use an under plate. Another is to deposit coatings with specific crystallographic orientations, which can strongly influence covering power and rate of pore closure.

Stress in coatings can also adversely affect properties. A variety of options are available for reducing deposit stress and these include: choice of substrate, choice of plating solution, use of additives and use of higher plating temperatures. A variety of theories have been postulated regarding the origins of stress but none of them covers all situations. Numerous stress measurement techniques are available and they vary from the simple rigid strip technique to sophisticated methods using holographic interferometers.

Corrosion is affected by a variety of factors including metallurgical, electrochemical, physical chemistry and thermodynamic. Often it is difficult to separate corrosion from many of the other property issues associated with deposits. When selecting a coating it is important to know its position with respect to its substrate in the galvanic series for the intended application. Besides galvanic effects, the substrate and the interfacial zone between it and the coating can noticeably affect the growth and corrosion resistance of the subsequent coating since corrosion is affected by structure, grain size, porosity, metallic impurity content, interactions involving metallic under plates and cleanliness or freedom from processing contaminants (Frankhental, 1975). Decorative nickel-chromium coatings developed for automotive industry applications are a good example of use of materials science and electrochemistry to improve corrosion resistance properties.

Wear, like corrosion, does not fit handily within the confines of a traditional discipline. Physics, chemistry, metallurgy and mechanical engineering all contribute to this topic. A particular feature of electrodeposition that is attractive for wear applications is its low temperature processing and ability to be applied to distortion prone substrates without increasing stress in the composite. Coatings that are used for various wear applications include chromium, electroless nickel, precious metals and anodized aluminium. Recent advances include ion implantation of chromium deposits with nitrogen to provide improved wear resistance and codeposition of

dispersed particles with electroless nickel. Microlayered metallic coatings also known as composition modulated coatings also offer promise. Although electrodeposited coatings are typically not effective at temperatures above 500 °C, composite coatings containing chromium or cobalt particulates in a nickel or cobalt matrix can be effective.

CHAPTER FIVE
EXPERIMENTAL STUDIES

5.1 Purpose

Use of calcium phosphate based ceramics as biomaterials and coatings in both dentistry and orthopaedics in particular dated back to 1980s (Suchanek et al., 1998). Being one of these, Hydroxyapatite [HA; chemical formular $Ca_{10}(PO_4)_6(OH)_2$] has been extensively studied lately due to its chemical and structural similarities to naturally occurring biological apatite in hard tissues. It can not be used directly in bulk form for implant production due to its inefficient mechanical properties (Fujishiro et al., 1995). However its use as coating materials continues to be a point of interest because of its excellent biocompatibility, bioactivity, stimulating effect on bone formation onto itself (Osseo-integration) (Yu-Peng Lu, et al., 2006). CaP structures with high solubility and porosities remain to be a main problem faced in practice today (Gu et al., 2003). Besides argument is still going on at present whether the degree of crystalline structure of HA in coating layers has anything to do to promote bio-compatibility and osseo-integration.

In dealing with the shortcomings of CaP coatings, to better control the film adherence particularly, various deposition technologies, electrochemical deposition (ECD) being the first (Lin et al., 2003), have been developed. When compared to the other deposition techniques, ECD methods have several advantages and are in the most important place with high flexibility to control the coating chemistry and characteristics because of several numbers of process variables they have.

The objective of this study was to form HA coatings on 316 Stainless Steel by using electrochemical deposition technique, and investigate the wear and corrosion behaviour of these coatings. The coatings were characterised by using X-ray diffraction (XRD), scanning electron microscope (SEM) with attached energy dispersive spectroscopy (EDS), optical microscope, image analyzer, Fourier transform infrared (FTIR) spectroscopy, differential thermal analyzer/thermogravimetry (DTA/TG). Electrochemical corrosion studies were also

employed to determine the corrosion characteristics of HA coatings on Stainless Steel substrates in lactated Ringer's solution at 37 °C by using potentiostat/galvanostat. The changes in morphology and chemistry of the coatings as a result of corrosion tests were investigated by conducting characterization before and after corrosion tests. Tribological and mechanical properties of the coatings were measured by dynamic ultra micro-hardness tester, scratch tester, and friction-wear tester.

5.2 Materials

0.042 M $Ca(NO_3)_2.4H_2O$ and 0.025 M $NH_4H_2PO_4$ were used as a test solution to electrochemically deposit hydroxyapatite on 316L stainless steel, which was supplied by Sandvick Company. The chemical composition of 316L is given in Table 5.1. Corrosion behaviour of the coatings was investigated in lactated Ringer's Solution supplied by Eczacıbaşı A.Ş..

Table 5.1 Chemical composition of 316 L stainless steel

Element	C	Cr	Fe	Mo	Mn	Ni	N	Si	P	S	Cu
%	0,03	17-19	Balance	2-3	2	12-14	0,1	0,75	0,03	0,03	0,5

5.3 Production of HA Coatings

Calcium phosphate coatings have been deposited on 316L SS substrates by electrochemical method with Gamry PC-750/4 potentiostat/galvanostat. Electrochemical deposition is an attractive process because highly irregular objects can be coated relatively quickly at low temperatures. Additionally, the thickness and chemical composition of coatings can be well controlled by manipulating varieties of process parameters. HA, the most interesting form of calcium phosphates was electrochemically deposited in several solutions at different temperatures. HA formation was accompanied by other forms of unstable calcium phosphate compounds such as dicalcium phosphate dihydrite [DCPD: $CaHPO_4.2H_2O$, (Brushite)] at some of the test temperatures examined.

A three-electrode system was used in this study. The saturated calomel electrode (SCE) was the reference electrode, graphite rod was the auxiliary electrode and 316 L SS was the working electrode. Figure 5.1 shows the three-electrode system schematically.

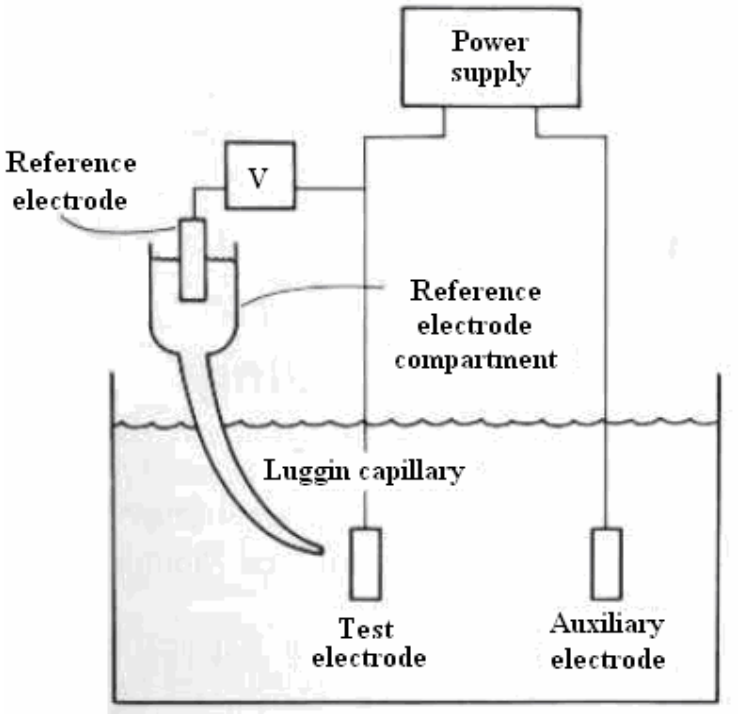

Figure 5.1 Three-electrode system equipment

Before electrodeposition, the surfaces of the 316L SS samples (with 9 mm diameter) were sandpapered in the order with 220, 400, 600, 800, 1000, 1200 with SiC abrasive papers firstly. Then these surfaces were polished to a mirror surface using 1 μ diamond paste. Later samples were rinsed with acetone in an ultrasonic bath for 15 minutes. Finally samples were washed with distilled water.

Cathodic polarization was conducted starting from open circuit potential to -3.0 V (vs. SCE electrode) at a rate of -0.5 mV/s at different temperatures. Coatings were produced potentiodynamically at various temperatures of 25, 37, 50, 60, and 70 °C. Test solution was so prepared that the molar ratio of Ca/P was 1.67. A different test solution with a molar ratio of Ca/P as 1, corresponding to the stoichiometry of Brushite was prepared, just to test out the chemical composition of the deposited film at 60 °C for comparison.

5.4 Characterization Studies

5.4.1 Solution Parameters

The rheological properties such as viscosity and shear stress of the electrolyte at various temperatures of 25, 37, 50, 60, and 70 °C were measured by Bohlin CVO 100 rheometer. The pH values were measured by a standard pH meter with Mettler Toledo electrode.

5.4.2 X-ray Diffraction (XRD)

The crystallography of the deposited, annealed, and calcinated specimens was analyzed by a Rigaku D/max-2200/PC X-ray diffractometry (XRD) with Cu Kα radiation and operated at a tube voltage of 40 kV and current of 20 mA.

5.4.3 Scanning Electron Microscope (SEM)

The surface morphology and microstructure of the coatings were observed by scanning electron microscopy (Jeol JSM-6060).

5.4.4 Energy Dispersive Spectroscopy (EDS)

The point and regional elemental analyses of the specimens' surfaces by X-ray mapping of the coatings were observed with a 500 Digital Processing (IXRF Systems, Inc.) energy-dispersive x-ray spectroscopy (EDS) attached to the SEM.

5.4.5 Fourier Transform Infrared (FTIR)

Fourier transform infrared (FTIR) spectroscopy was used to determine chemical composition of calcıum phosphate phases. The FTIR spectra were recorded by using Perkin Elmer Spectrum BX spectrometer with KBr pellet technique within the 2500-25000 nm wave length range.

5.4.6 Differential Thermal and Thermo Gravimetric Analysis (DTA/TGA)

Calcium phosphate compounds in forms of HA and Brushite in coatings and bone flour (biological HA) were examined by DTA/TGA to acquire information regarding phase transformations of the coating materials and the accompanying gravimetric changes at high temperatures. These analyses provide valuable information for process temperatures.

DTA/TGA analyses were used to optimize the heat treatment and observe the structural transformation of the CPP. DTA/TGA analyses of the powders obtained by scraping the coatings from the substrate and bone flour were conducted by using Shimadzu DTG-60H Thermo-gravimetric Analyzer at temperatures ranging 25-1000 °C (for the bone flour) and 25-600 °C (for the deposited coatings) at a heating rate of 10 °C/min.

5.4.7 Optical Microscope (with Image Analyzer Attachment)

The distribution of the crystals on the surface is an important parameter for ultra micro hardness tests. Therefore the distribution characteristics of the crystals were investigated by using Nikon ECLIPSE ME600D microscope supported with software called Lucia for image analysis.

5.5 Heat Treatment

Heat treatments applied to the coatings and bone flour were carried out by considering the DTA/TGA results. Accordingly the coatings were heated for 1 hour at 500 °C, and the bone flour was heated for 1 hour at 1000 °C.

5.6 Corrosion Tests of the Coatings

Electrochemical studies were carried out in lactated Ringer's Solution with a pH of 7,4 at 37 °C. Saturated calomel electrode (SCE) and graphite rod were used as the reference and auxiliary electrodes, respectively. The samples were immersed in the

electrolyte and the potential was monitored as a function of time with respect to SCE, until the potential reached a stable value. This stable value is called as corrosion potential or open circuit potential. Anodic polarisation was conducted under 0.1 V from open circuit potential to 3.0 V (vs. SCE electrode) at a rate of 5 mV/s.

The electrochemical studies cover the measurements of open circuit potential (OCP) and potentiodynamic polarisation. The critical parameters like corrosion potential (E_{cor}), corrosion current density (i_{cor}), and polarization resistance (R_p) were evaluated from these studies.

Porosities of the coatings were calculated by electrochemical methods using the fallowing equation (Oberlaender, 1992):

$$F = \frac{R_{p,m}}{R_p} \log\left(\frac{-|\Delta E_{cor}|}{\beta_a}\right)$$

where F is the total coating porosity; $R_{p,m}$ is the polarization resistance of the base material, R_p is the measured polarization resistance of the coated samples, ΔE_{cor} is the difference between the corrosion potentials of the surfaces without and with coating, and β_a is the anodic Tafel slope of the base material.

5.7 Mechanical Tests of the Coatings

Mechanical tests such as hardness, scratch, and wear tests were carried out on the coated samples to evaluate the mechanical integrity of the coatings.

5.7.1 Dynamic Ultra Micro Hardness (DUH)

Hardness, elastic modulus, and critical depth of the coatings were investigated by using Shimadzu DUH-W201, DUH-W201S ultra micro hardness tester. Tests conducted by this tester were performed under the load-unload test mode by applying a test force of 10 mN with a loading speed of 0,14 mN/sec. The ultimate force of 10 mN was maintained for 10 seconds.

5.7.2 Scratch

The scratch tests were conducted to evaluate the coating adhesion. Deposited specimens were scratched using SST-W101 SHIMADZU scratch tester with 2 μm/s scratch speed.

5.7.3 Wear and Friction

The wear and friction properties of the HA coatings were tested by using PLINT&PARTNERS Model TE 88 Multi Station friction-wear test machine. The coated samples with the worst and the best scratch test results were selected for the wear tests. Wear tests were done under the minimum load capacity of 49 N available on the test machine with 0.5 Hz frequency.

CHAPTER SIX
RESULTS AND DISCUSSION

6.1 Solution Characterization

Figure 6.1 shows the average values of the viscosity change as a function of increasing temperatures.

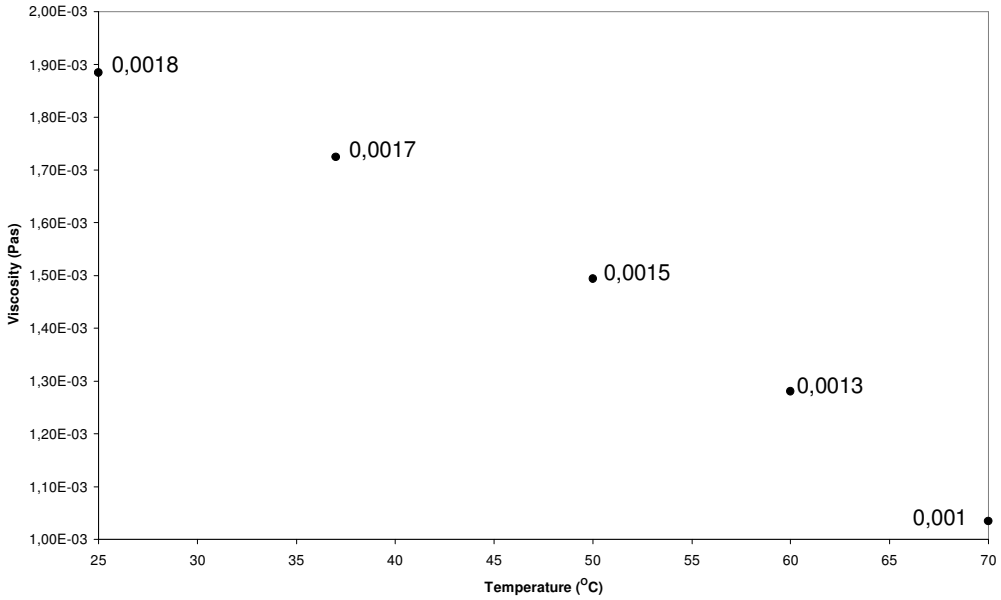

Figure 6.1 The change in average viscosities of the test solution with the Ca/P molar ratio of 1.67, as a function of temperature

As seen at the figure 6.1,viscosity decreases with increasing temperature.

Shear stress is proportionally related to the viscosity and increases with increasing viscosity. The change of shear stress at different temperatures is shown in Figure 6.2.

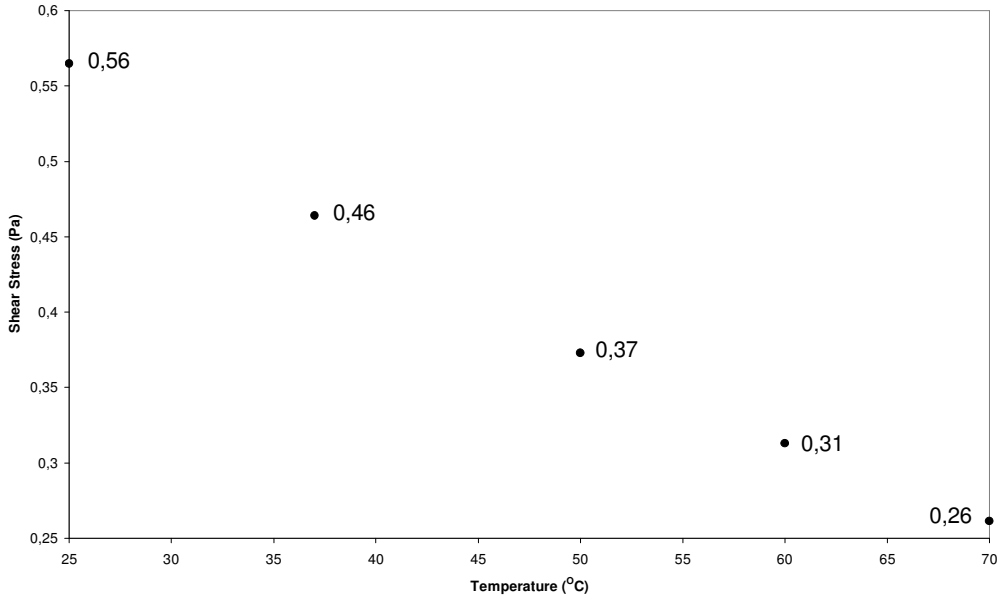

Figure 6.2 The average shear stress values of the test solution with the Ca/P molar ratio of 1.67, as a function of temperature

pH of the test solution is also an important parameter for the deposition process and decreases with increasing temperature as seen in Figure 6.3. This indicated the increasing rate of ionisation of water with increasing temperature.

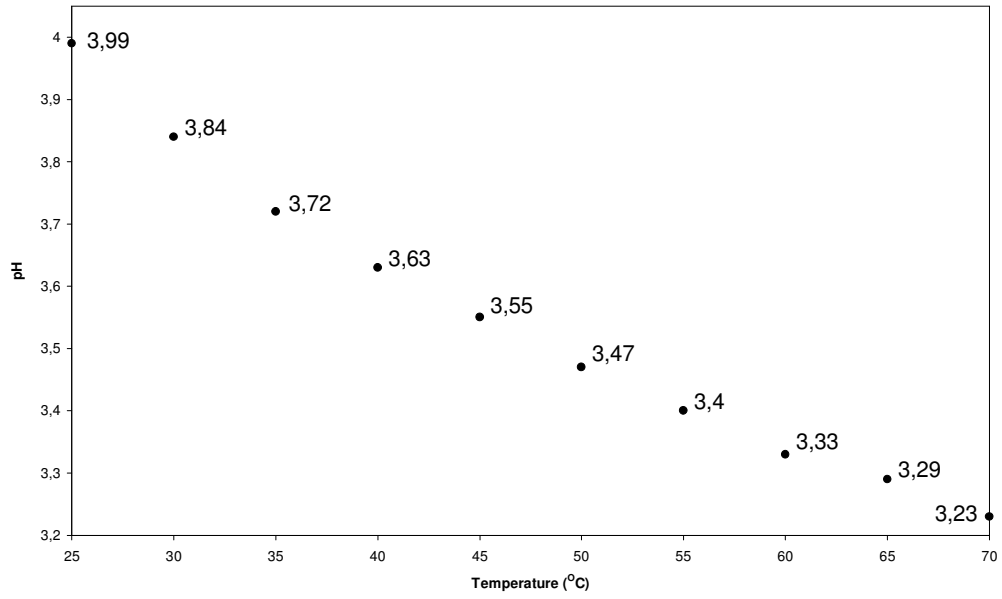

Figure 6.3 The change in pH of the test solution with the Ca/P molar ratio of 1.67, as a function of temperature

6.2 Production of the Coatings

Potentiodynamic cathodic polarization studies conducted to synthesize the electrochemically deposited coating yielded the following polarisation curves shown in Figure 6.4.

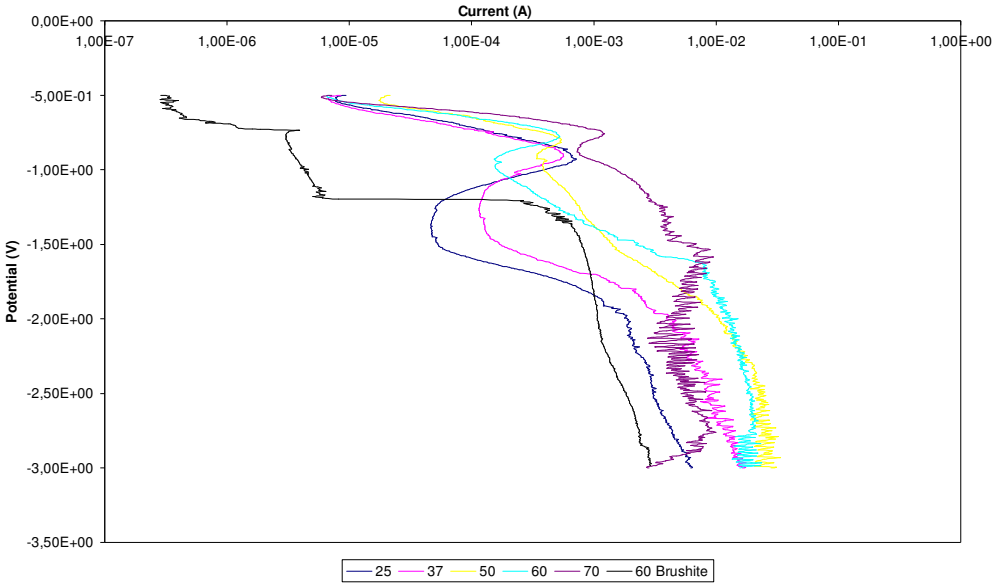

Figure 6.4 Cathodic polarization curves of the 316L SS in the test solution at different temperatures

6.3 Characterization of the Coatings

6.3.1 XRD

The XRD pattern of the coating, which was formed at 25 °C temperature, is given in figure 6.5. According to this pattern, coating includes only Brushite crystal (dicalcium phosphate dihydrite, DCPD) at the 25 °C temperature. It does not include any HA peak.

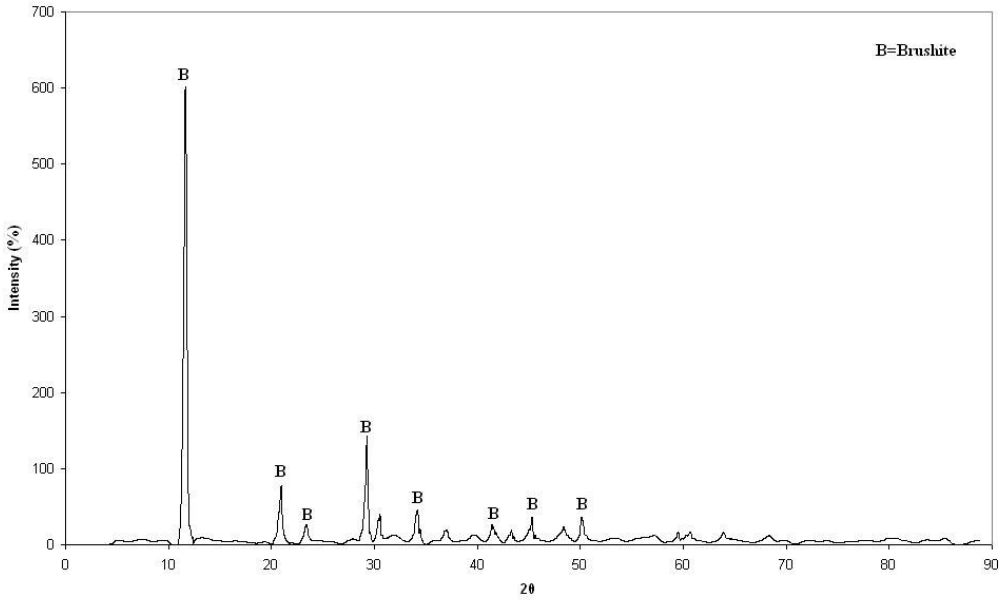

Figure 6.5 XRD pattern of the coating produced at 25 °C

Figure 6.6 shows the XRD pattern of the specimen, which deposited at 37 °C temperature. This pattern also indicated the existence of Brushite crystals in coating.

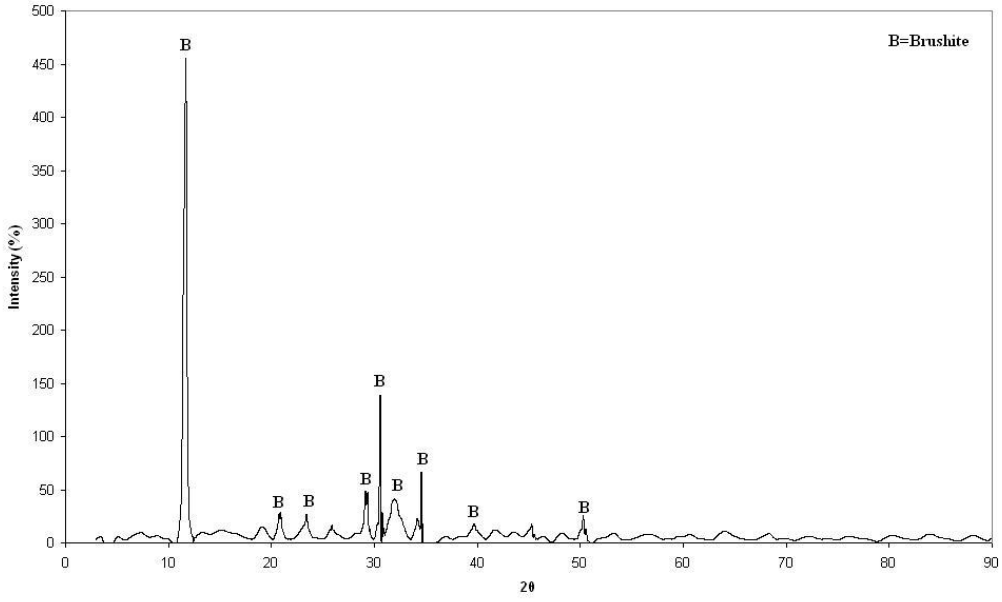

Figure 6.6 XRD pattern of the coating produced at 37 °C

The temperature level of 50 °C is a critical temperature for the all experiments conducted in this study, because HA formation started to take place at 50 °C

temperature for the first time in this process used throughout this study. As seen in Figure 6.7, the coating layer formed at 50 °C consisted of 100 % HA, with apparent picks of austenite from the substrate.

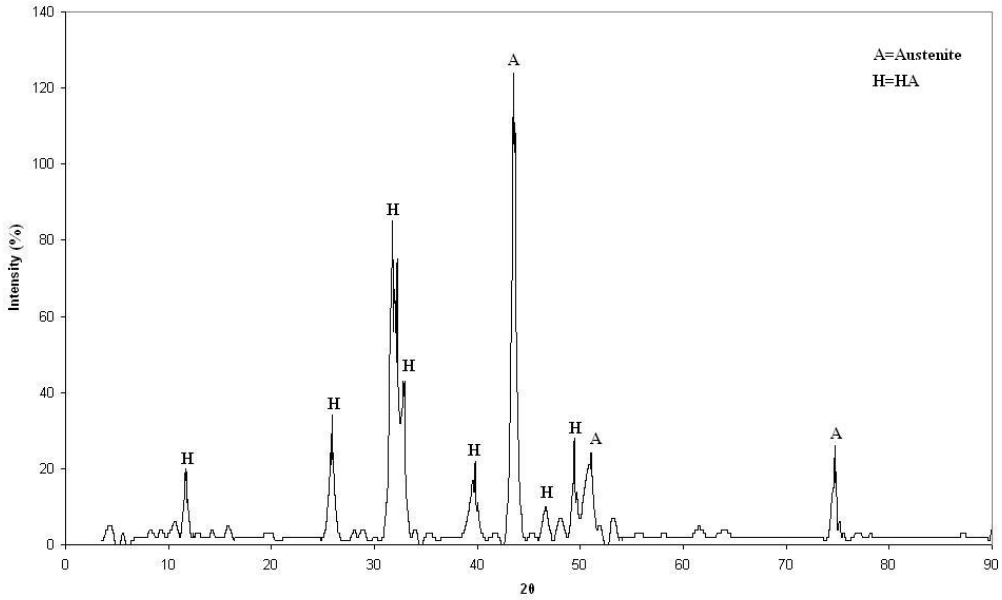

Figure 6.7 XRD pattern of the coating deposited at 50 °C

The coatings deposited at 60 and 70 °C also revealed all HA peaks. Figure 6.8 and 6.9 show XRD patterns of these coatings respectively.

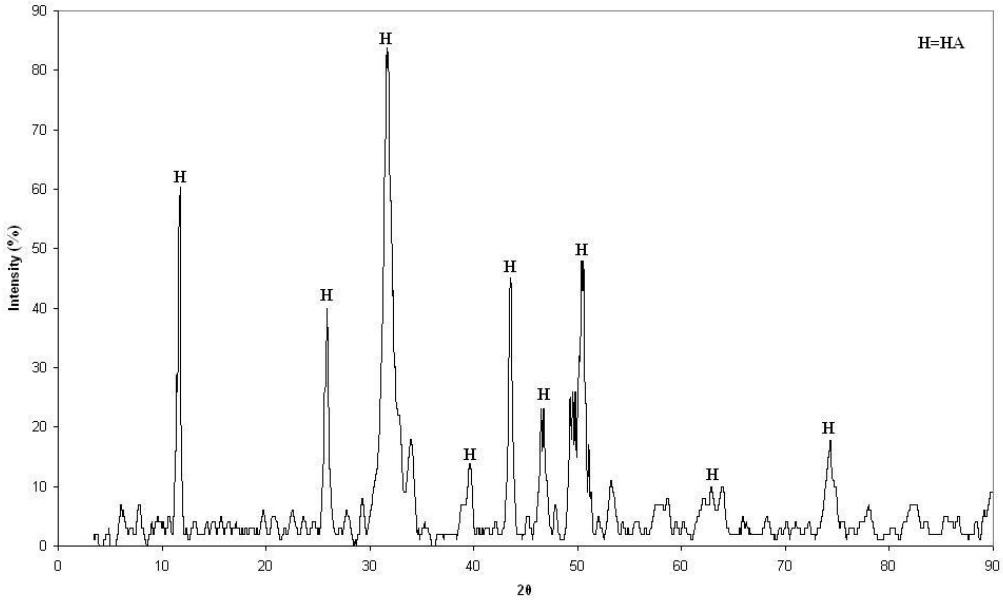

Figure 6.8 XRD pattern of the coating deposited at 60 °C

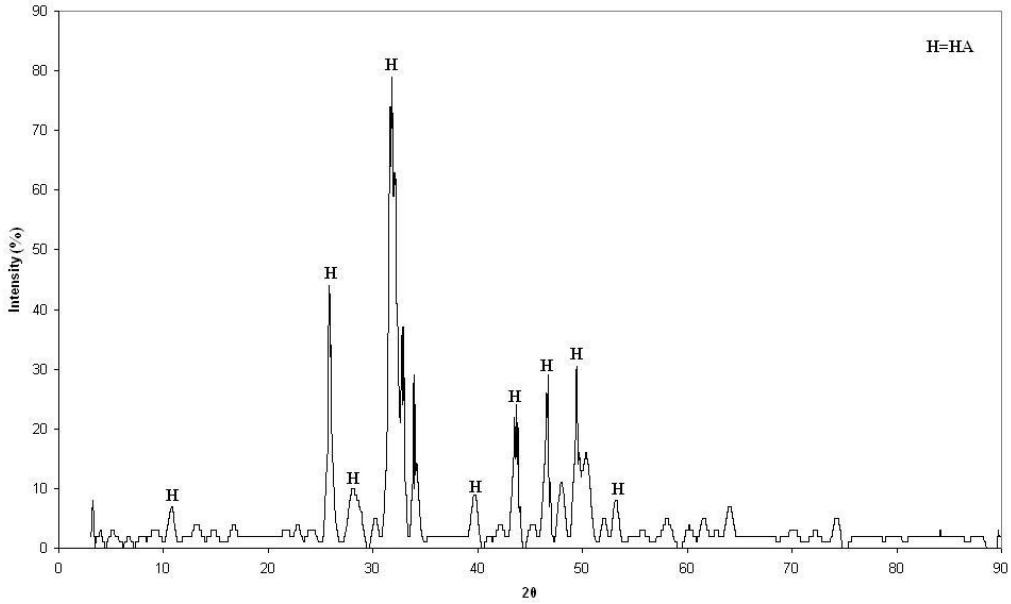

Figure 6.9 XRD pattern of the coating deposited at 70 °C

The coating deposited in a test solution with a Ca/P molar ratio of 1 at 60 °C revealed only Brushite crystals. Figure 6.10 demonstrates the XRD pattern of this coating. This could be assumed to indicate that both temperature and Ca/P ratio are equally important to produce HA coatings deposited by the method used in this study.

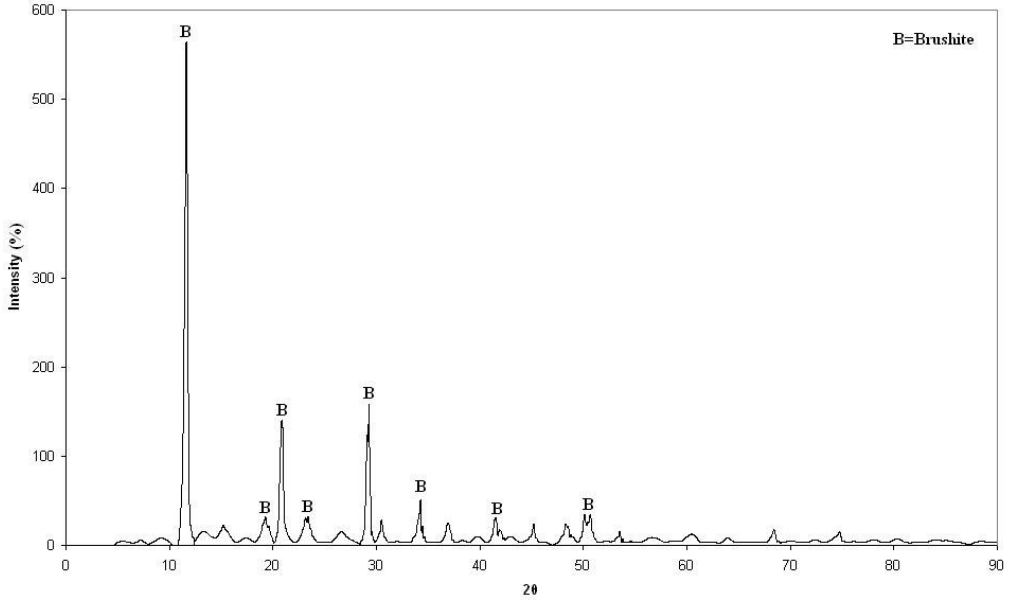

Figure 6.10 XRD pattern of the coating deposited potentiodymically in the test solution with a Ca/P molar ratio of 1 at 60 °C

As mentioned earlier, the temperature 50 °C is a critical temperature for the HA formation in the test solution with a Ca/P molar ratio of 1,67. The coatings deposited at the temperature levels of 25 °C and 37 °C in the same test solution of 1,67 molar ratio of Ca/P did not reveal any HA crystals indicating the significant effect of the temperature besides the molar ratio of Ca/P on the deposition procedures.

6.3.2 SEM

SEM photographs of the coatings deposited at 25 °C are shown in Figure 6.11. The structural composition of this coating consisted of mainly Brushite which presented a plate-like morphology.

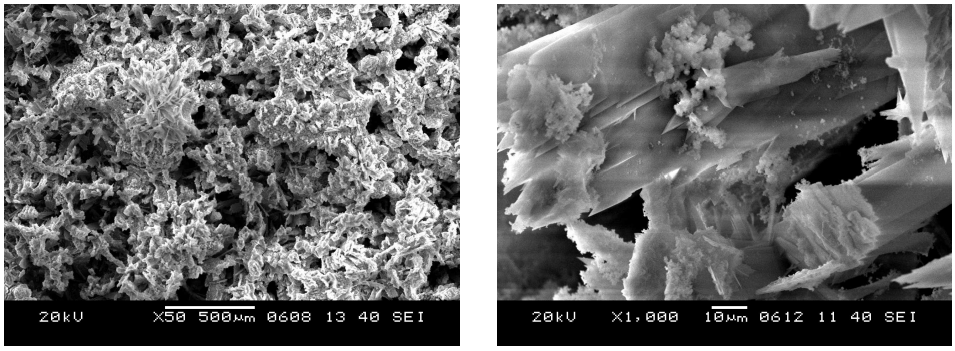

Figure 6.12 SEM photographs of the coating deposited at 25 °C

Figure 6.13 shows the SEM images of coating deposited at 37 °C. This coating also consisted in 100 % Brushite crystals which looked more needle-like particles rather than plate like ones as observed for the coating deposited at 25 °C.

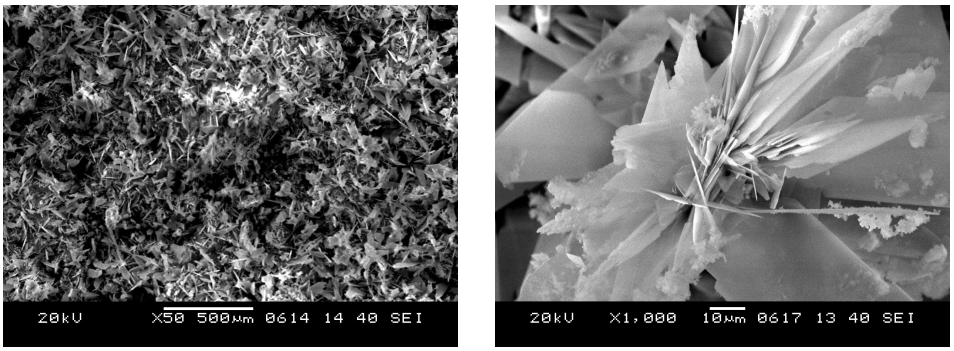

Figure 6.13 SEM photographs of the coating deposited at 37 °C

SEM images of Brushite crystals synthesized in the test solution with a Ca/P molar ratio of 1 at 60 °C are given in Figure 6.14. The microstructure of this coating displayed a smooth, plate-like morphology.

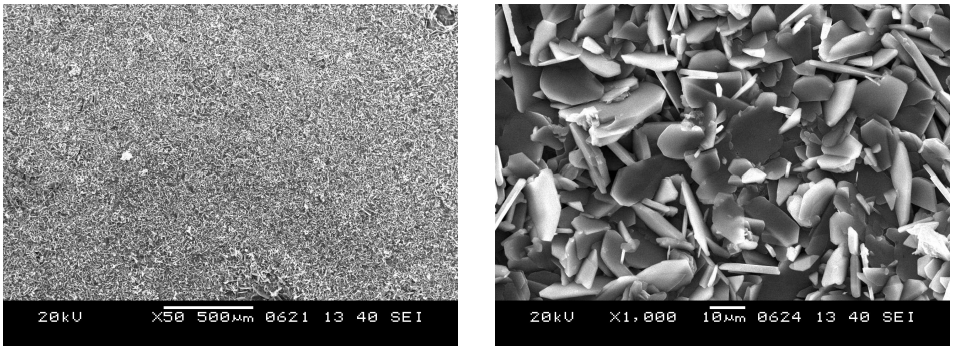

Figure 6.14 SEM photographs of the coating deposited potentiodymically at 60 °C in the electrolyte of 0.025 M $Ca(NO_3)_2.4H_2O$ and 0.025 M $NH_4H_2PO_4$

Figure 6.15, 6.16, and 6.17 show SEM images of the coatings deposited at the temperatures of 50, 60, and 70 °C respectively. As seen from the figures, the dimensions of HA crystals increased with increasing temperature. Planarity of HA crystals became more prominent as temperature rises. Consequential changes in mechanical and corrosion properties due to the morphological transformation could be expected.

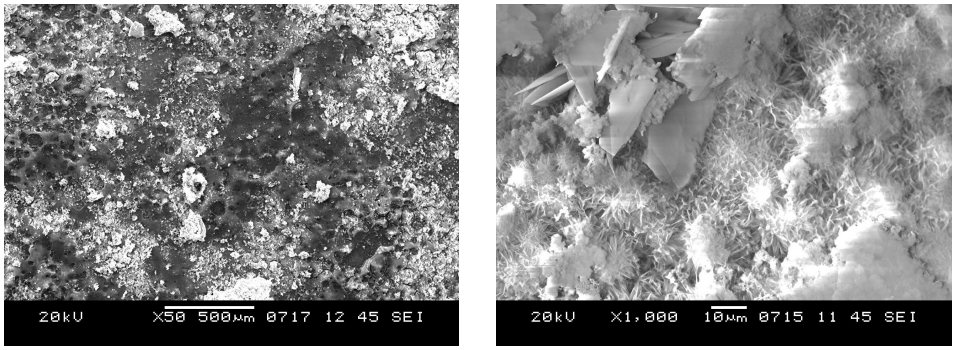

Figure 6.15 SEM photographs of the coating deposited at 50 °C

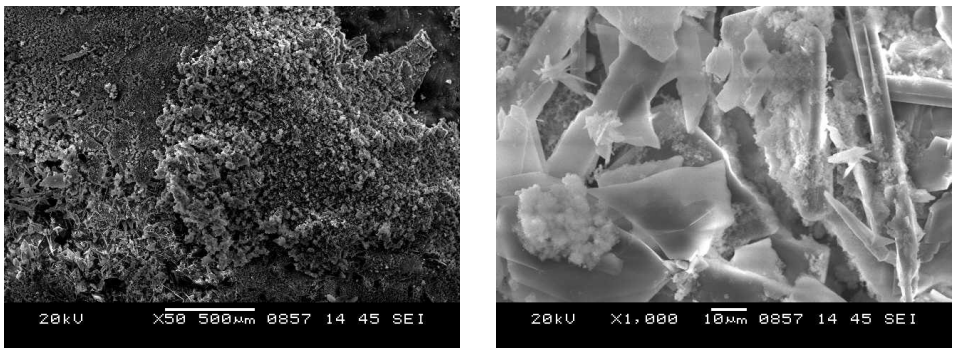

Figure 6.16 SEM photographs of the coating deposited at 60 °C

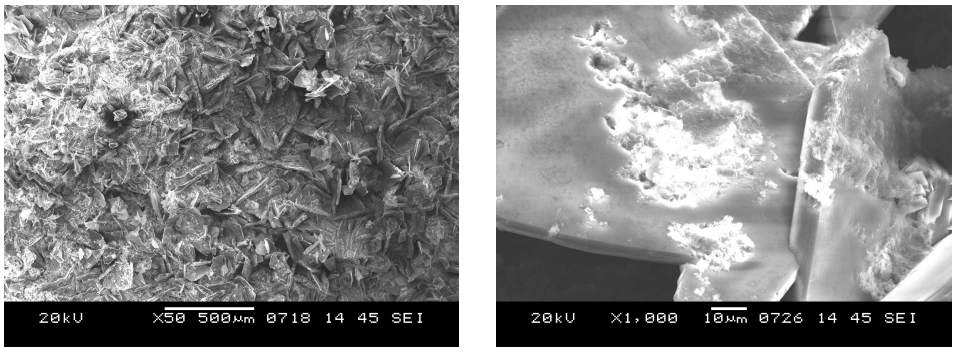

Figure 6.17 SEM photographs of the coating deposited at 70 °C

6.3.3 EDS

The weight percentage of the elements is given at the all figures. This means, Ca/P ratio expresses the mass ratio, but all these ratios were converted into the molar ratio by using needed calculations. Figure 6.18 demonstrates EDS analysis of the coating deposited at 25 °C. According to these data, Ca/P molar ratio in coating is 1.08, although the test solution was prepared with a Ca/P molar ratio of 1.67. Ca/P molar ratio of 1.08 lays between 1.67 and 1.0 corresponding to the stoichiometric values of HA and Brushite respectively.

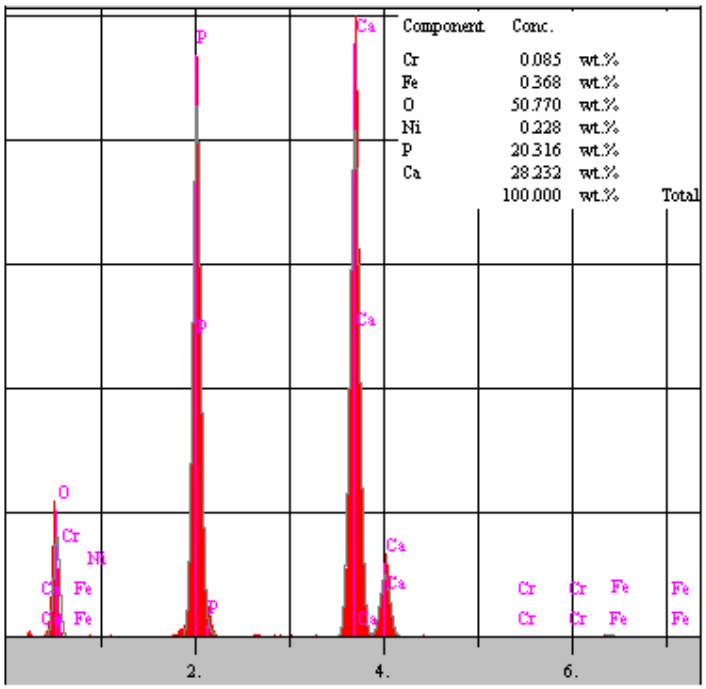

Figure 6.18 EDS analysis of the coating deposited at 25 °C

Figure 6.19 shows the EDS analysis of the coating deposited at 37 °C. This figure represents the molar ratio of Ca/P=1.16 for this coating. This is slightly higher than that of the coating deposited at 25 °C. For the solution with Ca/P molar ratio of 1 to promote the formation of HA crystals, solution temperature should be sufficiently high. As the solution temperature came closer to the limiting temperature of 50 °C, Ca/P molar ratio in coating approached 1.67. Coming closer to 50 °C caused an increase in the stoichiometric ratio of Ca/P. These results support the findings by Ban and Maruno, who reported that the coatings deposited at 5-37 °C were amorphous in a simulated body fluid, while the deposits produced in same solution at 52 and 62 °C contained HA (Ban et al., 1995).

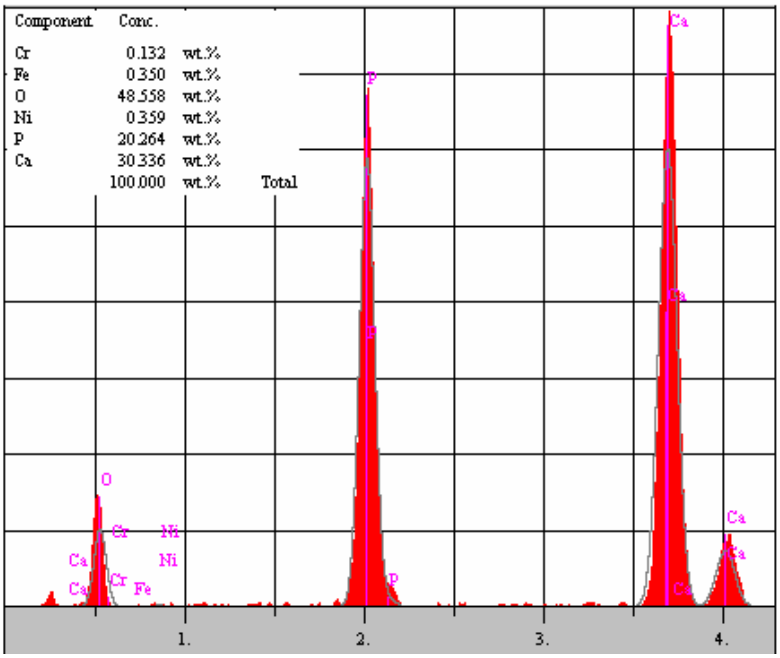

Figure 6.19 EDS analysis of the coating deposited at 37 °C

The EDS pattern of the coating deposited at 60 °C in the solution with a Ca/P molar ratio of 1 is given in the figure 6.20. As indicated in this figure the coating has Ca/P molar ratio of 0.8. This result stressed ones again the importance of chemical composition of the test solution. Temperature alone is not sufficient to produce HA films, unless the chemistry of the test solution is properly adjusted.

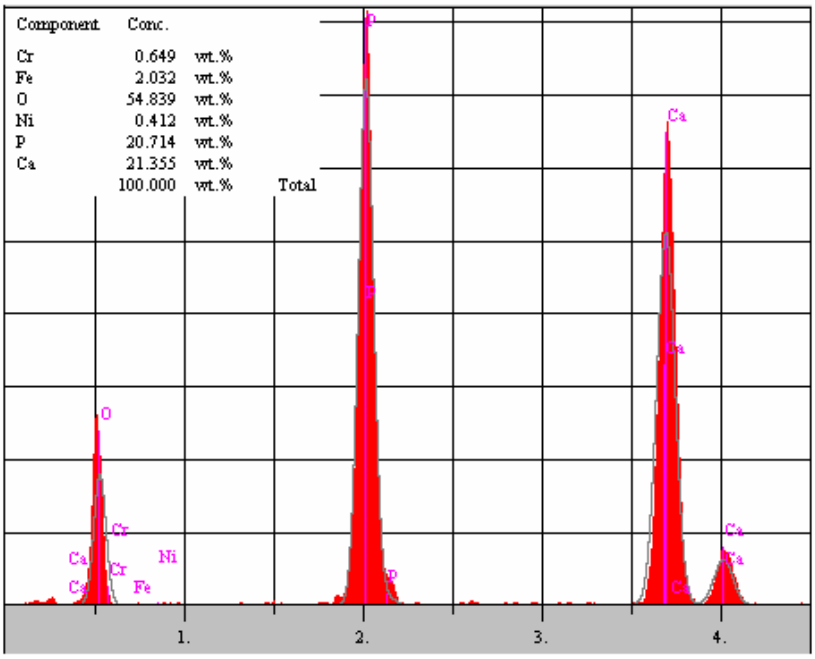

Figure 6.20 EDS analysis of the coating deposited at 60 °C in the solution with Ca/P molar ratio of 1

Figure 6.21, 6.22, and 6.23 show the EDS analyses of the coatings deposited at 50, 60, and 70 °C respectively. The corresponding Ca/P ratios of the films deposited at the mentioned temperatures were 1.16, 1.21, and 1.03 respectively, although the Ca/P molar ratio of the solutions was 1.67. Yet these temperatures and solution chemistry promoted the formation of HA crystals.

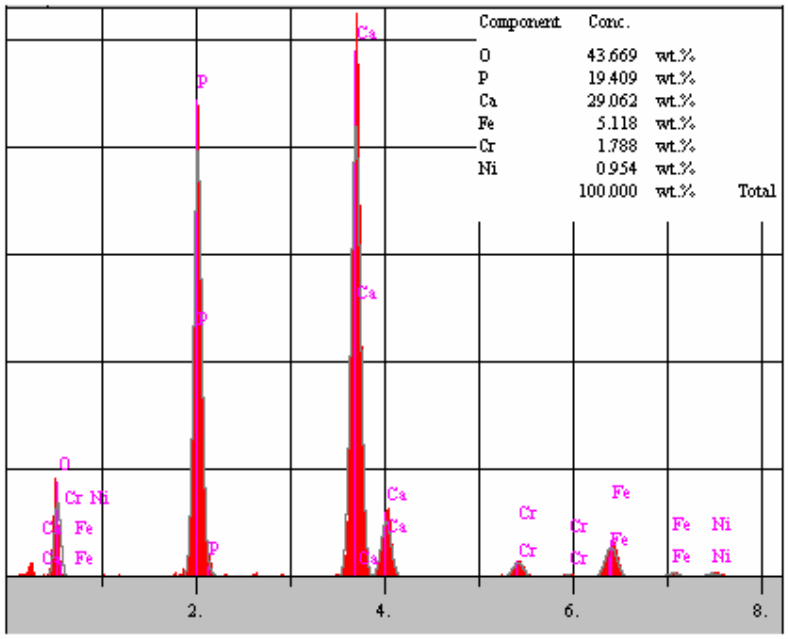

Figure 6.21 EDS analysis of the coating deposited at 50 °C

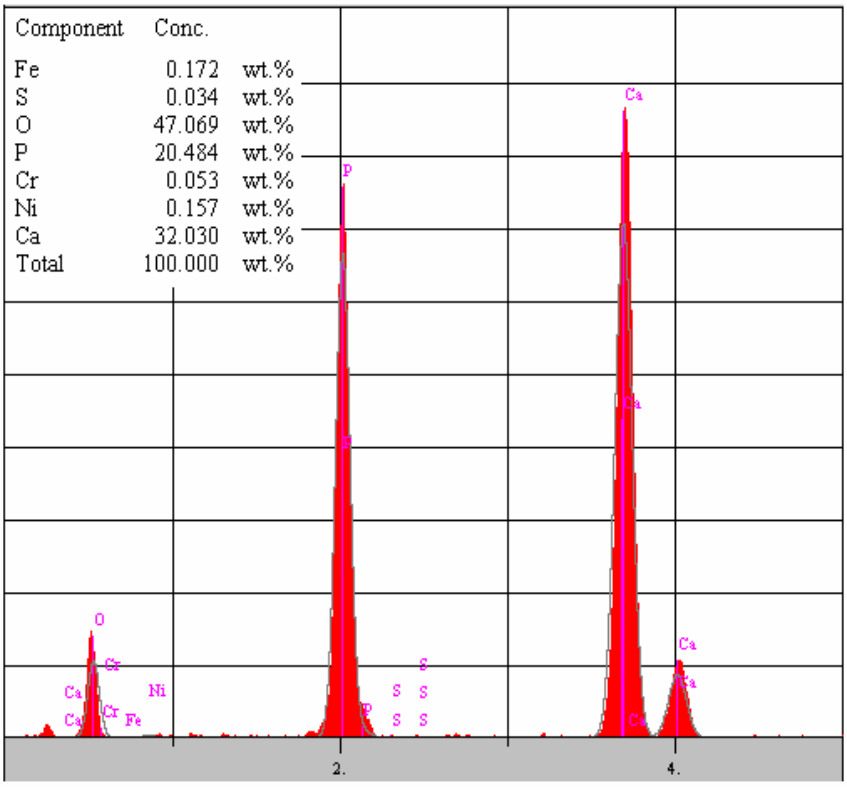

Figure 6.22 EDS analysis of the coating deposited at 60 °C

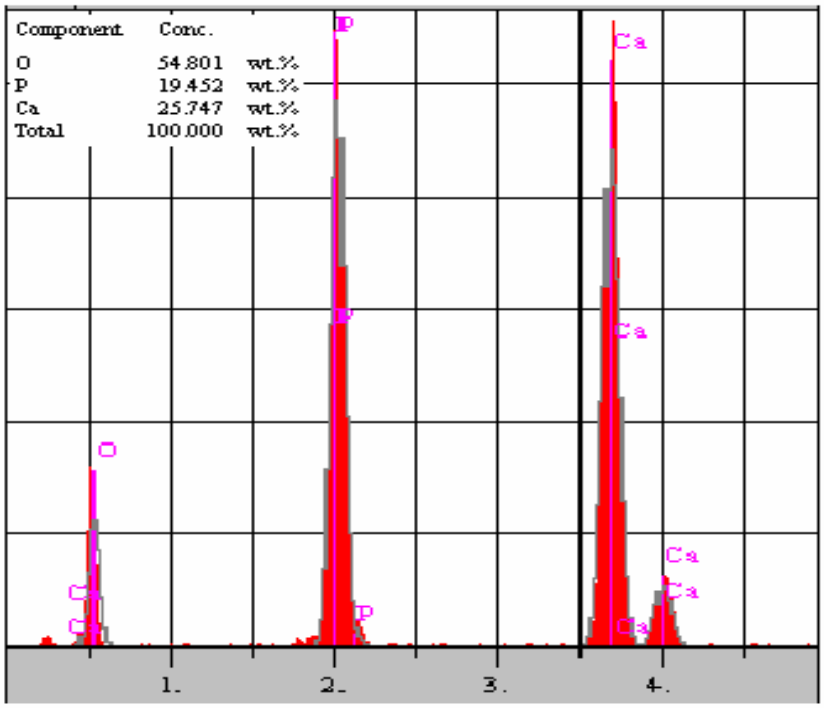

Figure 6.23 EDS analysis of the coating deposited at 70 °C

6.3.4 DTA/TGA

DTA/TGA analysis was carried out in order to determine the type of the reactions and the most suitable process for the film production. Figure 6.24 shows the DTA/TGA diagram of the bone flour. A phase transformation between ~ 400-600 ℃ is indicated in this diagram.

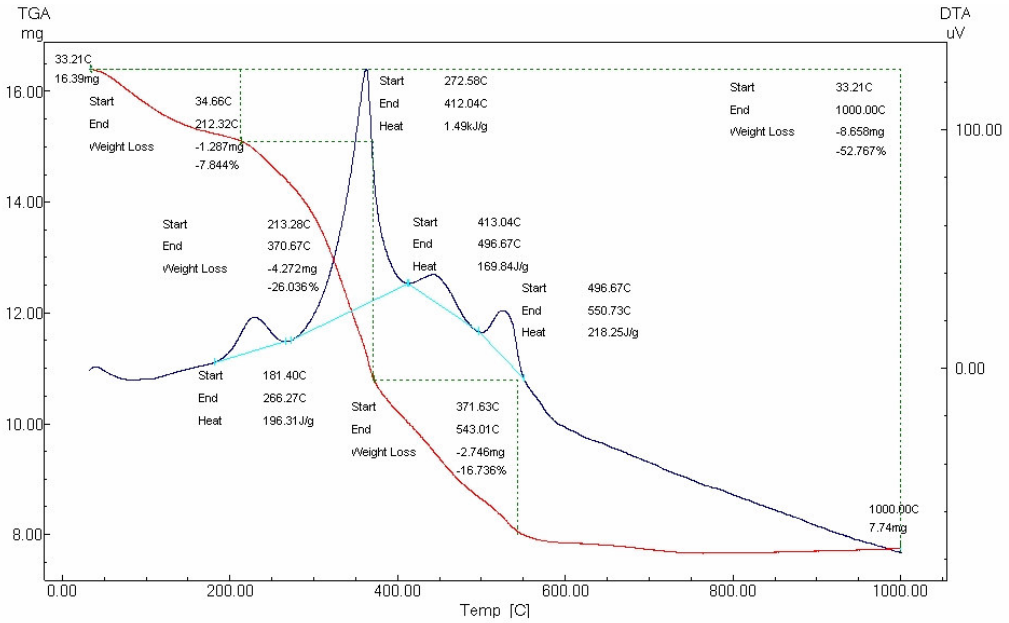

Figure 6.24 DTA/TGA diagram of the bone flour

Figure 6.25 shows the result of DTA analyses of scraped coating powders from the specimen surfaces. The scale of the Y-axis was not determined at this figure, because the curves were drawn with 10 % addition orderly. The reason of this addition was fitting of the curves into each other and it became difficult to seperate each other. Endothermic peaks were detected at 200 °C for the Brushite structure indicating a phase transformation at this temperature. Figure 6.26 shows the TGA results of the coating powders. The reason of the increase on the mass was oxidation of the phosphate phases with increasing temperature.

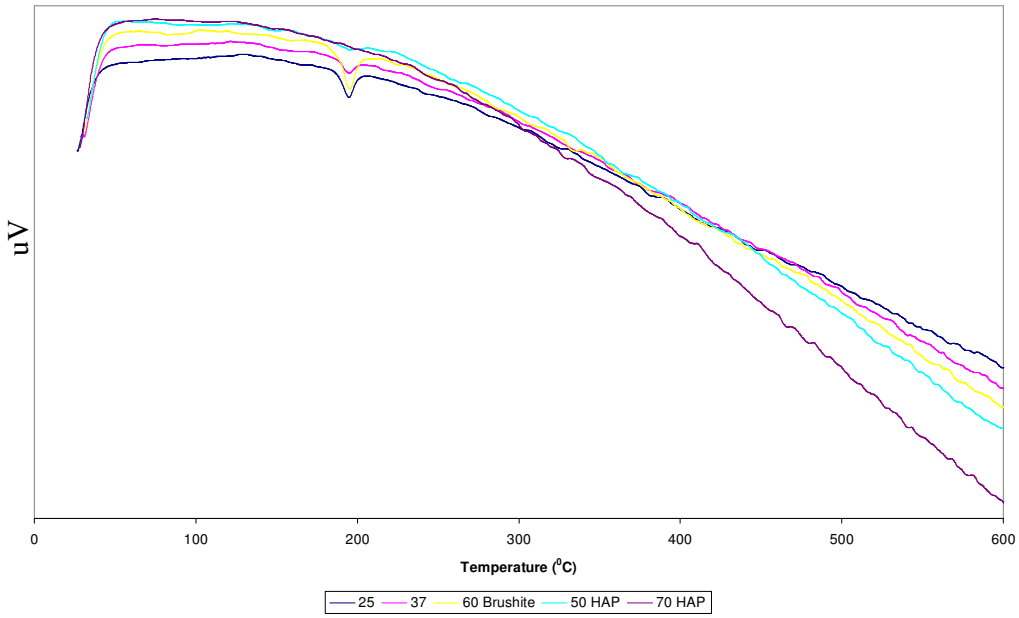

Figure 6.25 DTA diagram of the powders scraped from the specimen surfaces

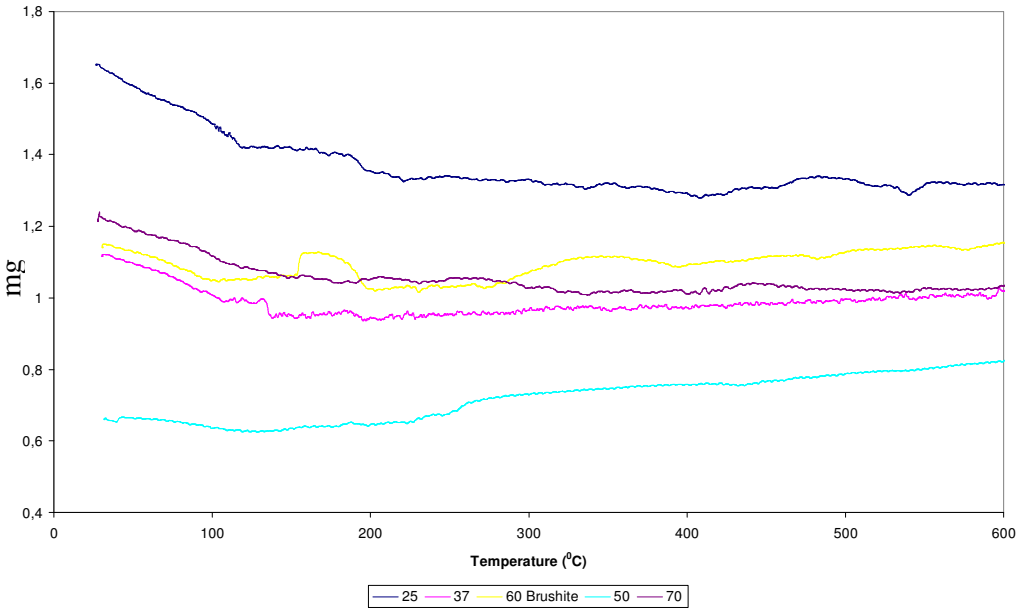

Figure 6.26 TGA diagram of the powders scraped from the specimen surfaces

6.4 Results of the Heat Treatment Procedure

Heat treatment was applied to the coatings and bone flour according to the DTA/TGA results.

6.4.1 XRD

Figure 6.27 shows the XRD pattern of the bone flour before heat treatment. As seen from the figure, bone does not have a certain crystal structure. It has semi-crystal structure, and the peaks belong to Calcium Phosphate Hydrate.

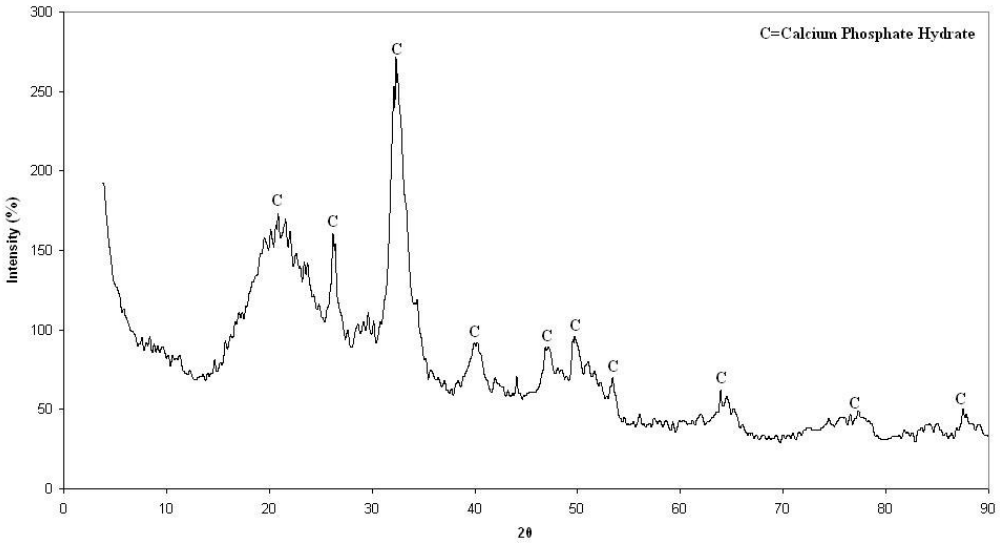

Figure 6.27 XRD pattern of the Bone Flour

After the heat treatment of the bone flours, a structural change appeared as shown XRD pattern in Figure 6.28. According to this pattern all powders transformed into the HA structure. This HA is called biological HA.

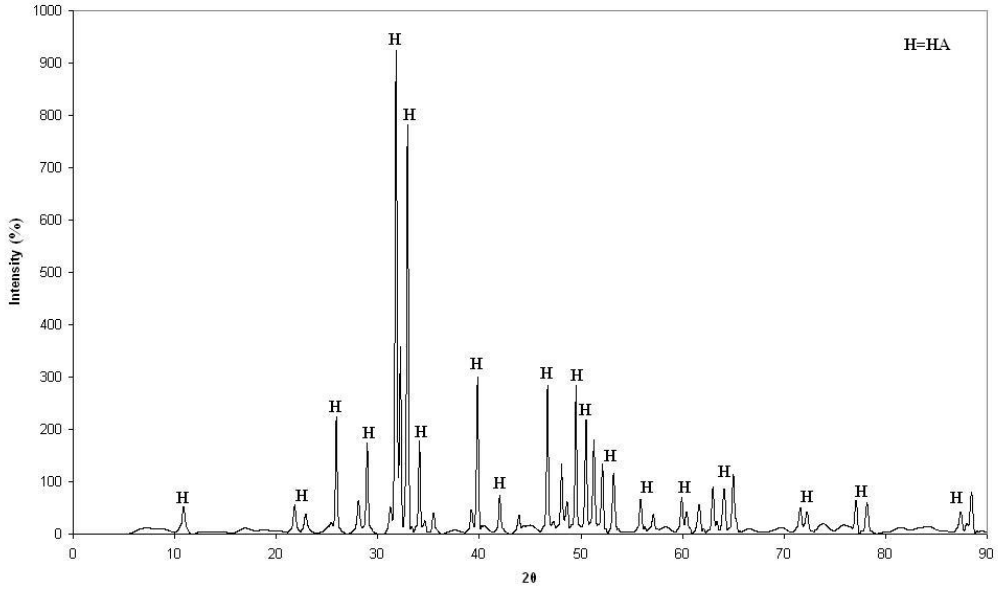

Figure 6.28 XRD pattern of the Bone Flour after calcinated for 1 hour at 1000 °C

The coatings consisted in Brushite crystals as produced in solution with the Ca/P molar ratio of 1,67 at 25 and 37 °C and in solution with the Ca/P molar ratio of 1 at 60 °C underwent a phase transformation to HA after heat treatment. Figure 6.29 shows the XRD pattern of the coating deposited at 25 °C. According to this pattern, transformation of Brushite to HA was partial, as indicated by some peaks still corresponding to the remaining crystals of Brushite in crystal structure. Some peaks corresponding to the substrate (316L) were also disclosed in this figure.

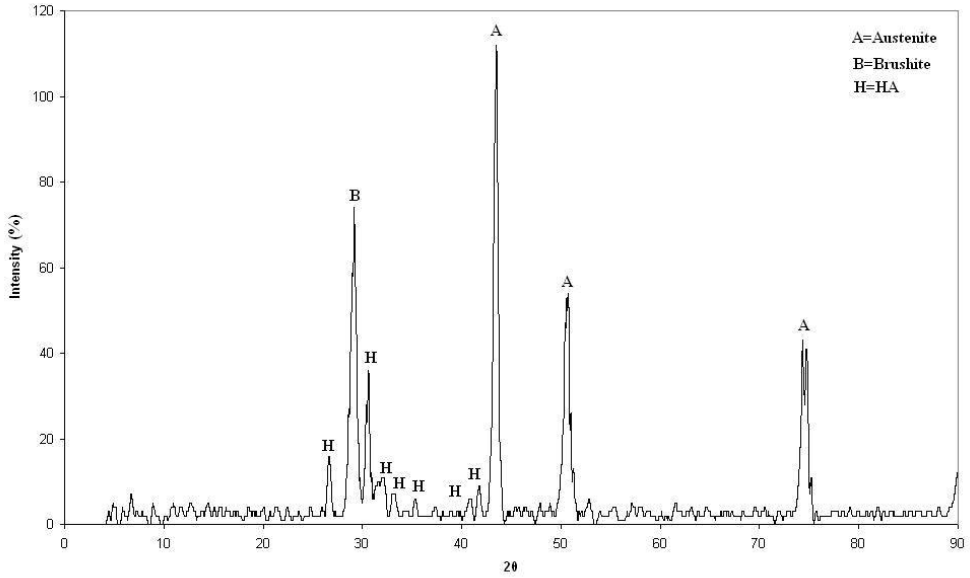

Figure 6.29 XRD pattern of the sample deposited at 25 °C and annealed for 1 hour at 500 °C

The coating deposited at 37 °C also went through full transformation into the HA crystals following the heat treatment as shown in Figure 6.30. Some peaks from the substrate were also apparent here.

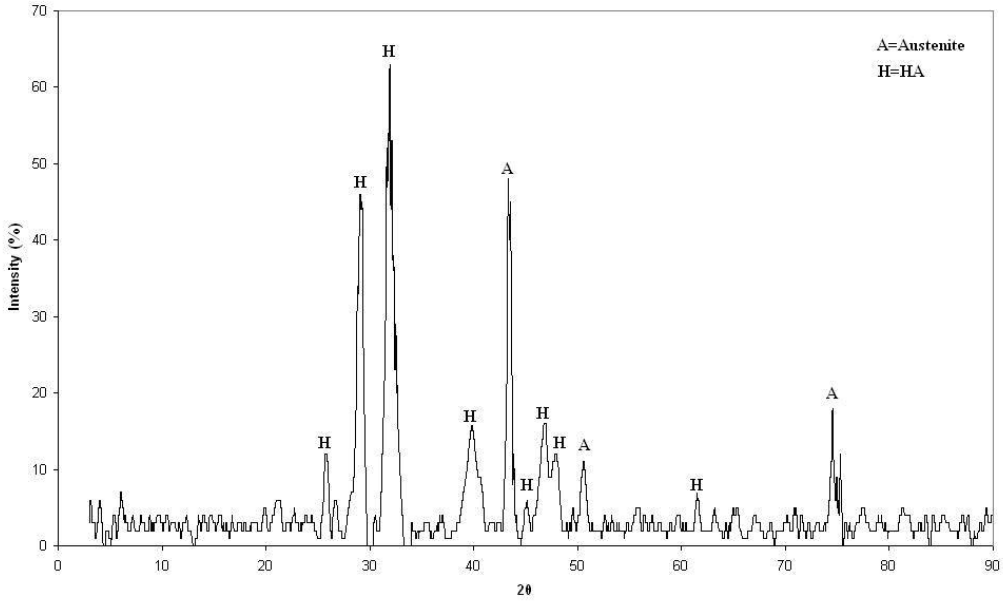

Figure 6.30 XRD pattern of the sample deposited at 37 °C and annealed 1 hour at 500 °C

The coating, which deposited at 60 °C in the solution with a Ca/P molar ratio of 1, went through a full phase transformation following heat treatment. As seen in Figure 6.31, XRD spectrum of this coating presented no peaks of Austenite and Brushite.

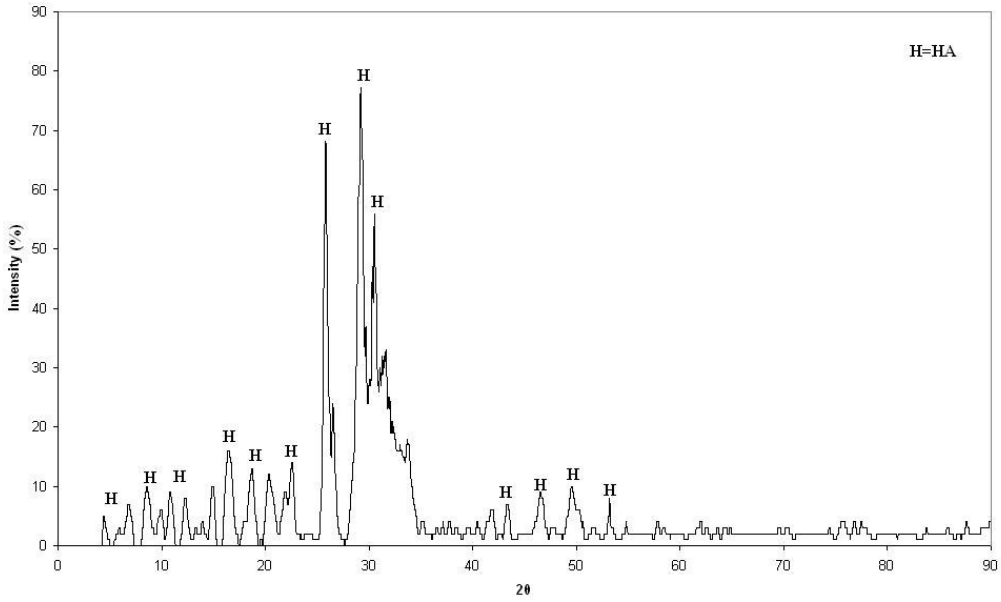

Figure 6.31 XRD pattern of the coating deposited at 60 °C and heat treated for 1 h 500 °C

Figure 6.32 shows the XRD patterns of the coating deposited at 50 °C. XRD patterns of the coating before and after heat treatment are superimposed in this figure for the sake of comparison.

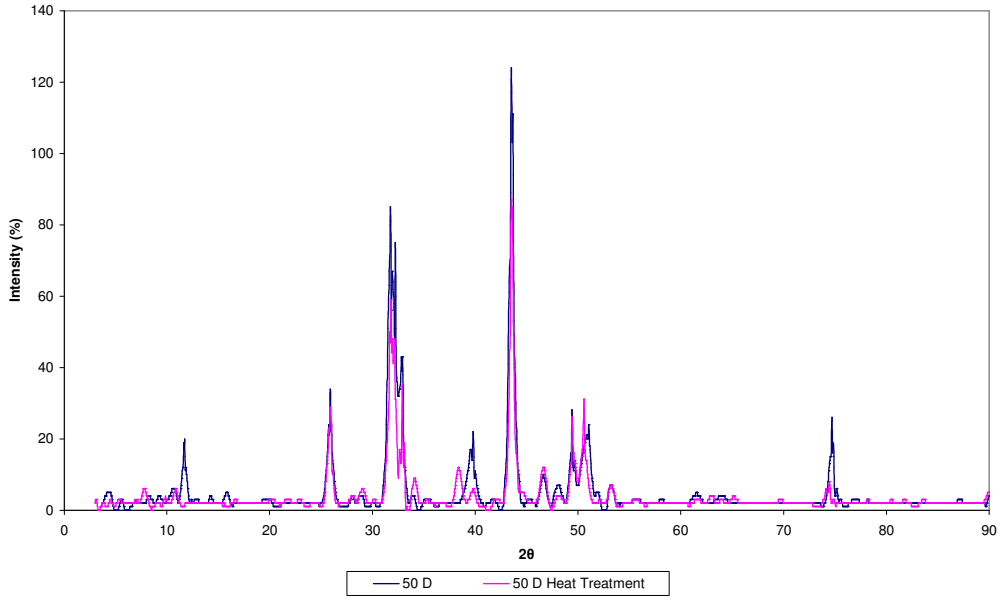

Figure 6.32 XRD patterns of the coatings: deposited at 50 °C (blue one), annealed for 1 h at 500 °C (pink one)

Figures 6.33 and 6.34 show XRD patterns of the coatings deposited at the temperatures 60 and 70 °C respectively. XRD patterns before and after the heat treatment of the relevant coating are superimposed here for comparison. Following heat treatment, the intensities of the HA peaks increased in both cases, at 70 °C in particular, as demonstrated in Figure 6.34.

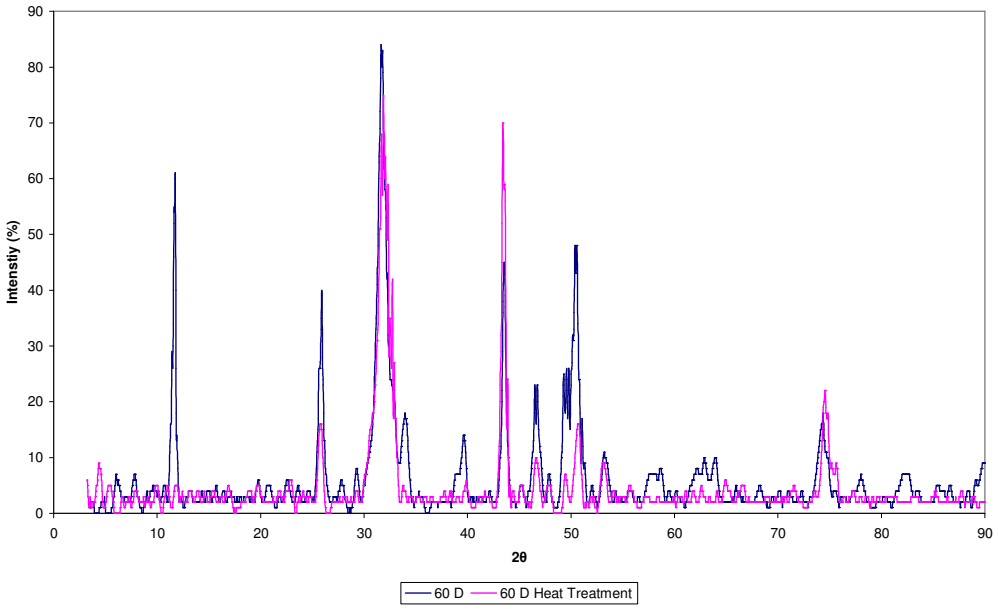

Figure 6.33 XRD patterns of the coatings: deposited at 60 °C (blue one), annealed for 1 h at 500 °C (pink one)

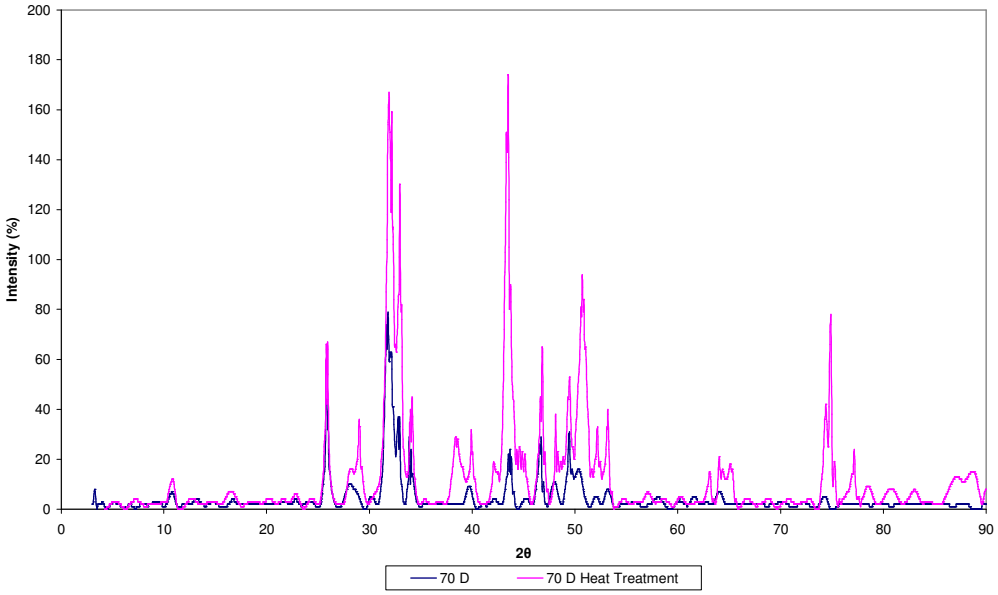

Figure 6.34 XRD patterns of the coatings: deposited at 70 °C (blue one), annealed for 1 h at 500 °C (pink one)

6.4.2 SEM

Figure 6.35 shows SEM image of the coating deposited at 25 °C and applied heat treatment. HA crystals in the forms of coarse needle-like and small plates are clearly seen in these images. The decrease in crystal sizes upon heat treatment is also clearly demonstrated here.

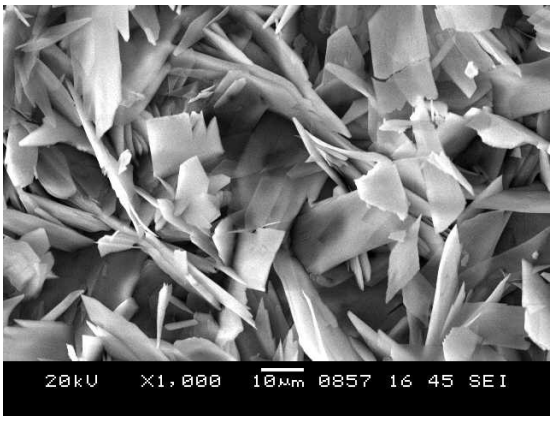

Figure 6.35 SEM image of the sample deposited at 25 °C and annealed (Brushite+HA)

Figure 6.36 shows the image of the deposited at 37 °C and heat treated for 1 hour at 500 °C. Brushite crystals seem to have disintegrated and accumulated into a form of HA agglomerates. Total transformation to HA crystals has taken place here upon heat treatment.

Figure 6.37 demonsrates the microstructure of the coatings deposited at 60 °C in the solution with Ca/P molar ratio of 1 and heat treated for 1 hour at 500 °C. The change from Brushite into HA is seen clearly from this figure. The big grains of the Brushite crystal transformed into the little HA crystals.

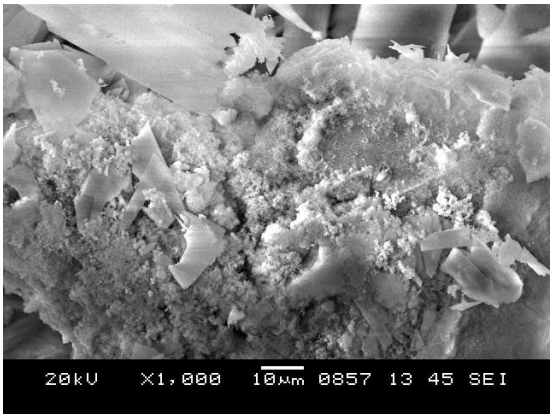

Figure 6.36 SEM image of the sample deposited at 37 °C and heat treated (HA)

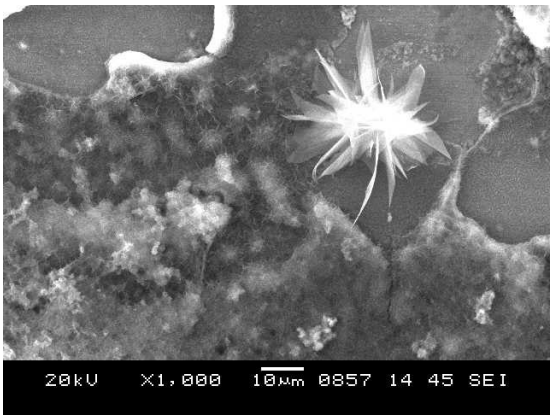

Figure 6.37 SEM image of the specimen deposited at 60 °C in the solution with Ca/P molar ratio of 1 and heat treated for 1 h at 500 °C (HA)

Figure 6.38, 6.39, and 6.40 show the surface morphology of the coatings all deposited in same solution having Ca/P molar ratio of 1.67 at 50, 60, and 70 °C respectively. There was no phase transformation in these coatings as expected. However, visible change in crystal structures has taken place in all cases.

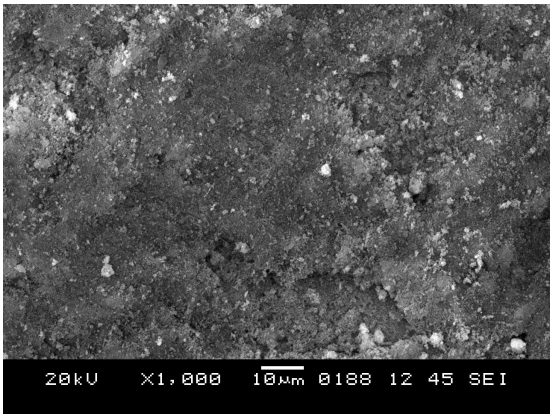

Figure 6.38 SEM image of the sample deposited at 50 °Cand annealed (HA)

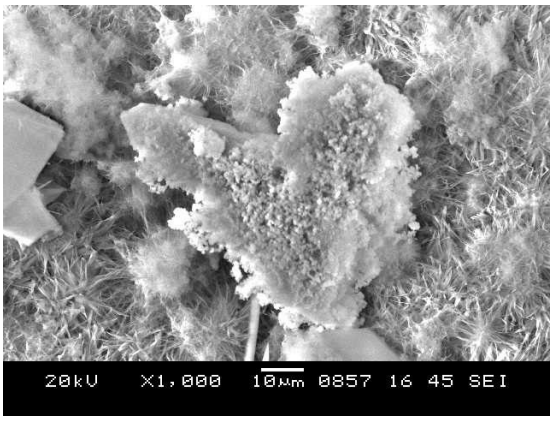

Figure 6.39 SEM image of the sample deposited at 60 °C and heat treated (HA)

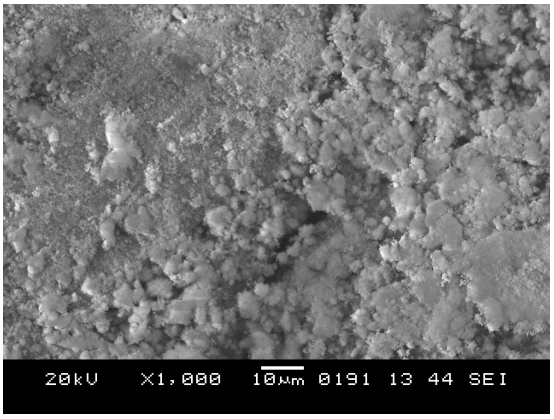

Figure 6.40 SEM image of the sample deposited at 70 °C and heat treated (HA)

6.4.3 EDS

Ca/P molar ratio of the coatings was measured by using EDS. The changes in the molar ratio of Ca/P of the coatings following the heat treatment are presented in Table 6.1.

Table 6.1 The change in Ca/P molar ratio of the coatings upon heat treatment

Coatings	Ca/P	Ca/P (After Heat Treatment)
25	1.08 (B)	0.93 (B+HA)
37	1.16 (B)	1.19 (HA)
50	1.16 (HA)	1.24 (HA)
60	1.21 (HA)	1.08 (HA)
70	1.03 (HA)	1.25 (HA)
60-B	0.8 (B)	0.94 (HA)

B: Brushite, HA: Hydroxyapatite

Results in this table indicated that the heat treatment resulted not only in phase transformation of the coatings, but also in the change of The Ca/P molar ratio in the coatings. Heat treatment has resulted increase in the molar ratio of Ca/P at all temperatures, except 25 and 60 °C.

6.4.4 FTIR

Figure 6.41 demonstrates the FTIR spectra of the Calcium Phosphate Phases (CPP).

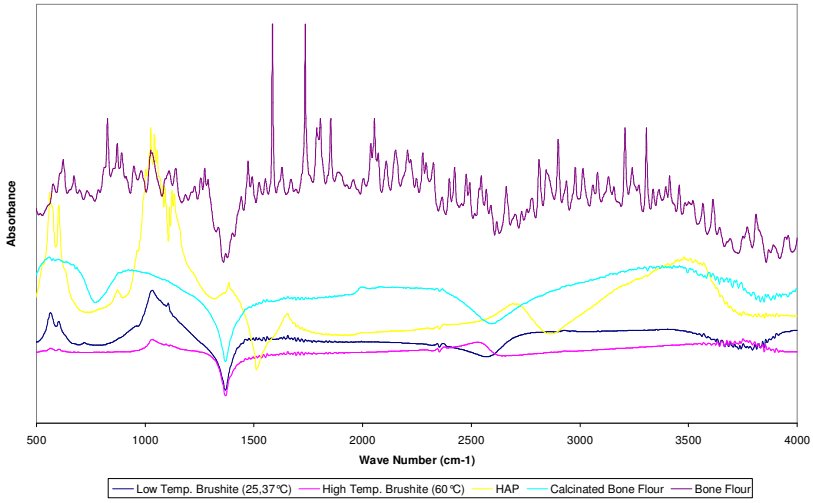

Figure 6.41 FTIR spectra obtained for different CPP

The peaks located around 1000 cm^{-1} and at 560–603 cm^{-1} are originated by phosphate modes of HA (Stoch et al., 2003). The broad band near 3400 cm^{-1} confirms the high water content characteristic. 1360 cm^{-1} peak belongs to the carbonate phase. Reaction given below (Rössler et al., 2002) may provide a simple explanation for phase transformation upon heat treatment, since this causes the loss of water changing the direction of the reaction to the left promoting the formation of HA crystals. HA crystals, which are rich in OH^- ions are likely to form upon the loss of water form Brushite.

$$CO_2 + 2OH^- \leftrightarrow CO_3^{2-} + H_2O$$

Brushite crystals and bone flour revealed carbonate peaks which also in line of the explanation given above for phase transformation in view of this reaction. Calcinated bone flour also revealed carbonate peak with high transmittance due to the presence of CO_2 in heat treatment atmosphere (Rössler et al., 2002). The peaks of the bone flour are not distinct and full of ridges. As indicated earlier (according to XRD data), bone flour has a semi-crystalline structure, the FTIR spectra of which resembles to the XRD spectrum, with its broadened and non-sharpness of the peaks.

6.5 Corrosion Tests of the Coatings

Figure 6.42 shows the anodic polarization curves of the coatings before heat treatment. All curves present a breakdown potential ranging between 100-400 mV_{sce}.

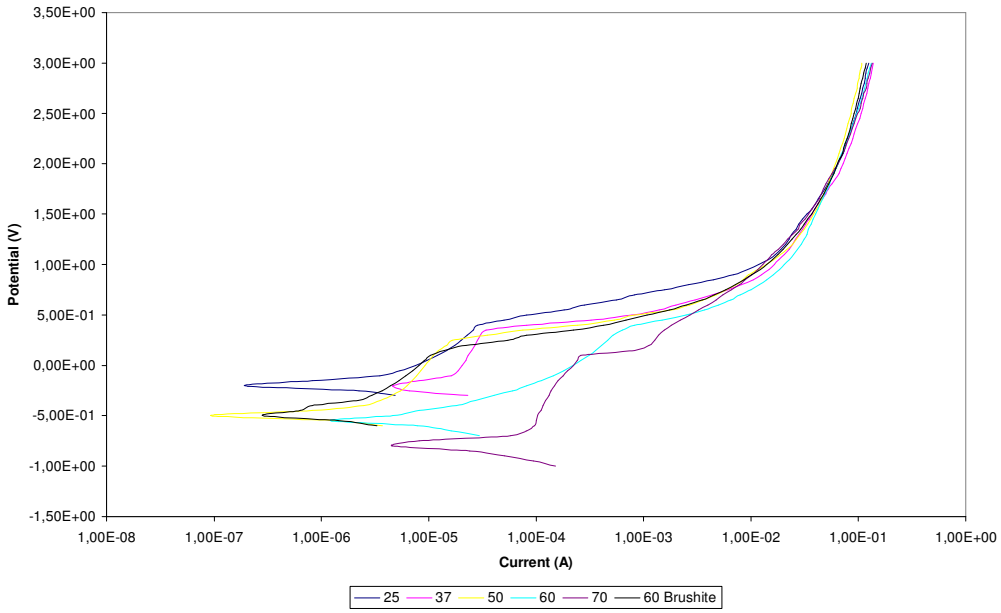

Figure 6.42 Anodic polarization curves of the untreated coatings in the lactated Ringer's Solution at 37 °C

Figure 6.43 shows the anodic polarization curves of the heat treated coatings which symbolised by H. All but 70 °C coating present also breakdown potential, but breakdown value seemed to have decreased here (btw. 0.0-235 mV_{sce}).

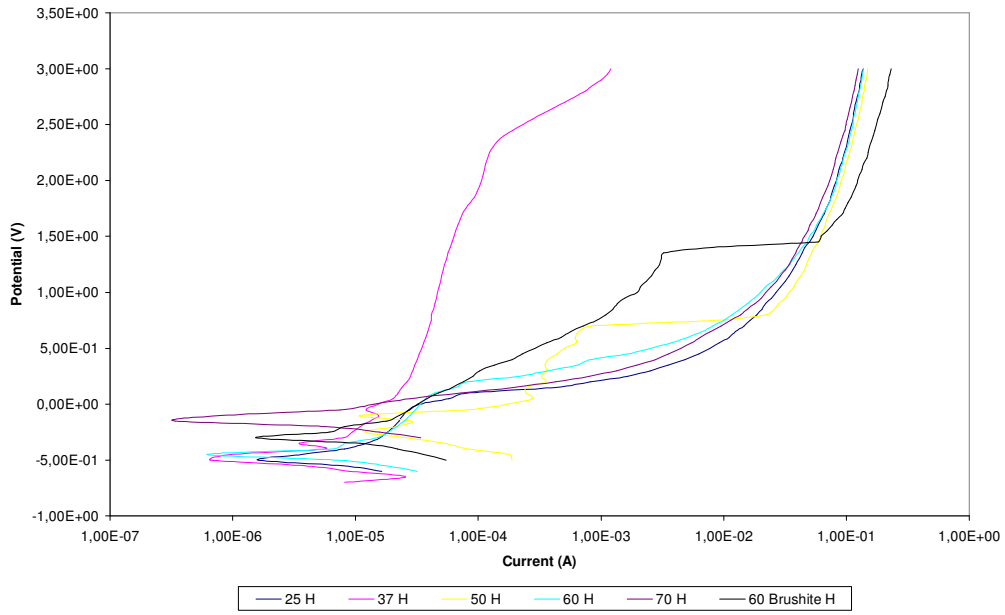

Figure 6.43 Anodic polarization curves of the heat treated coatings (1 hour at 500 °C) in the lactated Ringer's Solution

Table 6.2 lists the electrochemical parameters of the coatings obtained by corrosion studies.

Table 6.2 The values of the electrochemical parameters of all the coatings

Sample	E_c (mV) (SCE)	β_c (mV)	β_a (mV)	i_{cor} (Acm^{-2})	Pol Res R (mΩ)	Porosity (%)
316L	-150	1202	177.2	$5.08\ 10^{-7}$	$1.32\ 10^{8}$	-
25	-200	182.6	760.8	$3.05\ 10^{-7}$	$2.10\ 10^{8}$	0.35
37	-200	178.9	350.8	$7.14\ 10^{-6}$	$7.21\ 10^{6}$	10.06
50	-500	96.75	210.8	$1.46\ 10^{-7}$	$1.97\ 10^{8}$	0.2
60	-550	1076	71.39	$1.91\ 10^{-6}$	$1.52\ 10^{7}$	3.07
70	-800	160.8	177	$7.20\ 10^{-6}$	$5.09\ 10^{6}$	14.64
60 (B)	-500	124	510.2	$4.45\ 10^{-7}$	$9.75\ 10^{7}$	0.4
25 (H)	-500	913.9	174.8	$2.50\ 10^{-6}$	$2.55\ 10^{7}$	1.53
37 (H)	-500	1396	1024	$1.03\ 10^{-6}$	$2.49\ 10^{8}$	0.16
50 (H)	-250	1141	1015	$1.86\ 10^{-5}$	$1.26\ 10^{7}$	2.6
60 (H)	-450	1048	71.73	$9.64\ 10^{-7}$	$3.03\ 10^{7}$	0.99
70 (H)	-149	556	721	$5.28\ 10^{-7}$	$2.58\ 10^{8}$	1.15
60 (B-H)	-300	1041	733.4	$7.71\ 10^{-7}$	$2.43\ 10^{8}$	0.04

It is difficult to conclude anything concrete on the parameters shown in the table above. However, the coatings of HA seemed to increase E_c when heat treated. Brushite coatings, when transformed to HA upon heat treatment, decreased E_c. It is almost impossible to make a general statement for i_{cor} in regard with CPP (B or HA). The same statement includes porosity and polarisation resistance.

Figure 6.44 shows the SEM images and X-ray mappings of some elements on the untreated surface coatings following corrosion tests. These mappings show the distribution of some important elements, which came from the coatngs and Ringer's Solution.

Figure 6.45 demonstrates the SEM images for the untreated and treated coatings following corrosion tests. Affect of heat treatment on the microstructure of the coatings after corrosion tests is seen clearly from this figure. Especially, on the Brushite coatings the pits were seen clearly before heat treatment. But the opposite situation was observed for the HA coatings. On the HA coatings, after heat treatment pits became certain.

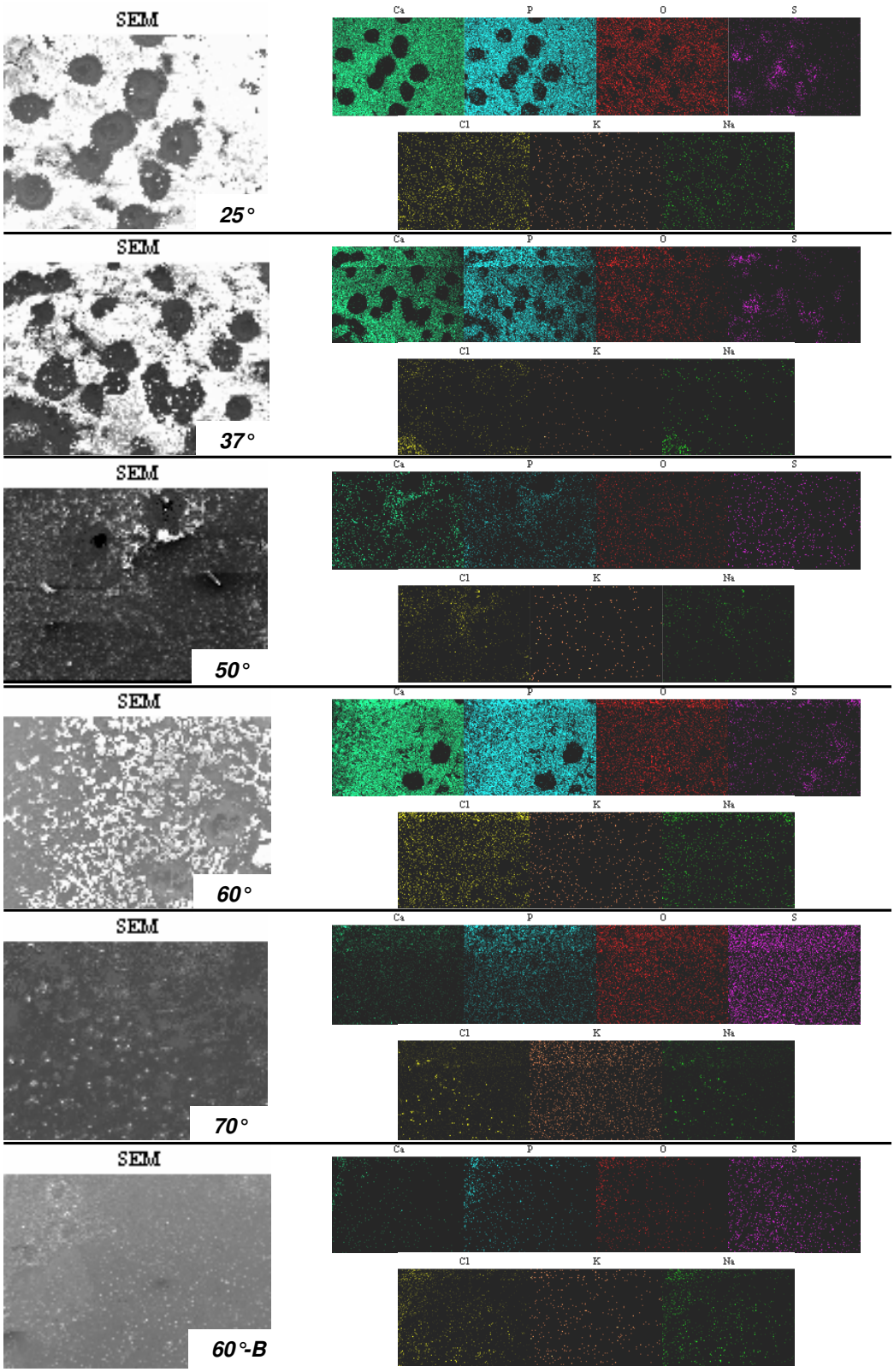

Figure 6.44 SEM images and X-Ray mappings of some elements for all coatings after corrosion tests

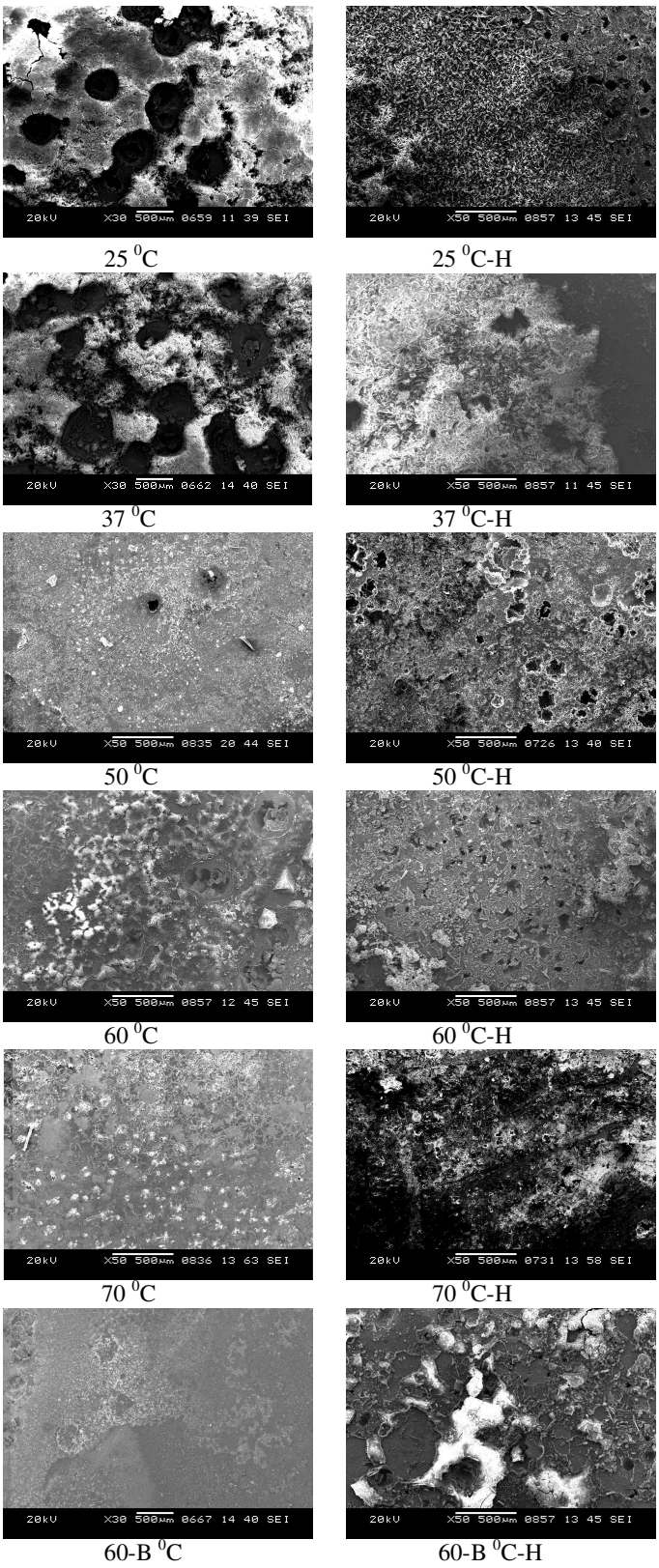

Figure 6.45 SEM images of the coatings after corrosion tests, objected in Ringer's Solution at 37 °C

6.6 Mechanical Tests of the Coatings

6.6.1 DUH

Topography of the coatings is an important parameter for the nano-indentation test. There is a crystal layer at the top of the coatings. This is not a homogenous layer. SEM image of a coating observed by mounting the sample vertically on the sample stage of SEM is given in Figure 6.46, as an example. This shows the possibility that the thickness of the deposited layer can be measured.

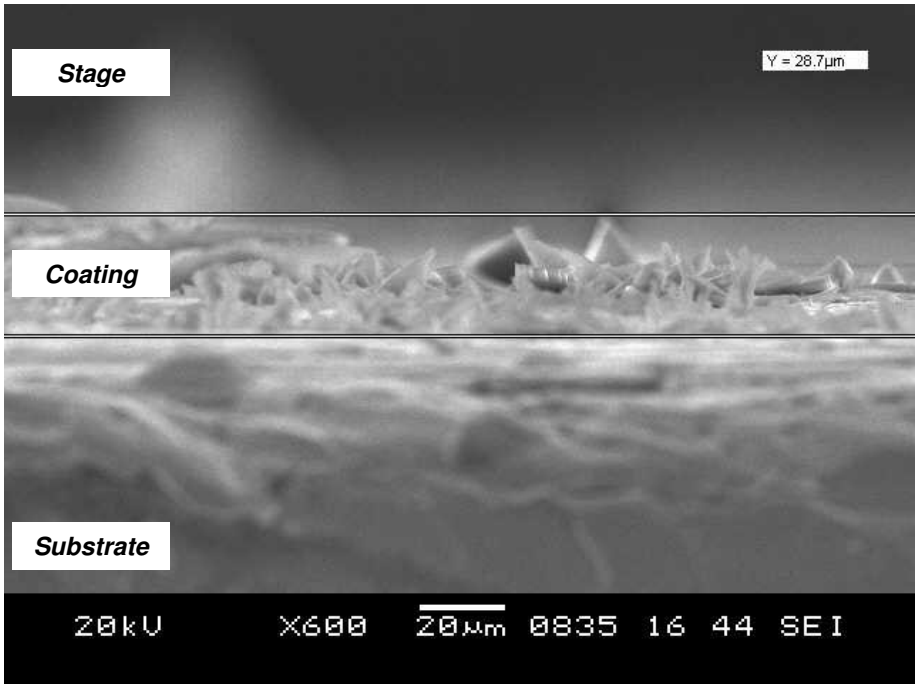

Figure 6.46 SEM image of a vertically mounted sample

The images and the size distribution of crystals on the surface of the coatings are shown in Figure 6.47 as obtained by using optical microscope and image analyzer. As seen from this figure crystal distribution on the surface is not in order. On the other hand, it was observed that dimension of the crystals increased with increasing temperature.

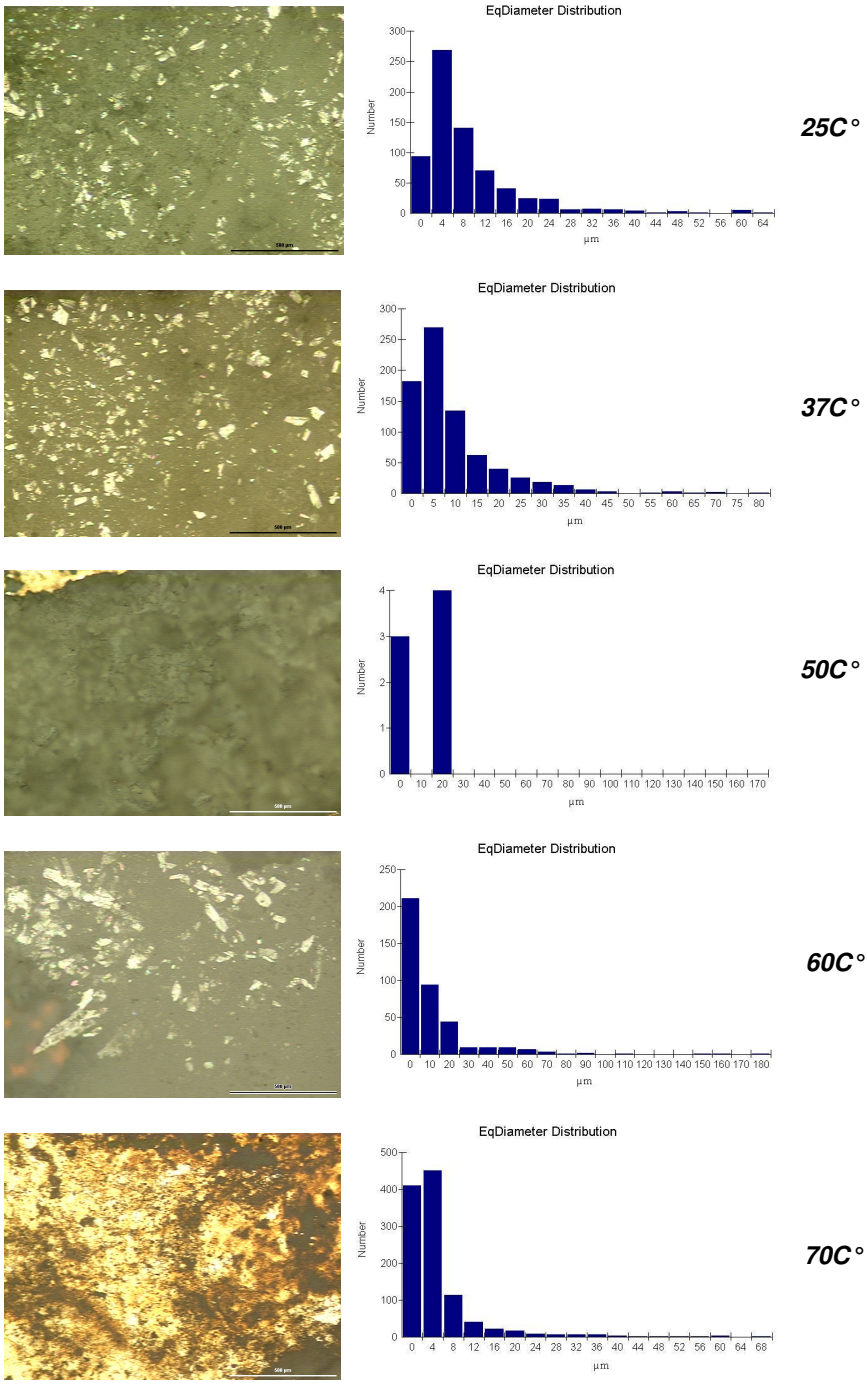

Figure 6.47 The optical images of the coatings and crystal distribution on these surfaces

Figure 6.48 shows the load-unload curve of the coatings before the heat treatment. The results of these curves are given at the Table 6.3.

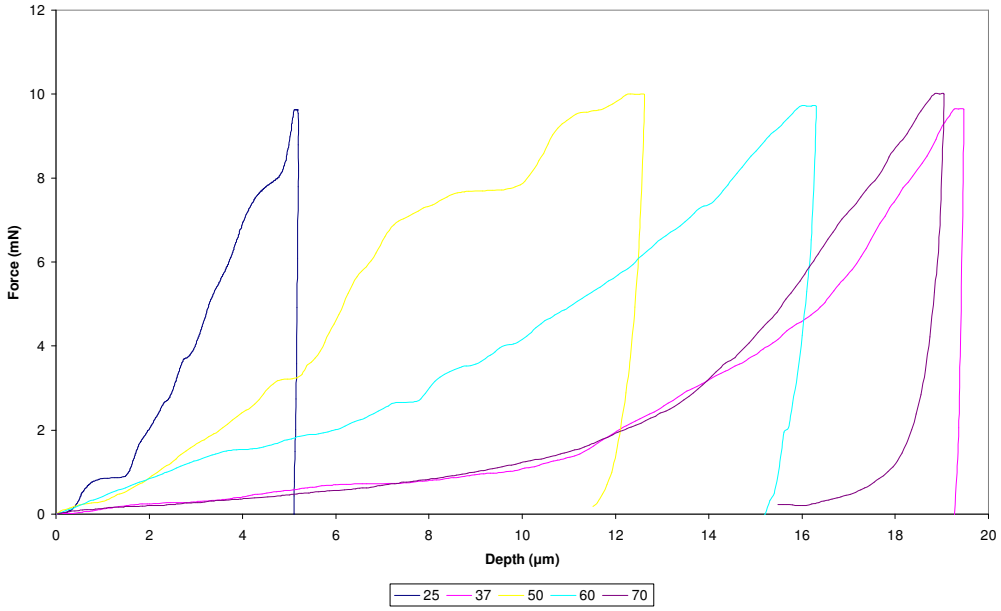

Figure 6.48 The load-unload curve of the coatings before heat treatment

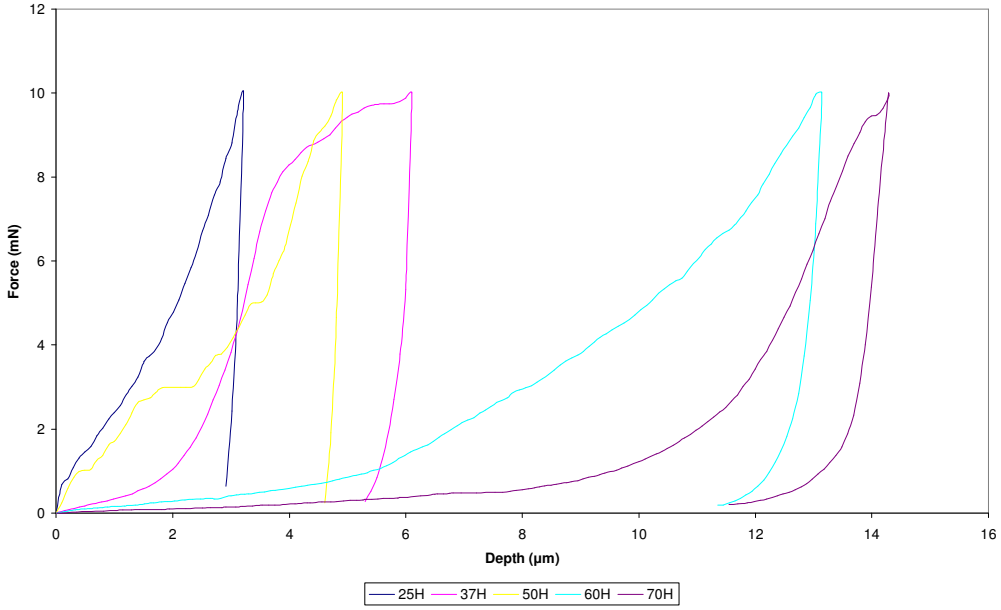

Figure 6.49 The load-unload curve of the coatings after heat treatment

Figure 6.49 shows the load-unload curve for the coatings after heat treatment. The hardness and the elasticity of the coatings studied were obtained by the use of these curves. The unload section of the curves provided the data to calculate the elasticity.

Table 6.3 The DUH results of all coatings before and after heat reatment

Deposition Temperature (°C)	**Hardness (MPa)**		**Elasticity (GPa)**	
	Before Heat Treatment	*After Heat Treatment*	*Before Heat Treatment*	*After Heat Treatment*
25	14.071	45.813	2.98	2.43
37	0.983	13.844	0.833	0.783
50	2.886	17.971	0.421	2.24
60	1.646	2.952	0.222	0.376
70	1.579	2.981	0.235	0.337

Table 6.3 shows the results of DUH tests for all coatings. As seen in the table all hardness values of the coatings increased following heat treatment process. On the other hand no meaningful results were obtained regarding the elasticity, due to may be an inhomogeneous distribution of porosity on the samples. However elasticity seems to have increased in general for the coatings deposited at the temperatures 50, 60, and 70 °C.

6.6.2 Scratch Test

Figure 6.50 and 6.51 show percent cartridge vs. force curves of the deposited specimens before and after heat treatment respectively.

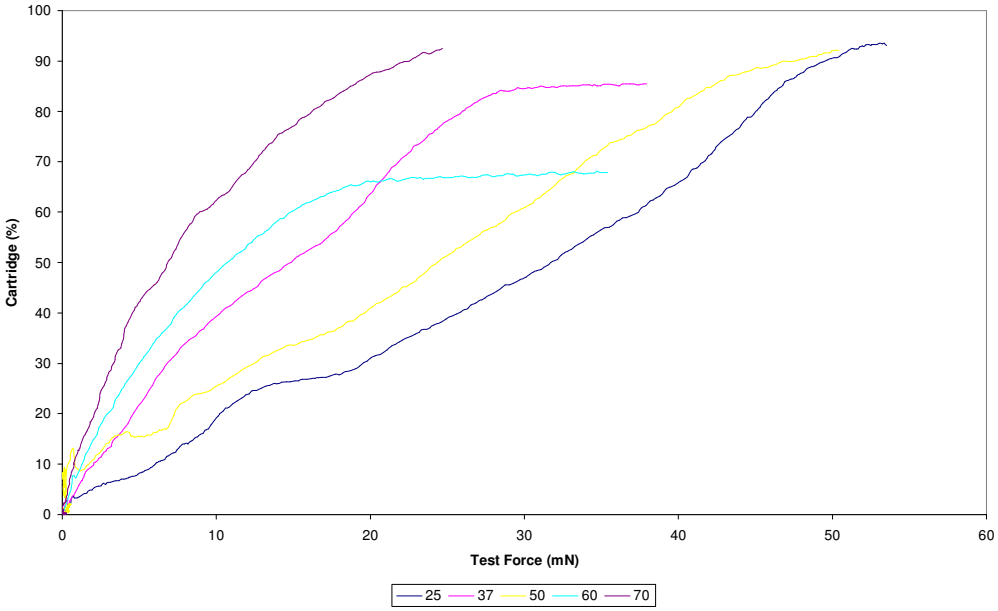

Figure 6.50 The cartridge (%)-force curve of all coatings before heat treatment

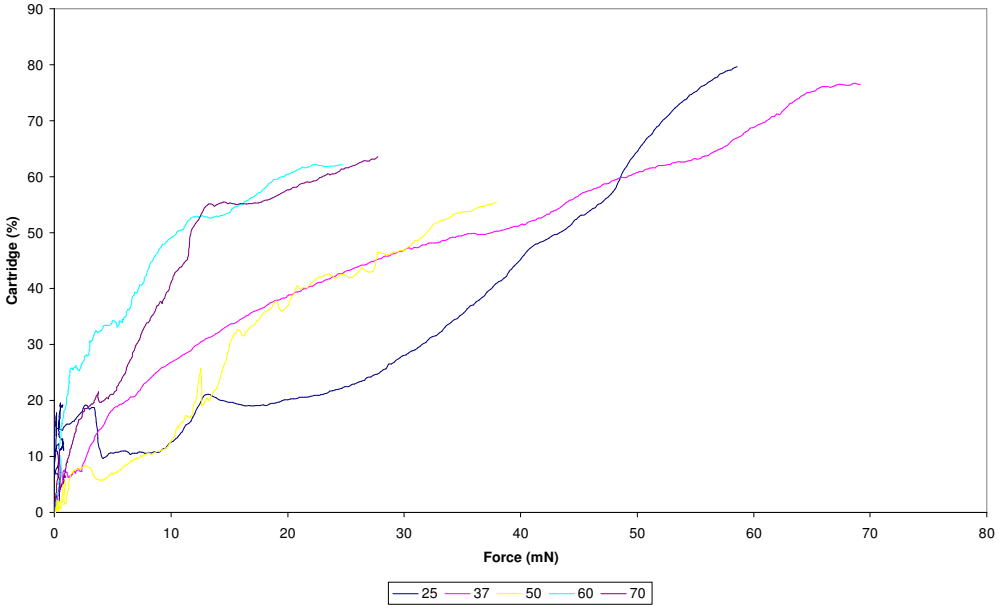

Figure 6.51 The cartridge (%)-force curve of the coatings after heat treatment

As seen from these figures % cartridge were found to decrease generally upon the heat treatment, indicating an increased adhesion of the coating to the substrate. The critical force is an important parameter for the scratch resistance. The point, where the slope of the curve in Fig. 6.50 and 6.51 deviates from linearity, is selected as a critical force. Table 6.4 shows the critical forces of all coatings.

Table 6.4 The scratch results of all coatings

Deposition Temperature (^{0}C)	**Critical Force (mN)**	
	Before Heat Treatment	*After Heat Treatment*
25	26.35	35.74
37	19.82	23.36
50	29.99	20.84
60	13.34	16.07
70	5.46	15.56

As seen from the Table 6.4 all the critical forces decreased with increasing deposition temperature without and with heat treatment with an exception of the untreated coating at 50 °C. Decrease in critical force means a decrease in adhesion strength to the substrate. Moreover, heat treatment caused an increase in the scratch resistance with one exception at 50 °C. This observation complied with the results of the DUH tests.

6.6.3 Wear Test

A cuople of coatings, namely the one deposited at 25 °C and heat treated and the other deposited at 70 °C and untreated, were chosen for wear testing. Figure 6.52 shows the wear test results of the coatings selected. In this figure, the curve No 1 (blue) presents the coating deposited at 25 °C and heat treated sample, and curve No 2 (pink) represents the untreated coating deposited at 70 °C. Wear tests were done under 49 N loads. This value was the lowest load available for the friction tester and yet was too high for these coatings considering the hardness results. Therefore wear properties of the coatings could not be assessed by these wear tests.

Figure 6.53 demonstrates the optical microscope images of the coatings before and after wear tests.

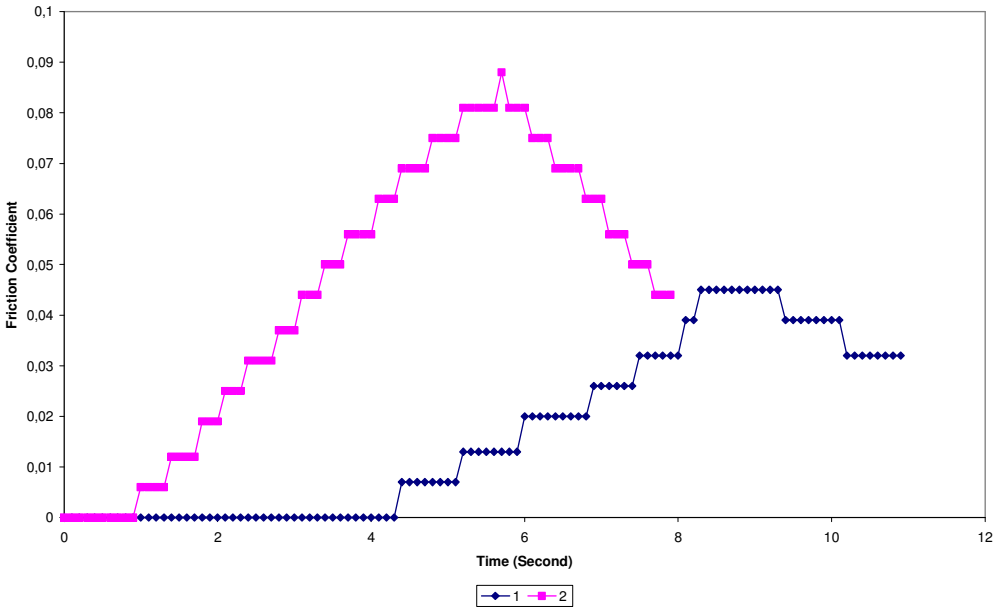

Figure 6.52 Friction coefficients vs. time curves of the coatings

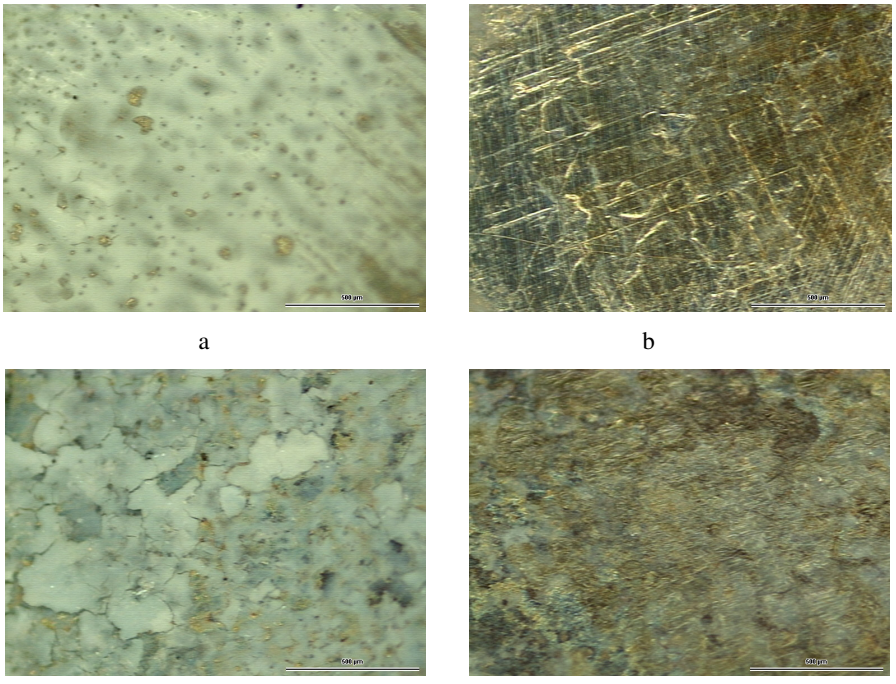

a b

c d

Figure 6.53 Optical images of the coatings; a) and b) represent coating No 1, before and after wear test respectively; c) and d) represent coating No 2 before and after wear test respectively

CHAPTER SEVEN
CONCLUSION

Calcium phosphate deposits on 316L SS substrate formed at different conditions by electrochemically from $Ca(NO_3)_2.4H_2O$ and $NH_4H_2PO_4$ solutions were obtained in the forms of Hydroxyapatite and Brushite. Heat treatments were applied to the coatings. Mechanical properties and corrosion behaviour of these coatings were investigated. The followings are the conclusions based upon the experimental works carried out in this study:

1. The temperature level of 50 °C is a critical temperature for all experiments conducted in this study, because HA formation started to take place at 50 °C for the first time in the process used throughout this study.
2. Molar ratio of Ca/P has the significant effect on the deposition performence besides the temperature.
3. Heat treatment procedure has an importance for the transformation of Brushite crystals into HA crystals.
4. The coating deposited at 70 °C and then heat treated at 500 °C for 1 hour exhibits the best corrosion resistance.
5. The coating deposited at 25 °C and then treated thermally at 500 °C for 1 hour has the best mechanical properties in all coatings regarding both hardness and scratch resistance together.

For further study, the kinetics of HA formation should be investigated, and the mechanical properties of the HA coatings should be improved.

REFERENCES

A Short History of Electroplating. (n.d.). Retrieved Juny 2006, from http://www.artisanplating.com/plating/index.html

Agraval C. M. (1998). Reconstructing the Human Body Using Biomaterials. *J. Met.*, Vol 50, 31-35.

Albee F. H. (1920). Studies in Bone Growth. Triple Calcium phosphate as a Stimulus to Osteogenesis. *Ann. Surg.* 71 32-36.

Aoki H., Kato K., Ogiso M. and Tabaka T. (1977). Sintered Hydroxyapatite as a New Dental Implant Material. *J. Dent. Outlook 49*. 567-575.

Ban S., Maruno S. (1995). *Biomaterials 16*. 977.

Barrows T. H. (1986). Degredable Implant Materials: a Review of Synthetic Absorbable Polymers and Their Applications. *Clin. Mater.* 1: 233.

Beevers C. A. and Melntyre D. B. (1956). The Atomic Structure of Fluorapatite and its relation to that of Tooth and Bone Mineral. Miner. Mag. 27. 254-259.

Birnbaum H. K. (1986). Hydrogen Embrittlement. Encyclopedia of Materials Science and Engineering, M. B. Bever, Editor, Pergamon Press. 2240.

Brunski J. B. (1996), Classes of Materials Used in Medicine, *Academic Press*.

Clark W. J., Driskell T. D., Hassler C. R., Tennery V. J. and McCoy L. (1973). Calcium Phosphate Resorbable Ceramics, A Potential Alternative to Bone Grafting. IADR Prog. & Abst. 52. Abstr. #259.

Daculsi G., Le Geros R. Z., Le Geros J. P. and Mitre D. (1991). Lattice Defects in Calcium Phosphate Ceramics; High Resolution TEM Ultrastructural Study. *J. Appl. Biomat. 2.* 147-152.

Davies D. and Whittaker J. (1967). Methods of Testing the Adhesion of Metal Coatings. Metallurgical Reviews, Review #112. 12, 15.

Davis J. R. (2003). Handbook of Materials for Medical Devices. *ASM International*

de Groot K. (1983). Ceramic of Calcium Phosphates: Preparation and Properties in Bioceramics of Calcium Phosphate. ed. K. de Groot (CRC Press, Boca Raton, FL.). 100-114.

de Groot K., Klein C. P. A. T., Wolke J. G. C. and De Blick-Hogervost J. M. A. (1990). Chemistry of Calcium Phosphate Bioceramics. Vol. H, eds. T. Yamamuro, L. L. Hench and J. Wilson (CRC Press, Boca Raton, Florida,). 3-16.

Denissen H. (1979). Dental Root Implants of Apatite Ceramics. Experimental Investigations and Clinical Use of Dental Root Implants Made of Apatite Ceramics. Ph. D. Thesis, Vrije Universiteit te Amsterdam.

Denissen H., Mangano C. and Cenini G. (1985). *Hydroxyapatite Implants.* (India: Piccin Nuova Libraria, S.P.A).

Dobbs H. S. (1982). Fracture of titanium orthopaedic implants. J. Mater. Sci. 17: 2398.

Ducheyne P., C. Kim S. and Pollack S. R. (1992). The effect of Phase Differences on the Time-Dependent Variation of the Zeta Potential of Hydroxyapatite. J. Biomed. Mater. Res. 26. 147-168.

Durney L. J. (1985). Hydrogen Embrittlement. Baking Prevents Breaking Products Finishing. 49. 90.

Ettel V. A., (1984). Fundamentals, Practice and Control in Electrodeposition-An Overview, Application of Polarization Measurements in the Control of Metal Deposition, I. H. Warren, Editor. Elsevier, Amsterdam.

Felder E. C., Nakahara S. and Weil R. (1981). Effect of Substrate Surface Conditions on the Microstructure of Nickel Electrodeposits. Thin Solid Films, 84. 197.

Fisher-Brandeis E., Dietert E. and Bauer G. (1987). Zur Morpologie Synthetisher Calcium-Phosphat-Keramiken In Vitro. A Zahnarztl. Implantol. III. 87.

Frankenthal R. P. (1975). Corrosion in Electronic Applications, Chapter 9 in Properties of Electrodeposits, Their Measurement and Significance, R. Sard, H. Leidheiser, Jr., and F. Ogburn , Editors. The Electrochemical Soc.

Frazza E. J. et al. (1971). A new absorbable structure. *J. Biomed. Mater. Res*.1: 43-58.

Fujishiro Y., Sato T., Okuwaki A. (1995), *J. Colliod, Interface Science*, 173: p-119.

Gilding D. K. et al. (1979). Biodegradable polymers for use in surgery, 1. *Polymer*.20:1459.

Glimeher M. J. (1984). "Recent Studies of Mineral Phase in Bone and its Possible linkage to the Organic Matrix by Protein-Bound Phosphate Conds." *Phil. Trans. R Soc., Lond.* B 304. 479-508.

Gorbunoff M. (1984). The Interaction of Proteins with Hydroxyapatite. J. Anal. Biochem. 136. 425-432.

Gu Y. W., Khor K. A., Cheang P. (2003). In vitro studies of plasma-sprayed hydroxyapatite/Ti-6Al-4V composite coatings in simulated body fluid (SBF). Biomaterials, 24. 1603–1611.

Hench L. L. (1985). Inorganic biomaterials: In Advances in chemistry series 245. *Materials chemistry–an emerging discipline (eds).* L V Interranate, L A Caspar, A B Ellis *(Washington DC: American Chemical Society)* p. 523.

Hench L. L., and E. C. Ethridge (1982). Biomaterials: An Interfacial Approach. Academic Press, New York.

Holleck H. (1986). Material Selection for Hard Coatings. J. Vac. Sci.Technol., A4(6). 2661.

Hubbard W. (1974). Phsiological Calcium Phosphate as Orthopedic Implant Material #6. Ph. D. Thesis, Marquette University.

Hulbert S. F. et al. (1987). Ceramics in Clinical Applications. *Elsevier science Pub. B. V*. Amsterdam. pp 189-213.

Jarcho M. (1976). Hydroxyapatite Synthesis and Characterization in Sense Polycrystalline Forms. J. Mater. Sci. 11. 2027-2035

Kay J. F. (1992). Calcium Phosphate Coatings for Dental Implants. Dent. Clin. North. Amer. 36. 1-18.

Kent J. N., Quinn J. H., Zide M. F., Guerra L. R. and Boyne P. J. (1983). Augmentation of deficient Alveolar Ridge with Non-Resorbable Hydroxyapatite Alone or With Autogenous Cancellous Bone. J. Oral. Maxillofac. Surg. 41. 429-435.

Lamb V. A. (1968). Plating and Coating Methods: Electroplating, Electroforming, and Electroless Deposition, Chapter 32 in Techniques of Materials Preparation and Handling, Part 3, R. F. Bunshah, Editor. Interscience Publishers.

Landau U., (1982). Plating-New Prospects for an Old Art, Electrochemistry in Industry, New Directions, U. Landau, E. Yeager and D. Kortan, Editors. Plenum Press, New York.

LeGeros R. Z. (1984). Incorporation of magnesium in Synthetic and Biological Apatites in Tooth Enamel IV, eds. R. W. Fearhead and S. Suga (Elsevier Science Publishers, Amsterdam,). 32-36.

LeGeros R. Z. (1991). Calcium Phosphates in Oral Biology and Medicine. Monographs in Oral Sciences, Vol. 15, ed. H. Myers (S. Karger, Basel).

LeGeros R. Z. and Tung M. S. (1983). Chemical Stability of Carbonate and Fluoride-Containing Apatites. Caries. Res. 17. 419-429.

LeGeros R. Z., (1988). Calcium Phosphate Materials in Restorative Dentistry: A Review. Adv. Dent. Res. 2. 164-183.

Lewitt G. E., Crayton P. H., Monroe E. A. and Conrate R. A. (1969). Forming Methods for Apatite Prosthesis. J. Biomed. Mater. Res. 3. 683-685.

Lin S., LeGeros R. Z., LeGeros J. P. (2003). Adherent octacalciumphosphate coating on titanium alloy using modulated electrochemical deposition method. J Biomed. Mater. Res., 66A. 819–828.

Lin T. C. (1986). Totally absorbable fibre reinforced composite from internal fracture fixation devices. Trans. Soc. Biomater. 9:166.

Mattox D. M. (1978). Thin Film Adhesion and Adhesive Failure-A Perspective", Adhesion Measurement of Thin Films, Thick Films, and Bulk Coatings, ASTM STP 640, K. L. Mittal, Editor, American Society for Testing and Materials. 54.

Monroe Z. A., Votowa W., Bass D. B., and McMullen J. (1971). New Calcium Phosphate Ceramic Material for Bone and Tooth Implants. J. Dent. Res. 50. 860-862.

Moss, A. J. et al. (1990). Use of selected medical device implants in the Unites States. Academic Press.

Nakahara S. (1979). Microporosity in Thin Films. Thin Solid Films, 64. 149.

Nakahara S. and Okinaka Y. (1983). Microstructure and Ductility of Electroless Copper Deposits. Acta Metall., 31. 713.

Nery E. B., Lynch K. L., Hirthe W. M. and Mueller K. H. (1975). Bioceramic Implants in Surgically Produced Infrabony Defects. J. Periodont. 46. 328-339.

Nguyen D., Thompson A.W. and Bernstein I. M. (1987). Microstructural Effects on Hydrogen Embrittlement in a High Purity 7075 Aluminum Alloy. Acta. Metall. 35. 2417.

Niwa S., Sawai K., Takahashi S., Tagai H., Ono M. and Fukuda Y. (1980). Experimental Studies on the Implantation of Hydroxyapatite in the Medullary Canal of Rabbits. Biomat. 1. 65-71.

Oberlaender B. C., Lugschneider E. (1992). Mater. Sci. Technol. 8. 657-665.

Paunovic M. and Schlesinger M. (1998). Fundamentals of Electrochemical Deposition. Wiley, New York.

Ratner B. D. et al. (1996). Biomaterials Science: An Introduction to Materials in Medicine. *Academic Press.*

Rickerby D. S. and Bull S. J. (1989). Engineering with Surface Coatings: The Role of Coating Microstructure. Surface and Coatings Technology, 39/40. 315.

Rodriguez F. (1982). Principles of Polymer Systems, 2nd ed. *McGraw-Hill. New York.*

Rosato D. V. (1983). Polymers, processes and properties of medical plastics: including markets and applications, in Biocompatible Polymers, Metals, and Composites. Lancester, PA. 1019-1067.

Rössler S. et al. (2002). Electrochemically assisted deposition of thin calcium phosphate coatings at near-physiological pH and temperature. *Institute of Materials Science, Dresden University of Technology, 01062 Dresden, Mommsenstr. 13, Germany.*

Rudzki G. J. (1983). Surface Finishing Systems. ASM, Metals Park, Ohio.

Safranek W. H. (1986). The Properties of Electrodeposited Metals and Alloys, Second Edition, American Electroplaters & Surface Finishers Soc.

Schlesinger M. and Paunovic M. (2000). Modern Electroplating (4th edition).*Wiley*. New York.

Schwartz M. (1982). Deposition From Aqueous Solutions: An Overview, Chapter 10 in Deposition Technologies for Film and Coatings, R. F. Bunshah, Editor. Noyes Publications, Park Ridge, New Jersey.

Sivakumar M., Kamachi Mudali U., Rajeswari S. (1994). Investigation of failures in stainless steel orthopaedic implant devices: Fatigue failure due to improper fixation of a compression bone plate. J. Mater. Sci. Lett. 13: 142–145.

Sivakumar M., Rajeswari S. (1992). Investigations of failures in stainless steel orthopaedic implant devices: Pit induced stress corrosion cracking. J. Mater. Sci. Lett. 11: 1039–1042.

Sridhar T. M. (2001). Synthesis, electrophoretic deposition and characterization of hydroxyapatite coatings on type 316L SS for orthopaedic applications. Ph D thesis, University of Madras, Chennai.

Sridhar T. M., Arumugam T. K., Rajeswari S., Subbaiyan M. (1997). Electrochemical behaviour of hydroxyapatite-coated stainless steel implants. J. Mater. Sci. Lett. 16. 1964–67.

Stoch A. et al. (2003). FTIR study of electrochemically deposited hydroxyapatite coatings on carbon materials. Journal of Molecular Structure 651–653. 389–396.

Suchanek W., Yoshimura M. (1998). Processing and properties of hydroxyapatite-based biomaterials for use as hard tissue replacement implants. *J. Mater. Res.13.* 94-117.

Visser S. A. et al. (1982). Biomaterials: An Interfacial Approach. Academic Press, NewYork. 50-60

Von Recum A. F. (1999). Handbook of biomaterials evaluation. Scientific, technical and clinical testing of implant materials 2nd edn. (Philadelphia: Taylor & Francis).

Williams D. (1990). An Introduction to Medical and Dental Materials. Concise Encyclopedia of Medical & Dental Materials, D. Williams, Ed., Pergamon Press and The MIT Press. p xvii-xx

Yankee S. J., Luckey H. A. and Johnson W. A. (1990). Thermal Spray Research and Applications. Proceeding of The Third National Thermal Spray Conference. Long Beach, USA.

Yip, C. S. et al. (1997). Thermal spraying of Ti6Al4V/hydroxyapatite composites coatings: powder processing and post-spray treatment. Journal of Materials Processing Technology. 65(1-3). 73-79.

Young R. A and Eliot J. C. (1966). Scale Bases for Several Properties of Apatites. Archs. Oral. Biol. 11. 699-707.

Yu-Peng Lu et al. (in press-to be published in 2006). Microstructural inhomogeneity in plasma-sprayed hydroxyapatite coatings and effect of post-heat treatment. Applied Surface Science.

Zhang J. M., Feng Z. D., Tian Z., Mechanistic W. (1998). Studies of electrodeposition for bioceramic coatings of calcium phosphates by an in situ pH-microsensor technique. Journal of Electroanalytical Chemistry. 452. 235-240.

Zimmerman M. C. et al. (1991). The design and analysis of a laminated degradable composite bone plate for fracture fixation. J. Biomed. Mater. Res. Appl. Biomater. 21 A (3): 345.